Universitat Autònoma de Barcelona

Tesis doctoral

Effects of phosphorus limitation and ocean acidification on coccolithophores in the Mediterranean Sea.

Angela María Oviedo Sabogal

Septiembre, 2015

Institut de Ciència i Tecnologia Ambientals (ICTA)
Universitat Autònoma de Barcelona (UAB)
Programa de Ciencia y Tecnología Ambientales

Co-directora:

Dr. Patrizia Ziveri
Profesora
ICTA-ICREA
Universitat Autónoma de Barcelona

Co-director:

Dr. Gerald Langer
Associated Researcher
Cambridge University

Acknowledgments

Several people were directly or indirectly involve in the development of this work and my thanks go to all who knew me during the last years, took the time to listen parts of this story or answered my doubts. First, to Patrizia Ziveri and Gerald Langer for their kind guidance from the beginning to the end. I could not feel more comfortable with my thesis directors, and of course, without the scientific discussions that we had, this thesis would have not been done.

The first activities within this work were the "culture experiments" at the Alfred-Wegener-Institute (AWI) in Germany: Thanks to Jelle Bijma for introducing me to the laboratories and research of the Biogeochemistry group. I would like to thank Kerstin Oetjen and Tina Brenneis for their continuous help in the laboratory during this time. Together with Beate Müller they did the POP measurements. I know how much work that implied: thank you. The Roscoff Culture Collection and specially Ian Probert are kindly acknowledged for providing the algae strains here used. It was a great experience to share the work and daily life with the scientists and crew members on board of the Meteor during the cruise 84-3. To all of them many thanks. Furthermore, to Toste Tanhua and Marta Álvarez for their contributions as coauthors of the article that resulted from this experience. Two mesocosm experiments gave me the opportunity to meet scientists form around the word and to filter tons of water together. Vincent Taillandier is gratefully acknowledged for analyzing and providing the CTD data and for its support during samplings; S. Alliouane for analyzing and providing the carbonate system data and J. Louis and C. Guieu for analyzing and sharing the nutrient data. A. Sallon, L. Maugendre, R. Gutierrez and M. Celussi for their support during samplings. The staff of the Observatoire Océanologique de Villefranche and the STARESO (Cordica, France) marine station are gratefully acknowledged for their logistic assistance.

To my colleagues and friends at ICTA: Mika, Anaid, Laura, Pati, Ana, Rahiman y Barbara, gracias por las risas compartidas. A Antonius, du hast mir den ersten "impulso" gegeben zu Barcelona wählen (o algo así).

A mis padres y a mi hermano que aceptaron, sufrieron y se alegraron con mi decisión de vivir al otro lado del Atlántico. Los tres han seguido este proceso y les estoy muy agradecida por estar siempre a mi lado. A mi familia Vincent y Mariana por ser un soporte diario durante gran parte de mi doctorado y por todo el amor recibido.

This research recieved funding from the European Community's Seventh Framework Programme under grant agreement 265103 (Project MedSeA) and the "Agencia de Gestión de Ayudas Universitarias y de Investigación (Becas FI)" of the Catalunya Generalität.

Index

Resumen

Esta tesis se desarrolló en el marco del proyecto Europeo Mediterranean Sea Acidification in a changing climate (MedSeA) (http://medsea-project.eu) con el fin de estudiar los efectos de la limitación por fósforo (P) y el incremento en la presión parcial de dióxido de carbono (pCO_2) sobre diferentes aspectos de la biología y ecología de los cocolitóforos. Tanto la concentración de nutrientes en los océanos como la pCO_2 están sujetos a variabilidad espaciotemporal natural. Sin embargo, los cambios climáticos globales antropogenicamente inducidos influirán fuertemente en estos dos parámetros. Las muestras de campo y las cepas de cocolitóforos usadas en los experimentos de cultivo provienen del Mar Mediterráneo, el cual es uno de los mares más pobres en P. Según las proyecciones sobre el cambio climático para diferentes escenarios, el Mar Mediterráneo es considerado un "hot spot" debido al rápido incremento en temperatura atmosférica y del agua marina y la reducción en precipitaciones en algunas regiones. Adicionalmente, en este mar posee una alta alcalinidad y un corto tiempo de residencia de sus aguas, lo que promueve una mayor absorción de CO_2, cambiando la química de las aguas (acidificación oceánica).

Esta tesis combina diferentes aproximaciones metodológicas, desde experimentos de cultivo y mesocosmos hasta observaciones de campo, para responder preguntas a diferentes escalas, de especies a comunidades. Los capítulos 2 y 3 se basan en experimentos de cultivo realizados con la especie *Emiliania huxleyi*, la más abundante de las especies actuales. Se investigaron los impactos de la limitación por P y la acidificación oceánica en cultivos monoclonales de *E. huxleyi*. Los parámetros analizados incluyen: tasa de crecimiento, densidad celular máxima, cuota celular de carbono orgánico e inorgánico, de fósforo y de nitrógeno y la morfología de sus coccolitos (Capítulos 2 y 3). En el Capítulo 2, los posibles impactos de la limitación por P se investigan en 6 cepas de la especie *E. huxleyi*, 4 de ellas aisladas en el Este del Mediterráneo (ultra-oligotrófico) y 2 en el oeste (oligotrófico a mesotrófico). Se demuestra que dichas cepas no representan ecogenotipos establecidos según la disponibilidad de P. Así mismo, que la limitación por P produce un sobre-consumo de carbono y no causa malformaciones de los coccolitos. El Capítulo 3 presenta los resultados de un segundo experimento diseñado para examinar los efectos de la acidificación oceánica en aguas pobres en P sobre una de las cepas de *E.*

huxleyi usadas en el experimento previo. Se demuestra que la combinación de dichos factores estresantes puede afectar negativamente las poblaciones de *E. huxleyi* ya que la cantidad de P que las células toman aumenta con el incremento en pCO_2, lo que disminuye la densidad celular máxima si el P es limitante. También se demuestra que la acidificación oceánica causa malformaciones en los coccolitos sin relación a la concentración externa de nutrientes. El Capítulo 4 presenta los resultados de dos experimentos de mesocosmos realizados en Córcega y Villefranche-sur-Mer (Francia). Estos se enfocan en cuantificar y entender los impactos de la acidificación oceánica en dos comunidades de cocolitóforos, ambas habitando aguas pobres en P. Los resultados de estos experimentos son: 1) Cambios en la pCO_2 no desencadenaron una sucesión en el fitoplancton, 2) La estructura de la comunidad de cocolitóforos no cambió bajo una elevada pCO_2. Sin embargo, un posible efecto de los nutrientes no puede ser excluido, como tampoco que los cambios sean de orden fenológico. 3) Altos niveles de CO_2 no causaron ningún efecto en la morfología de los coccolitos de *E. huxleyi* ni en su grado de calcificación. Entonces, en regiones oligotróficas, los nutrientes o cambios en la fenología de las diferentes especies pueden tener un mayor impacto sobre la comunidad de cocolitóforos que la pCO_2. Finalmente, el Capítulo 5 presenta los resultados del análisis de 81 muestras colectadas entre los 0 – 100 m de profundidad, en diferentes puntos del mar Mediterráneo, incluyendo un transepto de este a oeste (Meteor Research Vessel, campaña M84-3, Abril 2011). Los datos adquiridos proveen una descripción de la distribución de los cocolitóforos durante primavera, lo cual se relacionó con una amplia serie de variables ambientales medidas *in situ*. Estas observaciones sugieren un posible rol de parámetros relacionados con la química de carbonatos y también de la concentración de fosfatos en la distribución de los heterococolitóforos, fase del ciclo de vida que es la más abundante en el océano actual. Los holococolitóforos, por otra parte, se relacionaron con la concentración de nutrientes pero no con la química de los carbonatos, lo cual refuerza la importancia de considerar las dos fases separadamente cuando se analizan cambios en los ensamblajes de especies y de diversidad.

Se concluye que la limitación por P amplifica la respuesta a la acidificación oceánica dado que disminuye la densidad celular máxima que los cocolitóforos pueden alcanzar. Juntos, los resultados referentes a la limitación por P (Capítulo 2) y de otros estudios referentes a la acidificación oceánica (Meyer & Riebesell 2015) sugieren que *E. huxleyi* puede, en un

futuro océano limitado por nutrientes y acidificado, contribuir muy poco a la exportación de carbono inorgánico relativa a la exportación total de materia. Esto favorecería la remineralización en lugar del secuestro a largo tiempo de carbono.

Contrario a una hipótesis previa (Okada & Honjo 1975, Young & Westbroek 1991), la limitación por P no induce malformaciones en los coccolitos de *E. huxleyi* (Capítulos 2 y 3). Esto es también cierto para *C. leptoporus* (Langer et al 2012), pero el caso de *C. pelagicus* demuestras que dicha afirmación no puede ser generalizada (Gerecht et al 2014, 2015). Sin embargo, bajo una exposición prolongada a una elevada pCO_2 y en ausencia de selección entre clones, la acidificación oceánica causa malformación de los coccolitos irrespectivamente de la [P].

Summary

This thesis was conducted in the framework of the European Mediterranean Sea Acidification in a changing climate (MedSeA) project (http://medsea-project.eu). It studies the effects of phosphorus limitation and increased partial pressure of carbon dioxide (pCO_2) on different aspects of the biology and ecology of coccolithophores, an abundant and ubiquitously distributed group of calcifying phytoplankton. Both, oceanic nutrient levels and pCO_2 are subject to natural spatiotemporal variability, but the anthropogenic forcing in the world's climate are likely to have strong impacts on these two parameters. Field samples and the coccolithophore clones used in the culture experiments originate from the Mediterranean Sea, which is one of the most phosphorus (P) poor seas in the world. The Mediterranean is one of the most responsive regions to climate change and based on the results from global climate change projection scenarios is considered a "hot spot" for climate change with rapid increases in atmosphere and seawater temperature and decreased precipitation in some regions. It also has a high alkalinity, and the short residence time of surface water trigger a high absorption of anthropogenic CO_2, changing the water chemistry (ocean acidification).

The thesis combines different approaches from culture to mesocosm experiments and field observations, aiming to solve questions at different scale from species to community level. Chapters 2 and 3 are focussing on culture experiments performed on the most abundant modern coccolithophore species, *Emiliania huxleyi*. The experiments investigate the impacts of phosphorus limitation and ocean acidification on monoclonal *E. huxleyi* cultures. Parameters analysed include growth rate, maximum cell densities, cellular organic and inorganic carbon quotas, cellular nitrogen and phosphorus quotas, and coccolith morphology (Chapters 2 and 3). In Chapter 2 the possible impacts of P limitation are investigated on 6 *E. huxleyi* clones, 4 of them isolated in the eastern Mediterranean (ultra-oligotrophic) and 2 in the western Mediterranean (oligotrophic to mesotrophic). It is shown that no *E. huxleyi* ecogenotypes are established upon environmental phosphate availability in these clones. It is also shown that P limitation leads to an increase in cellular carbon quotas and does not cause coccolith malformation. Chapter 3 presents the results of a second culture experiment designed to test the combined effects of seawater acidification

under P limitation in one of the *E. huxleyi* clones used in the previous experiment. It is shown that the combination of these stressors may negatively affect *E. huxleyi* populations because the cellular P quota, i.e. the P requirement, increases with increased pCO_2. These higher cellular P quotas decrease maximum yield cell densities under P limitation conditions. It is also shown that ocean acidification causes coccolith malformation irrespectively of the seawater phosphate concentration. Chapter 4 presents the work performed in two mesocosm experiments conducted off Corsica and Villefrance sur Mer (France). They focussed on the quantification and understating of the impacts of ocean acidification on two different coccolithophore communities inhabiting P poor waters, and coccolithophore abundance in relation to diatoms and silicoflagellates. The results are: 1) A pCO_2 driven phytoplankton succession did not occur in the studied areas, 2) The coccolithophore community structure did not change with elevated pCO_2, an effect from nutrient concentrations can not be ruled out 3) Elevated pCO_2 had no effect on *E. huxleyi* coccolith morphology. Thus, in oligotrophic regions, nutrients or phenological trends in the different species may impose more constrains on the coccolithophore community structure than pCO_2 does. Finally, Chapter 5 elaborates on field data from 81 samples collected at depths from 0 – 100 m on an east to west transect in the Mediterranean Sea (Meteor Research Vessel, M84-3 cruise, April 2011). The acquired data are used to describe the spring-time coccolithophore distribution in the Mediterranean Sea, which was related to a broad set of *in situ* measured environmental variables. These observations suggest a possible role of seawater carbonate chemistry, but also [PO_4^{3-}] in determining the distribution of heterococcolithophores, the most abundant coccolithophore life phase. Holococcolithophores, on the other hand, thrived in oligotrophic areas and were not related to carbonate chemistry, which emphasizes the importance of considering holo- and heterococcolithophores separately when analyzing changes in species assemblages and diversity.

It is concluded that oligothrophy (i.e. P limitation) amplifies the response to ocean acidification in terms of maximum cell densities. That is, further decreases maximum cell densities. Results on P limitation (Chapter 2) and from other studies in ocean acidification (Meyer & Riebesell 2015) allowed to conclude that *E. huxleyi* might, in a future P-poor and acidified ocean, contribute relatively little inorganic carbon to exported matter, which would in turn favour remineralization over long term burial at depth.

Contrary to an older hypothesis (Okada & Honjo 1975, Young & Westbroek 1991), P limitation does not induce coccolith malformations in *E. huxleyi* (Chapters 2 and 3). While this is true for *C. leptoporus* as well (Langer et al 2012), the case of *C. pelagicus* shows that this finding cannot be generalized (Gerecht et al 2014, 2015). However, under a long time exposure to enhanced pCO_2 and the absence of clone selection, ocean acidification causes coccolith malformation irrespectively of the [P].

Chapter 1.

Introduction

1.1 The problem

There is no doubt that atmospheric concentrations of gases that produce a greenhouse effect have all increased since the industrial revolution due to human activity. Gases such as carbon dioxide (CO_2), methane (CH_4), and nitrous oxide (N_2O) increased by 40%, 150%, and 20%, respectively, in relation to pre-industrial levels (year 1750) and now substantially exceed the highest concentrations recorded in ice cores during the past 800,000 years (Stocker et al. 2013). Green-house gases absorb infrared thermal radiation emitted by the earth and also radiate some of this energy back to space, thus, they help regulating terrestrial climate by recycling solar energy in the atmosphere. From these gases, CO_2 is one of the major contributors to global climate change because it is present at a higher concentration with respect to other green-house gases (with the exception of water vapour) and it has a relatively long life-time in the atmosphere with respect to the most abundant water vapour. Then, its capacity to warm up the earth's surface is one of the highest (Stocker et al. 2013).

Atmospheric CO_2 levels, over the last 800,000 years as indicated by the ice-core data from Antarctica have fluctuated between 170 and 300 parts per million by volume (ppmv), corresponding with conditions of glacial and interglacial periods. In the Northern hemisphere. The highest pre-industrial value recorded in 800,000 years of ice-core record was 298.6 ppmv, in the Vostok core, around 330,000 years ago (Augustín et al. 2008, Zeebe & Caldeira 2008) . In industrial times atmospheric CO2 levels have increased drastically averaging 399 ppm in 2014 (Keeling et al. 2015). Nevertheless, emissions from fossil fuel combustion and cement production continue to increase: 9.5 [8.7 to 10.3] GtC yr^{-1} in 2011, which is 54% above the 1990 level (Stocker et al. 2013). Even further the mean rates of increase in atmospheric concentrations over the past century are unprecedented in the last 22,000 years (Stocker et al. 2013).

The rapid increased in atmospheric CO_2 affects the ocean in three main ways,: 1. CO_2 enters and leaves the ocean surface by molecular diffusion, once the gas dissolves in seawater, a series of chemical reactions modify the seawater carbonate chemistry decreasing its pH (Figure 1) and, in turn, it modifies other acid-base systems in seawater affecting the chemical speciation of some nutrients. 2. the global warming associated to anthropogenic CO_2 accumulation in the atmosphere is enhancing heat transfer to the sea surface. The ocean warming increases stratification in the water column, thus, reducing the input of nutrients into the upper photic productic layer. The first two process are further detailed in sections 1.1.1 and 1.1.2. respectively. 3. Ocean deoxygenation, i.e. the loss of dissolved oxygen (O_2) from the ocean which is bound to occur in a warming and more stratified ocean (Gruber 2011, Keeling et al. 2010).

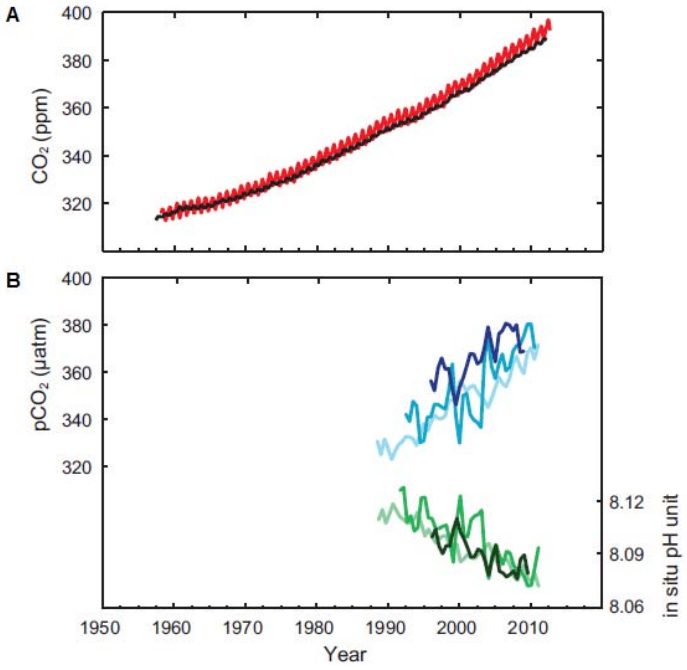

Figure 1.1 A. Atmospheric concentrations of carbon dioxide (CO_2) from Mauna Loa, Hawaii (in red) and South Pole (89°59'S, 24°48'W – in black); B. partial pressure of dissolved CO_2 at the ocean surface (blue) and in situ pH (green). Measurements are from three stations in the Atlantic (dark blue and dark green); and the Pacific Oceans (light blue and light green). Coordinates are specified in Stocker et al. (2013) from where the image has been taken and modified.

1.1.1 Carbonate chemistry modification: "Ocean acidification"

The ocean inventory of anthropogenic CO_2 represents ~45 – 50 % of fossil fuel CO_2 emissions over the industrial period (Sabine 2004, Khatiwala et al. 2013) or about ~30 %

of total human emissions and it is very likely that the global ocean inventory of anthropogenic carbon increased from 1994 to 2010 (Rhein et al. 2013). It is then clear that until now the ocean has been buffering the increase in atmospheric CO_2, and thus, climate change, by absorbing and sequestering carbon as CO_2. However, this up-take brings consequences to the ocean chemistry and ecosystems. Once atmospheric CO_2 dissolves into seawater, it forms carbonic acid (H_2CO_3) (Eq. 1.1). This unstable acid dissociates in bicarbonate (HCO_3^-) and hydrogen ions (H^+) (Eq. 1.2), the former continues to disassociate in carbonate ions (CO_3^-) and protons (Eq. 1.3).

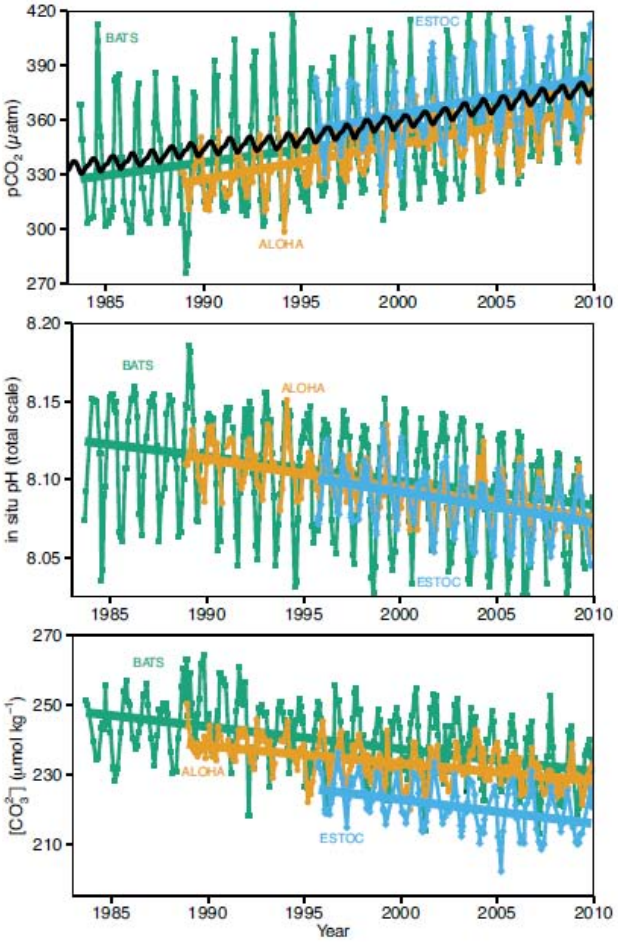

Figure 1.2 Trends in partial pressure of CO2, pH and carbonate ion concentrations at three different ocean time series (BATS, Bermuda Atlantic Times Series; ALOHA time sieries at Hawaii; and the ESTOC, North-east Atlantic time series at 100 km north of the Canary islands). Taken from (Rhein et al. 2013).

$CO_2 + H_2O \rightarrow H_2CO_3$ (Eq. 1.1)

$H_2CO_3 \rightarrow H^+ + HCO_3^-$ (Eq. 1.2)

$HCO_3^- \rightarrow H^+ + CO_3^{2-}$ (Eq. 1.3)

As a result, the distribution of the different carbon species are changed: $[CO_3^{2-}]$ decreases while, $[HCO_3^-]$ and $[H^+]$ increase. The release of hydrogen ions translates into decreased pH which is the reason why the process has been called "ocean acidification" (Figure 1.2). Ocean acidification also occurs from other chemical additions or subtractions in the ocean such as depositions of sulphur and nitrogen compounds from the atmosphere during rain (Gattuso & Hansson 2011). However, in the open ocean, the ocean acidification produced

by sulphur and nitrogen compounds is very small (< 2%) when compared to the acidification produced by the ocean uptake of CO_2 (Doney et al. 2007, Bates & Peters 2007).

The pH of ocean surface water has decreased by 0.1 since the beginning of the industrial era, corresponding to a 26% increase in hydrogen ion concentration (Orr et al. 2005; Feely et al. 2009) and the trend is expected to continue in the future (Ciais et al. 2013). Earth System Models project that by the year 2100, the decrease in surface ocean pH reaches 0.30 to 0.32 for RCP8.5 scenario (Figure 1.3) (Stocker et al. 2013). This equals a ~100 % increase in proton concentration and implies that average surface ocean pH will be lower than it has been for more than 50 million years (Pearson & Palmer 2000).

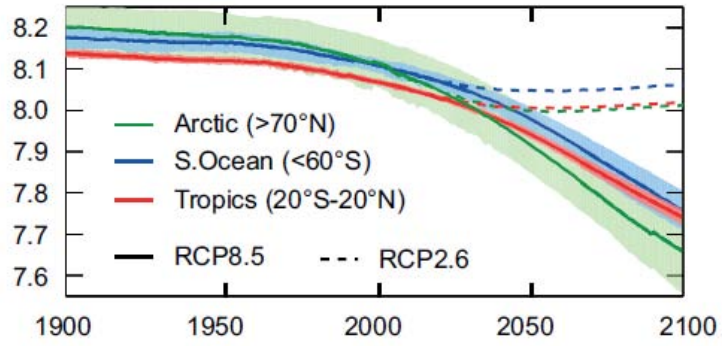

Figure 1.3 pH projections under two of the IPCC scenarios for the artic, southern ocean and the tropics [Taken from Rhein et al. (2013)]

The decrease in pH and parallel changes in the carbonate chemistry of seawater alters seawater chemical speciation and biogeochemical cycles of many elements and compounds (Doney et al. 2009). Here only the effects to calcium carbonate minerals and macronutrients (i.e.: phosphate) will be mentioned. Both, pose constrains for marine organisms to growth.

The fitness of organisms that use calcium carbonate ($CaCO_3$) and magnesium calcite to build up their skeletons or shells may be threatened by ocean acidification. The reasoning behind is that the dissolution and precipitation of these minerals are a function of the saturation state of seawater with respect to the particular mineral X (Ω_X). The saturation state of X is the product of the particular ions that form the mineral (i.e. for calcite and

aragonite: calcium and carbonate ion) divided by the solubility product which equals the equilibrium constant of the dissolution equilibria in seawater [see Zeebe and Gladrow (2001) for a detailed explanation]. It can be calculated according to:

$\Omega_X = [Ca^{2+}][CO_3^{2-}]/Ksp_X$; (Eq. 1.4)

Ocean acidification decreases the concentration of CO_3^{2-} in surface seawater, thus making more likely that Ω_X <1. In such case, the seawater is under-saturated with respect to the mineral phase and then, the dissolution of that mineral is thermodynamically favourable while the formation is not.

1.1.2 Several factors may promote phosphorus limitation in the future oceans

Nitrogen (N), phosphorus (P) and silicon are considered the major oceanic nutrients because primary producers (i.e.: phytoplankton and cianobacteria) consume these elements in the euphotic zone to assimilate them into carbon rich macromolecules. These nutrients, required in several metabolic processes, can be depleted from the ocean surface and then limit the growth of phytoplankton. Although N is believed to be the main limiting nutrient of ocean's productivity, large regions such as the subtropical north pacific (Karl 1999, Karl et al. 2001, Kim et al. 2014) have turned P limited in few decades. Even further, the sources of nitrogen to the ocean are expected to increase in relation to the input of phosphorus. For instance, atmospheric deposition of bioavailable N to the open ocean has tripled since 1860 (Moore et al. 2013) and atmospheric fluxes will likely become increasingly enriched in N relative to both iron and phosphorus (Moore et al. 2013). The projected increasing CO_2 emissions and enhanced stratification of the oceans may lead to an increase in global N fixation (Karl et al. 2001, Hutchins et al. 2007, Levitan et al. 2007). Even if species-specific (Hutchins et al. 2013), these changes in N fixation and atmospheric depositions could indirectly (i.e. biologically mediated) decrease P concentrations in the surface of the ocean.

Ocean acidification is also expected to alter the bioavailability of P for phytoplankton. This is because the acid-base equilibrium of the seawater is altered by the ocean´s uptake of

CO_2, affecting not only the carbonate acid-base system but many other compounds. Among them, the phosphoric acid-base system (Eq. 1.5) will be altered in a way that phosphate (PO_4^{3-}) concentrations are expected to decrease (Figure 1.4).

$H_3PO_4 = H^+ + H_2PO^{4-} = 2H^+ + HPO_4^{2-} = 3H^+ + PO_4^{3-}$; (Eq. 1.5)

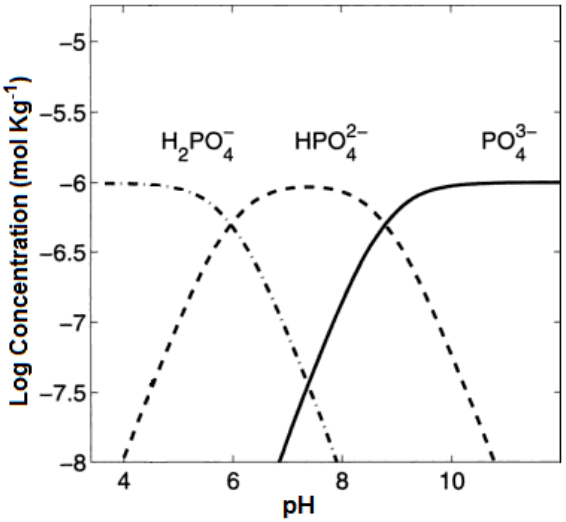

Figure 1.4 The concentrations of some of the different species in the phosphoric acid system that might be influenced by decreasing seawater pH, including phosphate (PO_4^{3-}). Modified from Zeebe and Gladrow (2001).

Oceanic phosphate concentrations are predicted to experience a further decline not only by the abovementioned chemical effects of enhance CO_2 uptake, but also because of the enhanced stratification of surface waters caused by increased heat content in the upper layers of the ocean. The globally averaged temperature difference between the ocean surface and 200 m increased by about 0.25ºC from 1971 to 2010 (Levitus et al., 2009). This change corresponds to a 4% increase in density stratification (Rhein et al. 2013). Although, global trends in oceanic nutrient concentration are not available due to the lack of long-time series data, thermal stratification is thought to explain the global trends to decreased net primary production and chlorophyll concentration (Figure 1.5) because it blocks the input of nutrients from the deeper layers, specially at low latitudes (Behrenfeld et al. 2006, Polovina et al. 2008, Irwin & Oliver 2009).

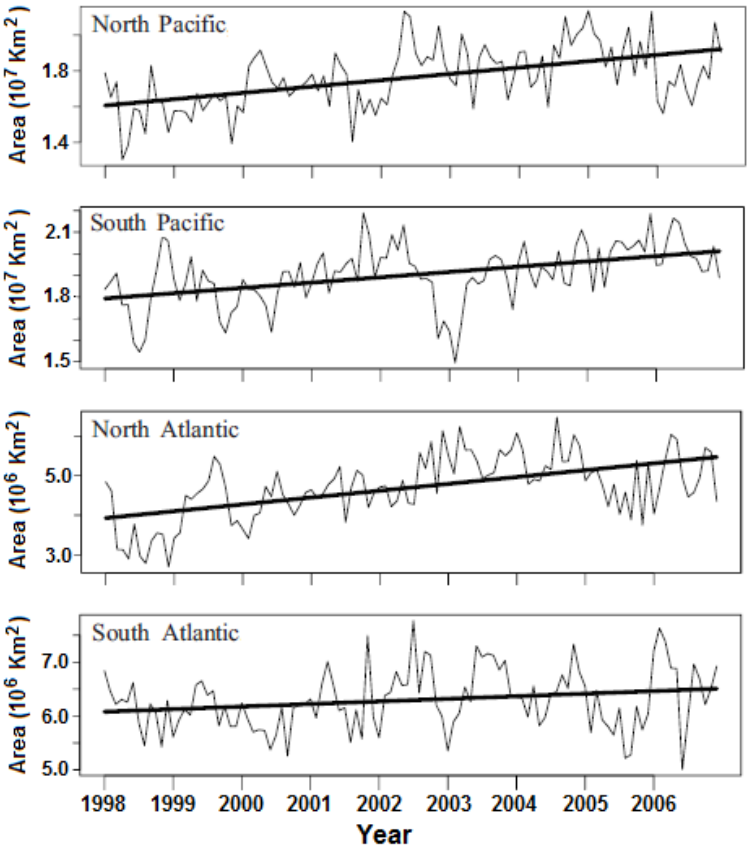

Figure 1.5 Annual monthly mean area with surface chlorophyll ≤ 0.07 mg Chl m^{-3} between 5º and 45º N/S latidude. Straight lines are the linear terms from the Generalized Additive Models. Taken from Polovina et al. (2008).

The expected increase in N fixation, the enrichment of N relative to P of the atmospheric depositions, the predicted changes in the phosphoric acid system of seawater and the thermal stratification of the water column bring the potential consequence of increasing P stress for phytoplankton. Decreased phosphate concentrations can be of great importance in areas which are already poor in P such as the North Pacific subtropical gyre (Karl 1999), the Western North Atlantic Ocean (Wu et al. 2000, Ammerman et al. 2003) or the Mediterranean Sea (Krom et al. 1991, Moutin & Raimbault 2002, Thingstad et al. 2005).

1.2 The subject under study

1.2.1. Coccolithophores

Marine phytoplankton contributes to ~ 40 – 50 % of the global primary production (Falkowski et al. 1998, Field 1998) and it is responsible for the functioning of the ocean

being at the base of the food web and a sink for atmospheric CO_2. Phytoplankton is divided into functional groups based on their impact on biogeochemical cycles (Iglesias-Rodríguez et al. 2002, Anderson 2005). The most studied functional groups of marine phytoplankton are usually nitrogen fixers (cyanobacteria), silicifiers (diatoms) and calcifiers (coccolithophores and some dinoflagellates). Coccolithophores (Haptophyta) are unicellular calcifying phytoplankton producing producing calcareous plates, called coccoliths interlocked to cover the cell (coccosphere). These organisms represent ~10% of global phytoplankton biomass (Tyrrell & Young 2009) and dominate in regions of moderate turbulence and nutrients. Coccolithophores evolved in the mid-Triassic period, but it was later, during the Cretaceous and throughout the Cenozoic, that coccoliths calcification accounted for up to 80% of the total marine $CaCO_3$ (Fabry 1989). Nowadays, coccolithophores contribute about half of the modern worldwide marine pelagic $CaCO_3$ sedimentation (Frenz et al. 2005, Broecker & Clark 2009). Given their high affinity for phosphate when compared to other phytoplankton groups (Riegman et al. 2000) they are particularly important in regions with low [P], where coccolithophores are a seasonally dominant group of the phytoplankton community (Siokou-Frangou et al 2010). Together with their dual contribution to the carbon cycle (section 1.2.2), and the possible detrimental effect of ocean acidification on the production of coccoliths, this make them one of the most interesting phytoplankton groups to study the combined effects of ocean acidification and P limitation.

Coccolithophores undergo a haplo-diploid life cycle, where both phases are capable of asexual reproduction (de Vargas et al. 2007). During the haploid phase holococcoliths, a type of coccoliths comprised of minute crystals (ca. 0.1 μm), are produced. During the diploid phase another type of coccolith, the heterococcoliths, are produced. They are comprised of a radial array of complex crystal-units (Young et al. 2003). However, many species do not calcify during part of their life cycle and certain species such as *Isochrysis galbana* or *Dicrateria inornata* probably do not calcify at all (de Vargas et al. 2007).

Currently, there are approximately 280 different morphologically defined coccosphere types (Young et al. 2003) (examples in Figure 1.6). The species quantification, however, is difficult to attain because the different life phases are heteromorphic. Coccolithophore have developed different growth strategies. Some species are typical of oligotrophic

conditions while others are “opportunistic”, bloom according to nutrient inputs (Ziveri et al. 2004, de Vargas et al. 2007). *Emiliania huxleyi* is the most abundant extant coccolithophore (Paasche 2002) and together with *Gephyrocapsa oceanica*, the only species known to form large seasonal blooms.

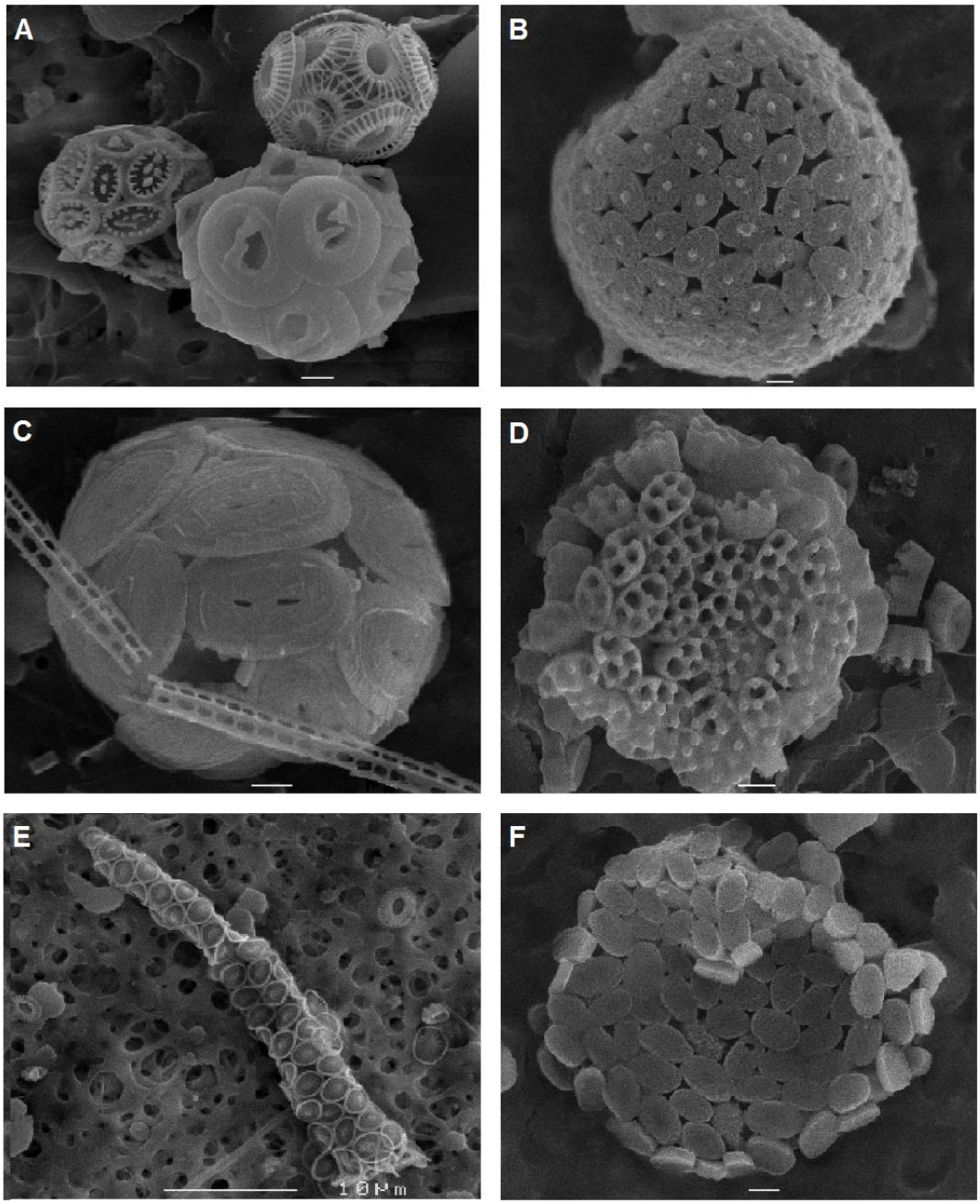

Figure 1.6 Coccolithophores from the Mediterranean Sea. Heterococcolithophores (A, C, E) and holococcolithophores (B, D, F). A, the species *Syracosphaera molischii, Gephyrocapsa oceanica* and *Emiliania huxleyi*; B, *Coronosphaera mediterranea* HOL hellenica-type; C, *Helicosphaera pavimentum*; D, *C. leptoporus* ssp. quadriperforatus HOL, E, *Syracosphaera prolongata*; and F, *Calyptrolithophora papillifera*.

1.2.2 The role of coccolithophores in biogeochemical cycles

There are three main mechanisms by which carbon is exported to the deep sea and remove in sedimentary record, the biggest reservoir of carbon. These mechanisms are called "carbon pumps" and can be divided into a physical and two biological pumps. The physical one, called "solubility pump" is based on the fact that colder waters of the bottom can hold more CO_2 at equilibrium with the atmosphere. The solubility pump accounts for approximately one-third of the total carbon exported to the sea bottom (Passow & Carlson 2012). The two biological ones are often called the "organic carbon pump" and the "carbonate pump" because the former refers to the sinking of particulate organic carbon (POC) from the surface ocean and the latter to the sinking and dissolution, in deep waters, of $CaCO_3$ particles. Together, they account for the other two thirds of the carbon exported to the sea-bottom, with the organic carbon pump exporting about 10 times more carbon than the carbonate pump (Sarmiento et al. 2002).

Coccolithophores contribute to the two biological carbon pumps by producing particulate inorganic carbon (PIC, i.e.: $CaCO_3$) through calcification and by producing POC via photosynthesis. Moreover, coccolithophore $CaCO_3$ can enhance sinking velocities of biogenic organic aggregates up to 100% (Ziveri et al. 2007, Lombard et al. 2013) and thus, even if coccolithophores are small phytoplankton whose cells might not contribute as much as larger phytoplankton cells to the POC sinking, their shells contribute greatly through the ballasting effect.

Coccolithophores are a main producer of dimethylsulphoniopropionate (DMSP), and have some of the higher cellular quotas found in phytoplankton (Keller 1989). DMSP can be converted into the volatile gas dimethylsulphide (DMS). The latter may form aerosol particles and contribute to clouds nucleation (Franklin et al. 2010), thus, scattering incoming radiation back into space and diminishing the greenhouse effect.

1.2.3 Coccolithophore responses to Ocean Acidification and P limitation

Under enhanced pCO_2, photosynthesis, and likely particulate organic carbon (POC) production are thought to be stimulated in species with poorly efficient carbon

concentration mechanisms, such as coccolithophores, were photosynthesis is not saturated at present pCO_2 (Paasche 1964, Buitenhuis et al. 1999, Rost et al. 2003, 2008, Bach et al. 2013). Observations from culture experiments showed that this statement cannot be generalized. On the other hand, it is clear that low PO_4^{3-} concentration limits coccolithophore growth whether by reducing exponential (i.e.: maximal) growth rate or by reducing the time cells can divide at maximum rate. For instance, a [PO_4^{3-}] of 0.009 ± 0.007 μmol L^{-1} limited coccolithophore growth in the eastern Mediterranean Sea (Kress et al. 2005). How the interaction of these two factors can act upon coccolithophore growth is still an open question. The available data suggest that under P limitation *E. huxleyi* cells can maintain its growth rate when passing from ~360 to 2000 μatm pCO_2 (Leonardos & Geider 2005) and at lower pCO_2 levels (Borchard et al. 2011, Engel et al. 2014). In the third Chapter of this work, the same aspect is analyzed for a strain isolated from the Mediterranean Sea.

While ocean acidification is expected to disrupt calcification (PIC production) through either the decrease in pH or the increase in CO_2 (Langer and Bode 2011, Bach et al. 2012), P limitation was suggested to enhance calcification (Paasche & Brubak 1994, Paasche 1998). It has been hypothesized that coccolithophores may increase their calcification rates when nutrients become limited. This could be related to calcification generating protons that can be used in exchange for nutrient ions (McConnaughey & Whelan 1997) or to the reduction of cytosolic free Ca^{+} ions that otherwise could precipitate PO_4^{3-} (Degens & Ittekkot 1986). Would that mean that the detrimental effects of enhanced pCO_2 on calcification would be attenuated in P poor waters? Current evidence suggest that the answer to this question is no. For instance, PIC production in two chemostat experiments running under low [P] decreased at the highest pCO_2 level tested (900 μatm) (Borchard et al. 2011) or did not change within the rage 180 to 750 μatm (Engel et al. 2014). These observations point towards a stronger effect of pCO_2 on calcification. This inference tallies well with recent results of P-limitation culture experiments showing that P-limitation does not lead to an increase in calcification rate (Langer et al 2012, 2013, Gerecht et al. 2015).

How the uptake of PO_4^{3-} may be affected by the combination of ocean acidification and P limitation is not obvious. Clearly, particulate organic phosphorus production (POPp) is expected to decrease with P limitation. However, in relation to ocean acidification this response is less clear. It has been hypothesized (Beardall & Giordano 2002) that increased pCO_2 reduces the need for carbon concentrating mechanisms (CCMs) which consume P, and in turn, it reduces the stress caused by nutrient limitation. So far, the experimental evidence to support or reject this hypothesis in the case of coccolithophores is not conclusive. So far, the results of two studies can be compared: In the study of Borchard et al. (2011) decreased POP quotas coupled with increased yield cell densities may indicate less stress from P limitation when the cells are exposed to the combination of P limitation and ocean acidification. This is consisted with the abovementioned hypothesis. On the other hand, in the study of Rouco et al. (2013) the combination of the two environmental factors caused no change in POP quotas. However, no data on maximum cell densities or growth rate is available which makes it difficult to estimate whether the stress caused by P limitation was reduced or not.

Coccolith morphology, which might be more instrumental in evolutionary success of coccolithophores than calcification rate (Langer et al. 2011), has been suggested to change due to ocean acidification, mostly by producing thinner coccoliths (Cubillos et al. 2007, Triantaphyllou et al. 2010, Beaufort et al. 2011, Meier et al. 2014) or by increasing the number of malformed coccoliths in culture experiments (Riebesell 2004, Langer et al. 2006, 2009, Rickaby et al. 2010, Bach et al. 2011) and in the field (Meier et al. 2014). PO_4^{3-} limitation has also been suggested to cause malformations (Okada & Honjo 1975, Kleijne 1990, Young & Westbroek 1991). Does that mean that high pCO_2 and low PO_4^{3-} will synergistically hamper coccolith morphogenesis? The question remains open.

Among coccolithophores, species-specific sensitivities of calcification rate and coccolith morphology to ocean acidification exist (Langer et al., 2006). Even further, coccolithophore species have different growth strategies (i.e.: specialized *vs* opportunistic; as exposed in section 1.2.1). These differences could affect the species distribution, assemblage composition and in turn, the biogeochemical contribution of coccolithophores to the different element cycles. Coccolithophore assemblage composition changes due to pH, in the North Sea and the Atlantic Ocean (Charalampopoulou et al. 2011). Experimental

manipulation of the seawater carbonate chemistry during mesocosm studies focused on *E. huxleyi* and little is known about how the coccolithophore community could respond to ocean acidification. All these experiments have been performed in eutrophic conditions or with nutrient additions and thus, nothing is known on how the coccolithophore community could respond to ocean acidification in a P limitation environment.

1.3 Research questions

In view of the predicted decrease in PO_4^{3-} concentrations (see section 1.1) three general questions are addressed in Chapter 2:

1) Can phosphorus limitation decrease *E. huxleyi* populations and affect their contribution to biogeochemical cycles?
2) Does phosphorus limitation affect the morphogenesis of coccoliths?
3) Are the strains isolated in P poor waters more resilient to P-limitation than strains isolated in areas with higher [P]?

Considering the combination of P limitation and ocean acidification, this work addresses (in Chapter 3) the following questions:

1) Will seawater acidification affect *E. huxleyi* population growth in P poor areas?
2) In P poor areas of the ocean, will seawater acidification affect the morphogenesis of *E. huxleyi* coccoliths?

Regarding the mesocosm carbonate chemistry manipulations performed to study the effects of ocean acidification on the phytoplankton community in an oligotrophic region (Chapter 4), the questions are:

1) Would coccolithophore growth still be enhanced by elevated pCO_2 under oligotrophic (i.e.: P poor) conditions? If so, would this lead to a dominance of coccolithophores over other phytoplankton groups?
2) Will community responses to elevated pCO_2 change depending on the initial coccolithophore assemblage? I compare the summer (Bay of Calvi, France) and the winter-spring (Bay of Villefranche-sur-Mer, France).
3) Will seawater acidification affect the coccolith morphogenesis of natural populations of *E. huxleyi* living in P poor waters?

Regarding the distribution of coccolithophores along natural environmental gradients (Chapter 5):

1) Is there any relationship between the coccolithophore species distribution and the carbonate chemistry or [PO_4^{3-}] of sea water?

1.4 The Mediterranean Sea: an ideal place for testing the effects of ocean acidification under P limitation conditions

The semi-enclosed Mediterranean Sea is an ideal place for exploring the questions posed in section 1.3 because:

1.4.1 The Mediterranean Sea features a strong gradient in PO_4^{3-} concentration

Due to its anti-estuarine circulation, nutrients are washed away towards the Atlantic Ocean. This generates a meso- to oligotrophic status in the western basin and an ultra-oligotrophic status in the eastern basin, with a gradient in PO_4^{3-} that goes from 0.05± 0.05µM in the west (Moutin & Raimbault 2002) to below detection limit in the east (≤ 0.01 µM, Krom et al. 1991, Moutin & Raimbault 2002). The later concentrations are considered among the lowest worldwide (Dugdale and Wilkerson, 1988). These conditions are maintained by the geological features of the sea, where the Sicilian Strait prevents deep-water exchange between the two basins.

In more detail: macro-nutrients mainly enter the Mediterranean Sea by river and groundwater discharges, atmospheric deposition and, in a lower extent, exchanges through the Straits of Gibraltar and of Bosphorus [The MerMex group (2011) and ref. therein). In the western Mediterranean, the more energetic air–sea exchanges and convection are believed to induce a more effective nutrient refueling of the euphotic zone than in the eastern basin where thermal stratification increases (The MerMex group 2011). Additionally, a part of the nutrients that are regenerated in the eastern basin are exported to the western basin by deep waters crossing the Sicily Channel (Béthoux et al. 1998, Schroeder et al. 2010). The western basin also exports nutrients via its intermediate water flow towards the Atlantic Ocean (Béthoux et al. 1998). In this thesis the PO_4^{3-} gradient that characterizes the Mediterranean Sea has been used to: 1) test whether *E. huxleyi*

ecogenotypes are established upon environmental phosphate availability in the selected strains, and 2) to sample different coccolithophore assemblages along an east to west transect in this sea and explore the relationship between the observed patterns and [PO_4^{3-}].

1.4.2 The Mediterranean Sea can buffer more atmospheric CO_2 than most oceans

The Mediterranean Sea is characterized by high alkalinity levels with a west to east increasing gradient that can be explained by the progressive evaporation and thus, increasing salinity, of the surface waters that flow west to east, as well as from the Black Sea inflow (Schneider et al. 2007). Together with river discharges, this constitutes the main contribution to total alkalinity (Schneider et al. 2007). The high alkalinity together with the active overturning circulation cells (Lee et al. 2011), permits to buffer more CO_2 than other oceans. In consequence, the water column inventory of anthropogenic CO_2 in the Mediterranean Sea is considerably higher than that for the Atlantic and the Pacific Oceans in the same latitude band, and higher than the actively ventilating East/Japan Sea (Schneider et al. 2010, Lee et al. 2011). Anthropogenic CO_2 is found throughout the entire water column of the Mediterranean Sea (Schneider et al. 2010).

An increasing west to east gradient exists for pCO_2 during all seasons (D'Ortenzio et al. 2008, Taillandier et al. 2012). Based on modelled satellite-data of the upper-mixed layer, these two studies locate minimum pCO_2 values in the Alboran Sea and maximum in the northern Ionian Sea and Levantine basin. Accordingly, the western basin acts as a sink for atmospheric CO_2 while the eastern acts as a source. Taillandier et al. (2012) further compared the periods 1979-1983 with the period 1998-2001 and showed that the western basin atmospheric CO_2 sink increased, whereas the eastern basin CO_2 source to the atmosphere weakened. Even further, the Mediterranean Sea as a whole, had apparently passed from acting as a net CO_2 source to the atmosphere in the1980s to be close to equilibrium with the atmosphere in the 2000s (slight sink of about 0.2 Gt C y^{-1}).

An estimate by Touratier and Goyet (2011) indicates that all water masses in the Mediterranean Sea are already acidified (0.14 to 0.05 pH unit). When compared to the typical value of 0.1 for the surface waters of the world ocean, the Mediterranean Sea

appears to be one of the regions that are the most impacted by acidification (The MerMex group 2011).

1.4.3 Coccolithophores are conspicuous in the Mediterranean Sea

Finally, coccolithophores are conspicuous all along the Mediterranean Sea (Knappertsbusch 1993, Ignatiades et al. 2009), and in its coastal waters (Dimiza et al. 2008, Garrido et al. 2014), which ensures sampling material for the field-based studies. Even further, coccolithophores contribution to the biogeochemsty of the Sea is important, especially in the eastern basin. Here these algae are the main contributor of biogenic $CaCO_3$ precipitation throughout the year (Knappertsbusch 1993, Ziveri et al. 2000, Malinverno 2003) and possibly explain high organic matter fluxes in the Ionian Sea through its ballasting effect (Malinverno et al. 2014).

Chapter 2.

Effect of phosphorus limitation on coccolith morphology and element ratios in mediterranean strains of the coccolithophore *Emiliania huxleyi*.

Published as: Oviedo AM, Langer G, Ziveri P (2014) Effect of phosphorus limitation on coccolith morphology and element ratios in Mediterranean strains of the coccolithophore *Emiliania huxleyi*. J Exp Mar Biol Ecol 459:105–113

Abstract

Six *Emiliania huxleyi* strains isolated in the Mediterranean Sea were grown under phosphorus limitation and replete (control) conditions in batch culture. We tested the hypothesis that increasing phosphorus limitation, resulting from ocean warming, will affect coccolithophores and change their contribution to the PIC:POC ratios. Four strains were isolated in the oligotrophic Algerian basin (western Mediterranean), and two strains in the extremely oligotrophic and often phosphorus depleted Levantine basin (eastern Mediterranean). Samples for particulate inorganic carbon, PIC; particulate organic carbon, POC; particulate organic phosphorus, POP; and total particulate nitrogen, TPN, were taken at equal cell densities in phosphorus limited and control culture conditions (harvesting in exponential and stationary phases respectively). Different morphological features of coccoliths were analyzed. Phosphorus limitation was inferred from: 1. a decrease in growth rate between 22% and 34% compared to phosphorus replete cultures; 2. a reduction in final cell density from ca. 2×10^6 cells/ml to ca. 8×10^4 cells/ml, and 3. markedly lower POP quotas of the limited cells. Differences in the phosphate uptake machinery are suggested based on the fact that three western Mediterranean strains decreased the phosphate concentration in the culture media until the detection limit in the first 3 experimental days

while 4–5 days were necessary for the other strains. Cellular carbon quotas increased in all strains under phosphorus limitation in comparison to their respective control cultures. The increase in POC quotas ranged between 179% and 260% and in PIC quotas between 43% and 201%. TPN quotas increased under phosphorus limitation between 31% and 86% in five out of six strains. POC:TPN increased in all strains, which suggests a change in the molecular composition of the cells when exposed to phosphorus limitation. Strain specific responses were also observed in the PIC:POC ratio, which decreased in five strains and did not change in another. Phosphorus limitation did not lead to malformations. However, morphological changes of coccoliths occurred, also in a strain specific way, namely the percentage of over-calcified coccoliths was altered by P limitation, but we observed all signs in the responses among different strains. Nevertheless, this morphological feature does not reflect the changes in calcite production (PICp nor PIC:POC). Strain specific responses were not related to the isolation location, suggesting that the isolated western and eastern strains do not represent distinct eco-genotypes featuring different phosphorus usage strategies.

2.1 Introduction

Coccolithophores (Haptophyta) are unicellular calcifying phytoplankton producing a shell comprised of calcareous plates, so called coccoliths. Coccolithophores are one of the most abundant phytoplankton, contributing ca. 10% to total global phytoplankton biomass (Tyrrell & Young 2009). *Emiliania huxleyi* (Lohmann 1902) Hay & Mohler in Hay et al. (1967) is among the most common bloom forming species (Brand 1994) and the most abundant coccolithophore in the modern oceans (Paasche 2002). This species is present in conspicuous numbers in both the western and the eastern Mediterranean (Knappertsbusch 1993, Malinverno et al. 2003). Coccolithophores play an important role in the carbon cycle, influencing the carbonate system of seawater by two types of effects: a production-effect and an export-effect. The former is brought about by the immediate effect of the CO_2 consumption (through photosynthesis, resulting in particulate organic carbon, POC, production) and CO_3^{2-} consumption (through calcification, resulting in particulate inorganic carbon, PIC, production). The export-effect rests on the ratio of calcite to organic carbon which sinks to depth (the so called rain-ratio). The sinking to depth of calcite, as opposed to organic material, substantially increases the portion of carbon which gets buried in the sediments and therefore potentially enters geological cycles (Klaas & Archer

2002, Van Cappellen 2003, Ziveri et al. 2007). Hence, a higher PIC:POC ratio of coccolithophores increases the probability of long term carbon burial. Apart from this biogeochemical role, coccolithophore calcite (i.e. coccoliths) probably has significance for the organism and its ecological/evolutionary success (Henriksen et al. 2003, Langer et al. 2011), although coccolith function remains unknown (Brownlee & Taylor 2004, Young 1994). The morphology of coccoliths is immensely sophisticated and its morphogenesis is known to be susceptible to environmental disturbances (e.g. Bach et al. 2012; Langer et al. 2006, 2010, 2011). It was hypothesized that macronutrient (nitrogen, N, and phosphorus, P) limitation represents an important disturbance resulting in the malformation of coccoliths (Okada & Honjo 1975, Kleijne 1990, Young & Westbroek 1991). In the future, the supply of nutrients (i.e. P and N) to the euphotic layer is predicted to decrease due to climate change induced stratification of surface waters (Behrenfeld et al. 2006, Bopp et al. 2013) and changes in ocean mixing and ventilation (Bopp et al. 2013). This poses two general questions: first, will P limitation affect the morphogenesis of coccoliths? Second, will P limitation alter coccolithophore cellular carbon quotas and therefore its contribution to overall PIC:POC of sinking matter? A particular aspect that can be used for testing the first question is the occurrence of malformed coccoliths. Using data from a mesocosm experiment, Båtvik et al. (1997) suggested that P limitation might lead to an increase in the percentage of malformed coccoliths in E. huxleyi. However, differences between treatments were lower than 8% and no associated error is shown. Paasche (1998), in a culture experiment, found little evidence to support the conclusion that nutrient limitation induces malformations. The selection of different genotypes can be a serious obstacle in finding a generic answer because strain-specific responses might occur. The latter were discovered with regard to salinity change (Brand 1984) and to change in carbonate chemistry of seawater (Langer et al. 2009, 2011). The reason for strain specific responses is a matter of current debate and a prevailing notion is that the particular environmental conditions the strains experienced in their natural habitat has shaped their response patterns with respect to changes in environmental parameters. This notion certainly fits the observation of Brand (1984) that coastal strains of *E. huxleyi* are more tolerant to salinity changes than open ocean strains. However, no relationship between the response patterns of different strains to carbonate chemistry changes and the particular carbonate chemistry of the sites of strain isolation could be observed (Langer et al. 2009, 2011). In the case of P limitation, the Mediterranean Sea provides an ideal testing ground for the hypothesis that

strain-specific responses can be traced back to features of the location of strain isolation. In the Mediterranean Sea, the average P concentration decreases from mesotrophic to extremely oligotrophic along a west–east gradient (Krom et al. 1991). Phosphorus concentrations in the Eastern basin are often below detection limit (<0.01 μM, Krom et al. 1991; Moutin & Raimbault 2002) and among the lowest worldwide (Dugdale & Wilkerson 1988). In the eastern Mediterranean, coccolithophores have been shown to be P limited (Kress et al. 2005). Similar data do not exist for the western Mediterranean. However, given the relatively higher nutrient concentrations in the western Mediterranean compared to the Eastern basin, it can be hypothesized that strains isolated in the Eastern basin are more resilient to P limitation than strains isolated in the Western basin. We compare two strains of *E. huxleyi* isolated in the Eastern basin to four strains isolated in the Western basin. Regarding the second general question posed above, namely will P limitation alter coccolithophore contribution to PIC:POC ratios of sinking matter?, different results have been observed. Borchard et al. (2011) and Langer et al. (2012a) using culture strains of E. huxleyi and *Calcidiscus leptoporus* (Murray and Blackman 1898) Loeblich and Tappan (1978) respectively, found no change in PIC:POC ratios under P-limitation, while in three other studies using *E. huxleyi* an increase of the PIC:POC ratio was reported in response to P limitation (Paasche & Brubak 1994, Paasche 1998, Riegman et al. 2000). These disparate results could stem from strain-specific responses, because different strains were used. On the whole, a direct comparison of the responses of different *E. huxleyi* strains to P limitation is obviously needed.

2.2 Methods

2.2.1 Strain selection

E. huxleyi strains were obtained from the Roscoff culture collection, isolated from the BOUM cruise in September 2008. We selected 2 strains from the Levantine basin in the eastern Mediterranean (33°37′N, 32°39′E): RCC1813 and RCC1817, and 4 strains from the south-western Mediterranean (39°6′N, 5°21′E): RCC1827, RCC1830, RCC1833 and RCC1812. Additional information about the strains can be found at: http://www.sb-roscoff.fr/Phyto/RCC/index.php?option=com_dbquery&Itemid=24.

2.2.2 Batch cultures

Six culture strains were grown under P limited and repleted (control) conditions in triplicate. Cultures developed in 2.3 l glass bottles and incubated in a climate cabinet (Rubarth Apparate GmbH, Germany) at 20 °C culture media consisted of 64% artificial seawater, ASW, (modified from Kester et al. 1967) and 36% natural North Sea seawater. Nutrients followed F/2 concentrations (Guillard & Ryther 1962), except for the no addition of P in the limited cultures. All culture media were then sterile-filtered through a 0.2 μm pore size cartridge.

Pre-experiments were done using 2 strains (RCC1813 and RCC1827) to test for the ideal initial P concentration which allowed for a cell density of ca. 1×10^5 cells/ml at stationary phase, later used in the experiments for P limitation treatments. This cell density provided sufficient sampling material for the selected analyses and prevented large changes in the culture media carbonate chemistry. P concentrations tested in the pre-experiments were: 0 μM (below detection limits), 0.14 μM, 0.35 μM, 0.50 μM and 35.18 μM. These concentrations were both, assumed from the performed dilutions as well as measured; the data presented here is the measured. During the experiment, all strains were grown at 0.2 μM for P limitation cultures and 35.0 μM [P] for control cultures.

Cell density at inoculation was 400 cells/ml. Limited cultures were sampled in stationary phase at ca. 1×10^5 cells/ml. Controls for each strain were harvested during the exponential phase, at the same cell density yielded by the respective limited culture. A small volume of each control was grown until the maximum yield to prove absence of limitation. Cell density and size were monitored daily (Multisizer III Coulter counter). Growth rates were calculated from exponential regression up to and including harvest day. Averages of triplicates and SD were used in tables and figures. Nutrients (PO_4^{3-} and NO_3^-) were also monitored on a daily basis using an Autoanalyzer Evolution III (Alliance Instruments) with detection limits of 0.1 μM for PO_4^{3-} and 0.3 μM for NO_3^-.

2.2.3. Carbonate chemistry

Alkalinity samples were filtered (Whatman GFF filter, 0.6 μm pore size), stored in 300ml borosilicate flasks at 4 °C, and measured in duplicate by potentiometric titration. Total alkalinity was calculated from linear Gran plots (Gran 1952). DIC samples were sterile-

filtered (0.2 μm pore size cellulose-acetate syringe filters) and stored in 13 ml borosilicate flasks free of head space and stored at 4 °C for 1 to 4 weeks until they were measured, in triplicate, using a Shimadzu TOC 5050A. The carbonate system was calculated from alkalinity, pH, PO_4^{3-}, and temperature, using the program CO2SYS (Lewis & Wallace 1998). Equilibrium constants of Mehrbach et al. (1973) refitted by Dickson & Millero (1987) were chosen.

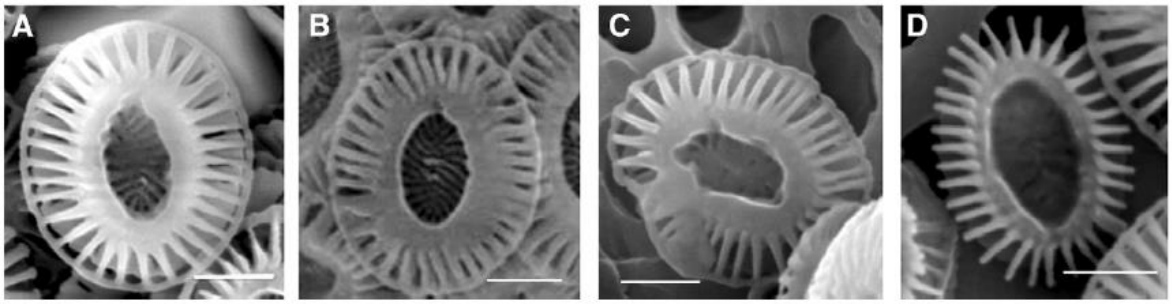

Figure 2.1. Example micrographs of the different coccolith classes: A. normally developed coccolith, B. normally developed but over-calcified coccolith, C. malformed coccolith (note the asymmetrical distal shield elements, shorter on the down-left side of the image and the deformed external rim) and D. incomplete coccolith (external rim missing). Scale bars represent 1 μm.

2.2.4. Coccolith morphology and coccosphere size

25 ml of culture was filtered onto polycarbonate filters (Sartorius, 0.25 μm) and dried at 60°C for 24 h. A piece of each filter was placed on aluminum stubs and sputter coated using a EMITECH K550X. Imaging was performed in a JEOL JSM 6300 SEM. At least 300 coccoliths per sample (Langer & Benner 2009) were analyzed (distal shield) and classified using captured images into: normal (inner tube circle, external rim and all distal shield elements were well formed and the latter were of the same size and symmetrically distributed around the inner tube circle); malformed (when two or more distal shield elements were asymmetrical) or incomplete coccoliths (when the external rim was not formed or only the inner tube circle was present). Normal coccoliths were sub-classified in over-calcified (when distal shield elements were thicker to the point that half or more were fused, usually but not always the inner tube circle was also thicker), and normally calcified coccoliths (when individual distal shield elements clearly displayed the space between them). Examples are given in Fig. 2.1. Although subjective by nature, our analysis of coccolithophore morphology provides robust, unbiased results which tally well with an objective biometrical classification (Bach et al. 2012; Langer et al. 2012b). Coccosphere

size was recorded from the Multisizer III Coulter counter data and from the same SEM images used to count and classify single coccoliths, in this case ca. 100 complete coccospheres per sample were measured (diameter) using the program GIMP v2.6. The two size data sets were compared.

2.2.5. Particulate organic and inorganic carbon and particulate nitrogen

Samples for total particulate carbon, TPC; total particulate nitrogen, TPN; POC and particulate organic phosphorus, POP, were filtered onto pre-combusted (500 °C; 12 h) GFF filters and placed in pre-combusted petri dishes (500 °C; 12 h). TPC and POC samples were then oven dried (60°C overnight) and stored until analysis at −20 °C. Before analysis, POC filters were treated with 230 µl of HCl (0.1M) to remove the inorganic carbon and oven-dried again. TPC, POC, and TPN were then measured on a Euro EA Analyzer (EuroVector). PIC was calculated as the difference between TPC and POC. Filters for POP were stored at −20 °C until analysis. Right before the analysis the samples were oven-dried for an hour, dissolved in a mixture of 35 ml Milli-q water and potassium peroxide and autoclaved (120 °C, 30 min) and left overnight in the autoclave. Samples were centrifuged after the addition of ascorbic acid and a mixture of reagents (sulphuric acid, ammonium heptamolybdate-tetrahydrate, potassium antimonyl-tartrate and distilled water). The absorbance of the resuspended samples was measured at 882 nm by colorimetric analysis of dissolved PO4 3− (Hansen & Koroleff 1999). Production of PIC, POC and POP was estimated from cellular inorganic and organic carbon contents and population growth rates according to the following equations.

PIC production = (PIC/cell)µ

POC production = (POC/cell)µ

POP production = (POP/cell)µ

where µ is the growth rate calculated from the growth curve until harvest day.

2.2.6. Statistics

Differences between the control and P limited cultures in each strain were assessed by ANOVA ($\alpha = 0.05$). Coccolith morphology data was transformed ($\log_{10}X$) to achieve a normal distribution of frequencies. Differences between coccosphere size by Coulter counter and by SEM measurements were assessed by T test.

2.3. Results

2.3.1. Population growth

Already in the pre-experiments (growing two strains at different P concentrations), differences were evident between the two strains: the eastern strain RCC1813 did not grow when no P was added while RCC1827 did (Fig. 2.2). During the experiment (six strains growing under P limited and control condition), [P] in the culture media decreased concomitantly with the increase in cell densities (Fig. 2.3). P limited cultures reached the stationary phase after 7 or 8 days in culture, depending on the strain. Control cultures reached similar cell densities at day 5 or 6. The stationary phase in control cultures was reached after 9 to 12 days. Limitation was evident by 1: a decrease in growth rate between 22% (RCC1817) to 37% (RCC1830), from 0.99–1.23 d^{-1} in controls to 0.66–0.82 d^{-1} in limited cultures (Table 2.1); 2: a reduction in final cell density from ca. 1.6 $\times 10^6$ – 2.0 x 10^6 cells/ml in controls to ca. 8 × 10^4 –1 × 10^5 cells/ml in P limited cultures (Fig. 2.3) and 3: up to 88% lower POP quotas in relation to controls (Table 2.1). All P limited cultures consumed the available P by the end of the experiment. However, the two eastern strains RCC1813 and RCC1817 took 5 days to reach the detection limit of the measurements, the western RCC1812 strain took 4 days and the other western strains took 3 days. In control cultures, [P] decreased from 35 μM to ≈17–23 μM in all strains but RCC1813. For the latter strain [P] in the culture media decreased until ≈10 μM (Fig. 2.3).

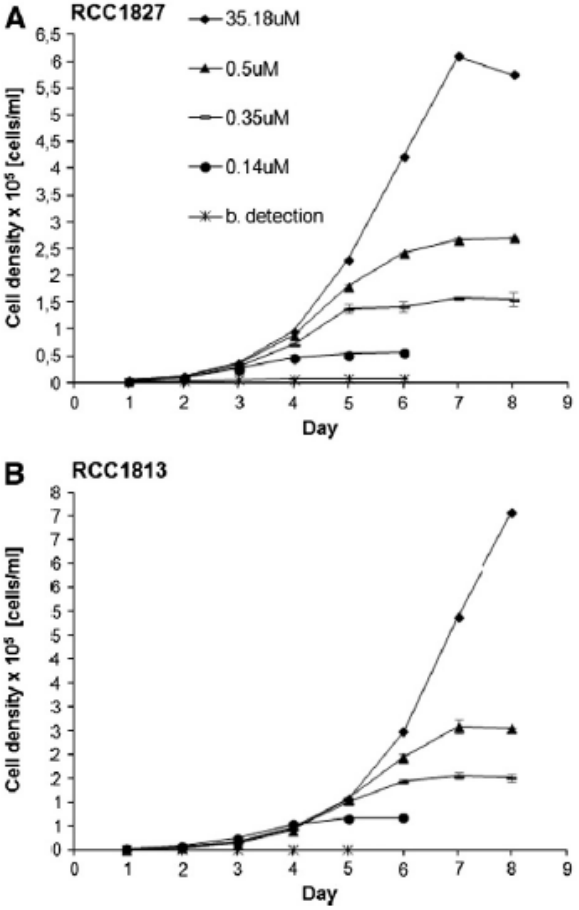

Figure 2.2 Cell densities at different [P] in the culture media during the pre-experiment. The lowest point was assumed to completely lack P, and the measurement was under detection limit (B. detection).

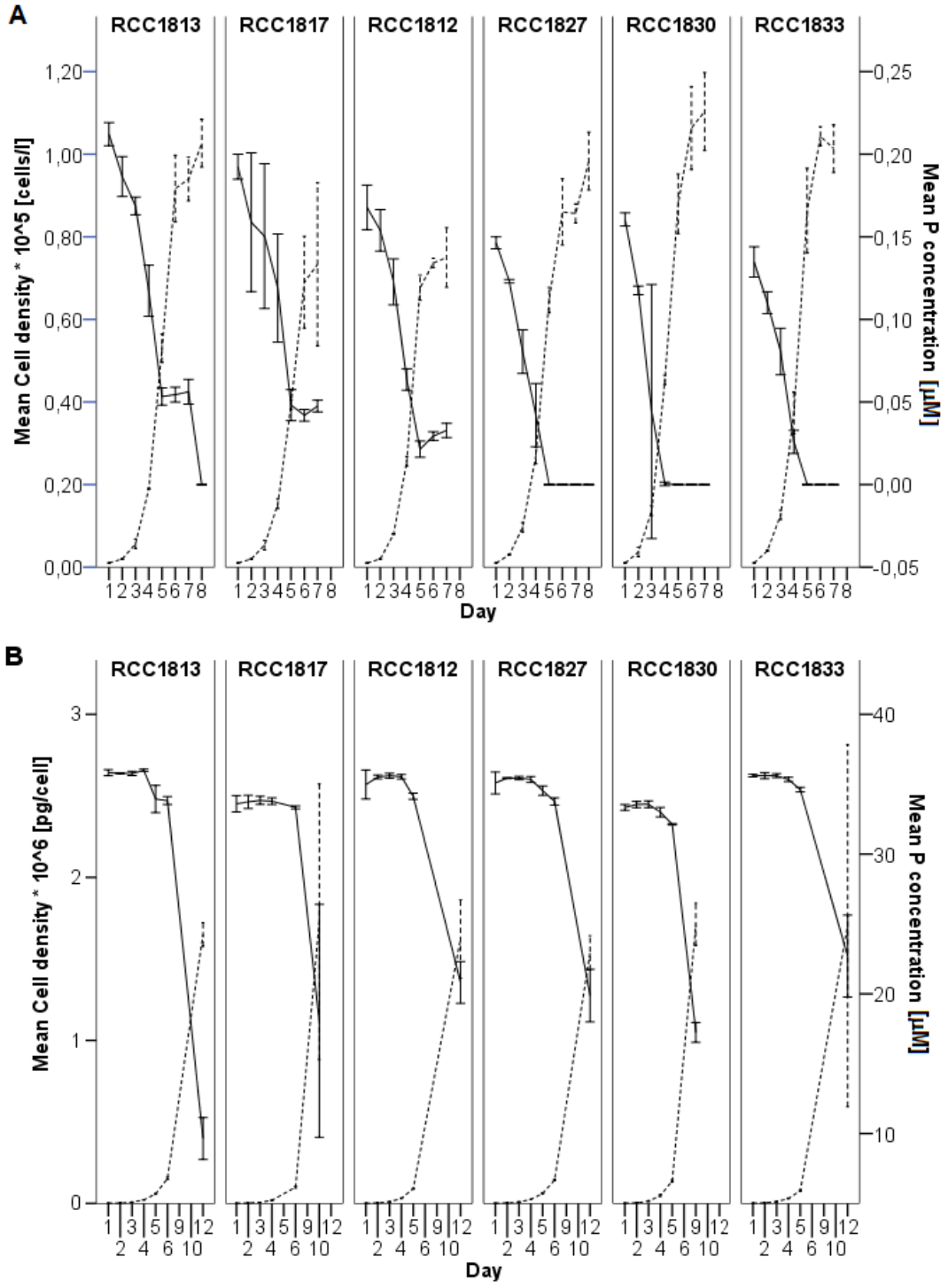

Figure 2.3 Mean cell density (dotted line) and [P] in the culture media (solid line), during the experiment. A, shows the data from the P limited cultures, until harvest day and B, the data from control cultures, which extents, beyond harvest day, until stationary phase (at day 9 to 12 depending on the strain). The first two strains at the left were isolated in the eastern Mediterranean Sea, while the others were isolated in the western Mediterranean.

Table 2.1 Elemental quotas and coccosphere size at harvest day, population growth rate and calculated elemental production, under phosphorus limited and control conditions.

	Eastern Mediterranean strains				Western Mediterranean strains							
	RCC1813		RCC1817		RCC1812		RCC1827		RCC1830		RCC1833	
	P limited	Control	P limited	Control	P limited	Control	P limited	Control	P limited	Control	P limited	Control
Growth rate (μ)	0.76	1.04	0.82	1.05	0.80	1.13	0.66	0.99	0.81	1.23	0.75	1.02
Standard deviation	0.01	0.01	0.02	0.02	0.01	0.01	0.00	0.01	0.02	0.03	0.01	0.00
PIC (pg/cell)	23.85	7.96	20.13	9.69	26.71	15.48	23.81	9.95	17.54	12.35	24.08	10.52
Standard deviation	0.75	0.51	2.95	0.49	0.29	0.15	0.65	0.05	1.43	0.63	0.88	0.32
POC (pg/cell)	23.47	8.41	30.08	8.44	35.38	11.51	24.31	7.94	32.36	10.54	22.22	7.84
Standard deviation	0.98	0.30	1.06	0.10	1.56	0.40	0.41	0.24	1.60	0.31	2.23	0.20
PON (pg/cell)	3.50	1.95	3.02	1.70	3.73	2.85	3.66	2.29	3.15	2.12	2.81	2.42
Standard deviation	0.09	0.10	0.54	0.46	0.20	0.05	0.05	0.06	0.10	0.11	0.12	0.14
POP (pg/cell)	0.02	0.09	0.02	0.17	0.03	0.12	0.02	0.09	0.01	0.09	0.02	0.08
Standard deviation	0.00	0.00	0.00	0.01	0.00	0.00	0.00	0.00	0.00	0.00	0.00	0.00
PIC:POC	1.02	0.95	0.67	1.15	0.76	1.35	0.98	1.25	0.54	1.17	1.09	1.34
Standard deviation	0.06	0.09	0.07	0.04	0.03	0.04	0.02	0.04	0.03	0.03	0.10	0.07
Coccosphere size[a] (μm)	5.95	4.11	5.71	4.37	5.26	4.35	5.82	4.44	6.46	5.21	5.52	4.40
Standard deviation	0.05	0.07	0.09	0.05	0.03	0.13	0.03	0.05	0.04	0.09	0.09	0.06
Coccosphere size[b] (μm)	6.90	5.47	6.35	5.39	6.24	5.86	6.62	5.71	7.13	5.80	6.44	5.81
Standard deviation	0.17	0.09	0.22	0.04	0.08	0.09	0.18	0.05	0.18	0.04	0.60	0.21

[a] Data from Multisizer III Coulter.
[b] Data from SEM images.

Changes in TA or DIC between the initial and final carbonate chemistry were close or smaller than 10% under replete conditions and roughly 20% under limitation (Supplementary material). The difference in TA between P limited cultures and controls at the end of the experiment ranged between 9% (RCC1813) and 15% (RCC1833).

2.3.2. Coccolith morphology and coccosphere size

P limitation did not cause malformations. In fact, in 4 strains the percentage of malformed coccoliths slightly decreased (F from 11.11 to 80.73, p = 0.05) and in RCC1817 and RCC1833 it did not change (F =0.50, p = 0.552 and F = 1.19, p = 0.332 respectively) (Table 2.2). We do not take this to mean that P limitation is beneficial for coccolith morphogenesis, though. The percentage of incomplete coccoliths increased in one strain (RCC1827, F = 23.66, p = 0.008), and it did not change significantly in the other 5 strains. The percentage of normal developed but over-calcified coccoliths increased significantly in RCC1827 (F =9.41, p = 0.037) and in RCC1830 (F = 9.05, p = 0.040); it decreased in RCC1833 (F= 17.22, p= 0.014) and it did not change in the others (F b 5.81, p N 0.05). Coccosphere diameter at harvest day was between 21% and 44% higher under P limitation according to Counter coulter data and ca. 21% according to the measurements from SEM images. For all samples, SEM derived sizes were between 0.6 and 1.5 μm larger (t=−15.94, p= 0.000).

Table 2.2 Percentage of coccoliths in the different morphological classes and standard deviation of triplicate incubations.

	Normally developed				Malformed	SD	Incomplete	SD
	Over calcified	SD	Normally calcified	SD				
RCC1813 control	11.7	8.7	40.2	8.6	22.1	3.4	26.1	4.6
RCC1813 P limited	28.3	9.2	34.2	6.4	14.7	1.4	22.9	2.6
RCC1817 control	26.6	20.9	53.7	20.6	14.8	0.7	4.9	0.3
RCC1817 P limited	41.9	9.6	36.0	13.8	13.7	2.9	8.4	3.4
RCC1812 control	28.8	9.9	36.1	10.5	32.1	2.6	2.9	1.4
RCC1812 P limited	50.4	9.2	25.0	9.1	19.4	1.1	5.1	2.5
RCC1827 control	34.8	3.8	20.1	2.2	42.7	2.7	2.4	0.4
RCC1827 P limited	49.0	7.0	18.5	2.0	26.7	6.3	5.8	1.6
RCC1830 control	46.3	9.8	22.8	7.5	23.3	4.0	7.6	3.9
RCC1830 P limited	65.4	5.0	15.8	2.7	10.5	0.9	8.2	3.7
RCC1833 control	42.9	14.0	44.4	12.3	8.1	0.8	4.7	1.3
RCC1833 P limited	8.6	2.9	80.3	1.8	7.2	1.1	4.0	2.5

2.3.3. Element quotas and ratios

POC and PIC per cell increased in all strains (F from 124.02 to 3594.92, $p < 0.05$ for POC and F from 33.20 to 3610.39, $p < 0.05$ for PIC); often, the increase in POC was up to 260% (Fig. 2.4). The increase in PIC per cell ranged between 43% and 201%. PIC:POC decreased between 19% and 54% relative to the control in five strains (F from 13.39 to 718.80, $p < 0.05$) and it did not change in RCC1813 ($F = 1.20$, $p = 0.335$) (Fig. 2.4). An increase in TPN between 31% and 86% was observed in five strains (F from 13.29 to 399.68, $p < 0.05$) while no change was observed in RCC1833 ($F = 4.43$, $p = 0.103$) (Fig. 2.5). POC:TPN and TPN:POP largely differed from Redfield ratios when cells were P limited. These ratios increased in all strains (F from 14.20 to 3909.05, $p < 0.05$) under P limitation (Fig. 2.5). POC production increased in all strains ($F > 88.69$, $p < 0.05$), while PIC production increased in 5 strains ($F > 28.74$, $p < 0.05$) and did not change in RCC1830 ($F = 1.16$, $p = 0.342$). TPN production increased in two of the tested strains RCC1813 and RCC1827 ($F = 120.42$, $p = 0.000$ and $F = 16.24$, $p = 0.16$ respectively) and did not change in the others (F between 0.25 and 5.02, $p > 0.05$).

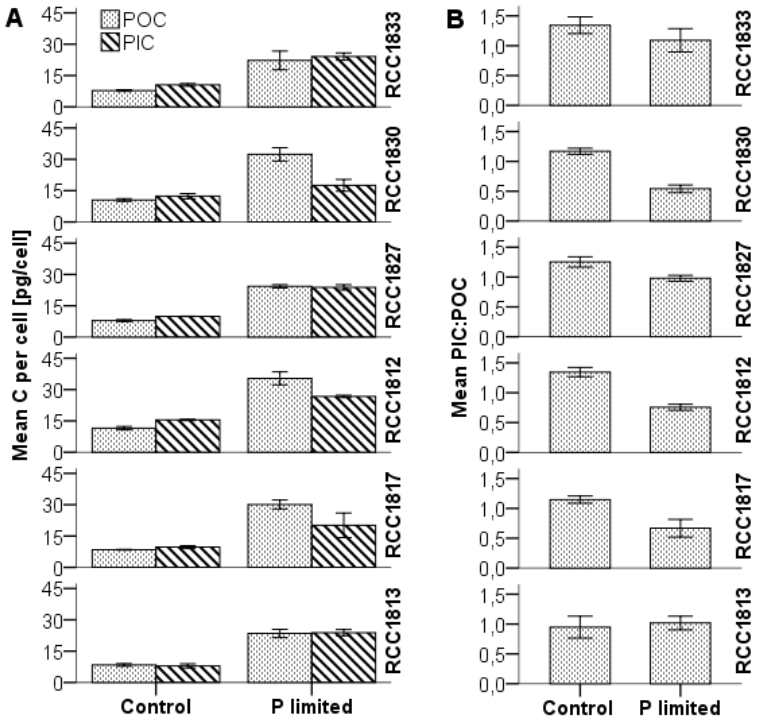

Figure 2.4 Mean POC and PIC quotas and B, mean PIC:POC ratio at harvest day under phosphorus limited and replete (control) conditions. Error bars represent the standard deviation. The first two strains from down to up were isolated in the eastern Mediterranean Sea, while the upper 4 strains were isolated in the western Mediterranean.

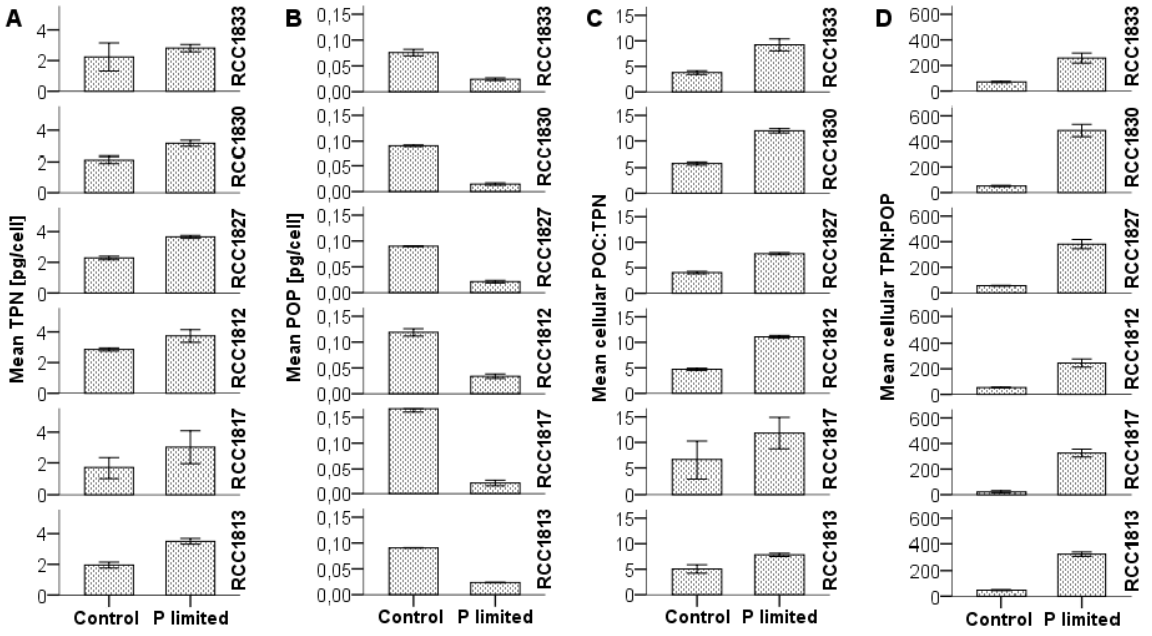

Figure 2.5 A, Mean TPN quotas; B, mean POP quotas; C, mean cellular POC:TPN ratio, and D, mean cellular TPN:POP ratio at harvest day under phosphorus limited and replete (control) conditions. Error bars represent the standard deviation. The first two strains from down to up were isolated in the eastern Mediterranean Sea, while the upper 4 strains were isolated in the western Mediterranean.

2.4. Discussion

2.4.1. Population growth

In the six *E. huxleyi* Mediterranean strains, the stationary phase was reached at markedly lower cell densities under P limitation than the one achieved under control conditions (Figs. 2.2 and 2.3). Final PO_4^{3-} concentrations as well as the final cell densities differed in the tested strains (Fig. 2.3). The strains RCC1813, RCC1817 and RCC1812 took from 4 to 5 days to draw down the PO_4^{3-} concentration under detection limits, while the other strains took 3 days (Fig. 2.3). RCC1817 and RCC1812 also displayed considerably lower final cell densities (ca. 80% of the average of the other four strains). Taken together, these two observations might indicate that both RCC1817 and RCC1812 are unable to use PO_4^{3-} as efficiently as the other strains. Interestingly, RCC1812was isolated in the western Mediterranean and RCC1817 in the Eastern basin, refuting the hypothesis that strains isolated in the Eastern basin are more resilient to P limitation (at least in terms PO_4^{3-} usage, we will discuss other data below). The latter inference is further supported by the pre-experiment data shown in Fig. 2.2. In this experiment different initial PO_4^{3-} concentrations were tested for two strains and we observed that the eastern RCC1813 did not grow when no PO_4^{3-} was added (only ASW) while the western RCC1827 did. Based on our data we cannot tell what the reason for the different PO_4^{3-} usage efficiencies is but the findings of Riegman et al. (2000), who observed two different types of alkaline phosphatase (PAse) kinetics under P limitation in *E. huxleyi* (one constitutively and the other inducible at low growth rates) might be suggestive in this context. It remains to be tested whether the observed differences in P usage efficiency are based on different PAse activities.

2.4.2. Coccolith morphology and coccosphere size

Coming back to the question whether P limitation will affect the morphogenesis of coccoliths in *E. huxleyi* (referred in Section 1) we start off with a discussion of malformations and test the possibility that eastern Mediterranean strains are more resilient to P limitation than western strains. Malformations indicate a disturbance of the coccolith shaping machinery (Young & Westbroek 1991, Langer et al. 2010) and it was argued that such a disturbance has negative consequences for coccolithophores in terms of evolution/ecology (Henriksen et al. 2003, Langer et al. 2011). Although malformations

occur more frequently in culture samples than in field samples (Langer et al. 2006, 2012b), they can be conspicuous in the field (Okada & Honjo 1975, Kleijne 1990). Based on field data the latter authors suggested macro-nutrient limitation to be the main cause for malformations and so did Young & Westbroek (1991) based on data obtained from cultures. However, the latter hypothesis could not be confirmed in a batch culture study using *C. leptoporus* (Langer et al. 2012a). Båtvik et al. (1997), contrarily, suggested that their mesocosm-derived *E. huxleyi* morphology data support the nutrient-hypothesis (Okada & Honjo 1975, Kleijne 1990). A closer inspection of their morphology data, however, reveals that the effect is so small that they cannot serve to support the notion of a detrimental effect of nutrient limitation.

In accordance with this re-interpretation of the Båtvik et al. (1997) data, Paasche (1998), in a thorough experimental study using *E. huxleyi*, found no evidence for an increase in malformations due to P limitation. Since the latter author used only one strain of calcifying *E. huxleyi*, the question remained whether other strains might have reacted differently. Our own data strongly suggest that this is unlikely, because we did not observe an increase in malformations due to P limitation in any of the six strains tested (Table 2.2). This observation, on the one hand, does not entail that there are no strains which show such an increase. On the other hand, it implies that a susceptibility of *E. huxleyi* morphology to P limitation is a rare phenomenon, if it exists at all. The term "insensitive morphogenesis" here specifically refers to the normal shaping (i.e. absence of tetratological malformation, Young & Westbroek 1991) of coccoliths. Taken together with the available data on *C. leptoporus* (Langer et al. 2012a), our data points to the notion that coccolithophore morphogenesis is insensitive to macro-nutrient limitation suggested by the latter authors.

Although coccoliths continued to be normal in shape, P limitation caused other morphological features to change. One of them was coccosphere size. We measured complete spheres by two ways: using the Multisizer III Coulter counter and measuring them from SEM images. In both cases, P limitation was observed to increase the size of coccospheres in five out of six strains ($F > 88.69$, $p < 0.05$ for both measurement types). However, SEM derived sizes were between 0.6 and 1.5 μm larger ($t=-15.94$, $p = 0.000$). We argue that this is due to the fact that the Coulter counter registers only the cell size and not the coccosphere size. The Coulter counter measures the change in resistance imposed

by the particles, on the assumption that these particles are non-conducting; which is not the case of calcite. It is possible that, in a coccosphere, the coccoliths arranged in different layers facilitate the penetration of electrolyte solution into the coccosphere. This layer of intricate coccoliths and spaces in between would then have a lower resistance than the cells. The coulter counter could possibly read this as background electrolyte solution. Instead, a single coccolith, solid in the proximal shield, might have a higher resistance than its surrounding electrolyte solution. Iglesias-Rodriguez et al. (2008) also found that Coulter counter coccosphere volume data were smaller when compared to flow cytometry derived data, they could not determine the cause for this difference. Comparing coulter counter with light microscope derived measurements or measuring the same culture with and without coccoliths, is needed to test this hypothesis.

Another morphological feature that changed with P limitation is coccolith over-calcification (see Section 2.4 for definition). The latter parameter did increased significantly in RCC1827 ($F = 9.41$, $p = 0.037$) and in RCC1830 ($F = 9.05$, $p = 0.040$); displayed a marked decrease in RCC1833 ($F = 17.22$, $p = 0.014$) and it did not change in the others ($F < 7.61$, $p > 0.05$). While this observation clearly suggests the importance of strain-specific responses, the strain specificity cannot be traced back to the location of strain isolation. P limitation induced an increase in over-calcified coccoliths, accompanied by an increase in the calcium content per coccolith, in another *E. huxleyi* strain (Paasche 1998), not originating from the Mediterranean Sea. However, considering our results the increase in over-calcification in response to P limitation cannot be regarded as a common phenomenon in *E. huxleyi*, but rather as a strain-specific feature.

2.4.3. Element quotas and ratios

An interesting question is whether morphological features of coccoliths, such as over-calcification, can be related to calcite production. If so, there might be the possibility to establish a morphology based PIC production proxy, which would help assessing past coccolithophore PIC production (Beaufort et al. 2011). In the context of carbonate chemistry induced changes in calcification it was, for instance, shown that coccolith weight and calcite production (i.e. PIC production) are positively correlated (Bach et al. 2012). In the study by Paasche (1998) several calcification related parameters increased due to P

limitation, namely percentage of over-calcified coccoliths, coccolith calcium (i.e. PIC) quotas, cellular PIC quotas, and PIC:POC ratio. Interestingly, PIC production did not change. Hence the relationship reported by Bach et al. (2012) does not hold for P limitation in the *E. huxleyi* strain investigated by Paasche (1998). The question whether the latter relationship holds for the six strains investigated in our study is not easily answered. The reason for this is not only that we did not analyze coccolith weight, but also that our determination of PIC production under P limitation is not accurate. Briefly, under nutrient limitation the batch approach as employed by us necessarily leads to an incorrect determination of growth rate at harvest day and therewith production (please refer to Langer et al. (2012a) for a detailed reasoning). However, we can analyze the relative change between PIC and POC production, the PIC:POC ratio (please note that growth rate cancels here). In both RCC1827 and RCC1830 the PIC:POC ratio decreases in response to P limitation but the decrease is more pronounced in RCC1830 ($F = 91.24$, $p = 0.001$ and $F = 718.80$, $p = 0.000$ respectively). It can therefore be concluded that these two strains display similar responses with respect to over-calcification, but strain RCC1830 shows a stronger decrease in PIC production when normalized to POC production than does strain RCC1827 (Fig. 2.4). It is also conspicuous that five out of six strains decrease the PIC:POC ratio in response to P limitation (Fig. 2.4). Out of these five only RCC1833 displays a decrease in over-calcified coccoliths, while the others show an increase or no change. Taken together, these observations support the findings of Paasche (1998), that there is no correlation between the change in the percentage of over-calcified coccoliths and the change in PIC production.

There is no uniform trend in the change in PIC:POC ratio due to P limitation. As already mentioned, in our study only strain RCC1813 showed no change in PIC:POC ratio, while in all other strains it decreased. Hence the response is clearly strain-specific. The strain specificity could be the reason why results of other studies are discrepant. Paasche (1998) and Riegman et al. (2000) reported an increase in the PIC:POC ratio, while Borchard et al. (2011) showed a constant PIC:POC ratio. The fact that every possible trend (increase, no change, decrease) was already observed, although less than a dozen strains were investigated (Table 2.3) clearly suggests that the variability in response patterns is high in *E. huxleyi*. It is consequently impossible to make any predictions concerning the change in *E. huxleyi*'s PIC:POC ratio under putatively more severe P limitation in the future. In case

of the C:N ratio (Fig. 2.5), however, the response pattern seems to be uniform. All six strains studied here, as well as the ones studied by Borchard et al. (2011), Riegman et al. (2000) and even one *C. leptoporus* strain (Langer et al. 2012a) increased the C:N ratio in response to P limitation (Table 2.3). The stark difference between the response patterns of PIC:POC and C:N ratios could stem from the fact that the production of (in)organic C-compounds is less affected by P limitation than the production of organic N-compounds. Within the C-compound (including calcite) producing pathways it seems that it is highly variable whether PIC or POC production is more affected. It should also be mentioned that the C:P and N:P ratios markedly increased under P limitation, which is to be expected because P is the element in short supply. On the whole, C:N and N:P ratios of *E. huxleyi* change under P limitation in a consistent manner, while the PIC:POC ratios show a great strain specific variability in response patterns.

Table 2.3 Summary of coccolithophore responses to phosphorus limitation in different batch or continuous (including also semi-continuous) experiments. The horizontal arrow symbolizes no change in the variable; while the pointing up and pointing down arrows symbolize an increase and a decrease, respectively. A 10% of difference threshold was set to define a significant increase or decrease in the data from other studies. In Müller et al., 2008 control values were compared to early stationary phase values. In Borchard et al., 2011 the 900pCO2 treatments were not taken into account.

Species	Strain name or code	Culture type	Growth rate (μ)	POC quota	POC p	PIC quota	PICp	POP quota	POPp	TPN quota	TPNp	Coccosphere size	PIC:POC	C:N	Reference
E. huxleyi	RCC1813	Batch	↓	↑	↑	↑	↑	↓	↓	↑	↑	↑	↔	↑	This study
E. huxleyi	RCC1817	Batch	↓	↑	↑	↑	↑	↓	↓	↑	↔	↑	↓	↑	This study
E. huxleyi	RCC1812	Batch	↓	↑	↑	↑	↑	↓	↓	↑	↔	↑	↓	↑	This study
E. huxleyi	RCC1827	Batch	↓	↑	↑	↑	↑	↓	↓	↑	↑	↑	↓	↑	This study
E. huxleyi	RCC1830	Batch	↓	↑	↑	↑	↔	↓	↓	↑	↔	↑	↓	↑	This study
E. huxleyi	RCC1833	Batch	↓	↑	↑	↑	↑	↓	↓	↔	↔	↑	↓	↑	This study
C. leptoporu	RCC1135	Batch	↓	↑	↑	↑	↑	↓	↓	↔	↔	n.a	↔	↑	Langer et al. 2012a
E. huxleyi	CCMP371	Batch	n.a	n.a	n.a	↑	n.a	n.a	n.a	↔	n.a	↑	n.a	n.a	Müller et al. 2008
E. huxleyi	BOF92	Continous	↓	↑	↓	↑	↑	n.a	n.a	n.a	n.a	n.a	↑	n.a	Paasche and Brubak 1994
E. huxleyi	BOF92	Continous	↓	↑	↓	↑	↔	n.a	n.a	n.a	n.a	↔	↑	n.a	Paasche 1998
E. huxleyi	PML B92/1	Continous	↓	↑	↓	↑	↓	↔	↓	↔	↓	↔	↔	↑	Borchard et al. 2011
E. huxleyi	L	Continous	↓	↑	↓	↑	↔	↓	↓	↔	↓	↑	↑	↑	Riegman et al. 2000

Finally, although *E. huxleyi* strain-specific responses to P limitation were observed in: PO_4^{3-} usage, TPN quotas, PIC production, PIC:POC, in the degree of coccolith calcification and other morphological features, none of these differences between strains can be attributed to the strain isolation location. The absence of a pattern among the inter-strain response variability indicates that no *E. huxleyi* ecogenotypes are established upon

environmental P availability in these strains. Supplementary data to this article can be found online at http://dx.doi.org/10.1016/j.jembe.2014.04.021.

2.5. Supplementary data

Table 2.4. Supplementary data on carbonate chemistry calculated from measured TA and pH in the culture media at harvest day. Shift in CO_2, TA and DIC were calculated as the difference between the carbonate system measured on day 0 and the one on harvest day.

	RCC1813		RCC1817		RCC1812		RCC1827		RCC1830		RCC1833	
	P limited	Control	P limited	Control	P limited	Control	P limited	Control	P limited	Control	P limited	Control
pH	8.14	8.15	8.02	8.12	7.92	8.07	8.03	8.04	8.13	8.14	7.91	8.02
Standard deviation	0.01	0.03	0.01	0.07	0.01	0.01	0.01	0.01	0.01	0.00	0.01	0.01
TA (µmol/Kg)	2276	2514	2241	2519	2158	2477	2188	2432	2065	2358	2141	2524
Standard deviation	5	12	22	7	32	45	7	24	5	13	21	6
DIC (µmol/Kg)	1990	2163	2019	2187	1985	2176	1966	2150	1803	2026	1974	2245
Standard deviation	4	18	19	50	28	43	10	22	5	13	19	6
CO3 (µmol/Kg)	205	229	163	217	129	195	161	181	182	210	126	182
Standard deviation	1	11	5	28	5	4	4	2	5	1	2	0
Ω (µmol/Kg)	5.0	5.6	4.0	5.3	3.2	4.8	3.9	4.4	4.4	5.1	3.1	4.4
Standard deviation	0.0	0.3	0.1	0.7	0.1	0.1	0.1	0.1	0.1	0.0	0.0	0.0
CO2 shift (µatm)	-194	-176	42	-12	25	-101	-100	-77	-91	-62	36	-37
Standard deviation	1	25	15	75	17	11	14	4	10	3	6	3
TA shift (µmol/Kg)	-366	-159	-373	-100	-485	-196	-454	-241	-549	-261	-502	-149
Standard deviation	5	12	22	7	32	45	7	24	5	13	21	6
DIC shift (µmol/Kg)	-406	-227	-289	-92	-406	-212	-427	-237	-506	-253	-417	-142
Standard deviation	4	19	19	51	28	43	10	22	6	13	19	6

Chapter 3.

Ocean acidification and phosphorus limitation alter cellular P content and lead to lower maximum cell densities in a Mediterranean strain of *Emiliania huxleyi*.

Article in preparation

Abstract

The *Emiliania huxleyi* strain RCC1827, isolated in the Mediterranean Sea, was grown in batch culture to test the effects of the combined increase in seawater pCO_2 and phosphorus limitation on population growth, cellular C, N and P quotas and coccolith morphology. Maximum cell densities decreased due to phosphorus limitation at all pCO_2 levels indicating that all cultures were P limited. However pCO_2 further decreased maximum cell densities only if cultures were also P limited. Growth rate deceased with pCO_2 in both nutrient conditions (36% and 47% in P limited and replete conditions respectively). At all pCO_2 levels, P replete cultures reached higher cell densities than P limited cultures. This results were linked to an increase in cellular P storage with increasing pCO_2. The low PO_4^{3-} concentration in P limited cultures and higher increased P demand resulted in lower maximum cell densities in these cultures. It is concluded that under nutrient replete conditions *E. huxleyi* is more resilient to changes in pCO_2 than when P stressed. Increased pCO_2 caused malformation of coccoliths, though malformations occurred irrespectively of the P availability. Increased pCO_2 did not affect the degree of calcification of coccoliths (i.e.: under-calcified, normaly-calcified or over-calcified). This suggests that in oligotrophic regions the degree of calcification, as seen in SEM images, is not a good proxy for carbonate chemistry parameters.

3.1. Introduction

Approximately 30% of current CO_2 emissions are being absorbed by the ocean (Rhein et al. 2013). As a result, the ocean´s carbonate chemistry is altered. That means, the pH, carbonate ion (CO_3^{2-}) and calcium carbonate saturation state (Ω) of seawater decrease while bicarbonate ion (HCO_3^-) increases. This phenomenon has been called "Ocean Acidification" (Caldeira & Wickett 2003). Estimates indicate that by the year 2100, the average surface ocean pH could be lower than it has been for more than 50 million years (Pearson & Palmer 2000). In parallel to these changes, rising surface seawater temperature, another consequence of enhanced CO_2 emissions, obstructs the input of nutrient rich water from the deeper ocean into its surface, reducing phytoplankton growth (Behrenfeld et al. 2006). In the case of nitrogen, this could be partially compensated by an increase in nitrogen fixation expected to occur as a response to enhanced column water stratification and increased pCO_2 (Karl et al. 2001, Hutchins et al. 2007, Levitan et al. 2007) and the increase in nitrogen enriched atmospheric depositions (Moore et al. 2013). Thus, the abundance of phosphate relative to nitrogen is expected to decrease. Additionally, ocean acidification itself decreases phosphate concentrations, throughout modification of the phosphoric acid system with decreased pH [for details see Zeebe & Gladrow (2001)**]**.

Within phytoplankton, coccolithophores are a group of particular interest with respect to the combined effects of ocean acidification and P limitation. On the one hand, they cover their cell with plates (coccoliths) made of calcium carbonate whose production and durability is believed to be hampered by the ongoing ocean acidification. On the other hand, Given their high affinity for phosphate when compared to other phytoplankton groups (Riegman et al. 2000) they are particularly important in regions with low [P], such as the Mediterranean Sea, where coccolithophores are a seasonally dominant group of the phytoplankton community (Siokou-Frangou et al. 2010). Coccolithophores contribute about half of the modern worldwide marine pelagic $CaCO_3$ sedimentation (Frenz et al. 2005, Broecker & Clark 2009), which in turn contributes to ballasting organic carbon (Lombard et al. 2013). Therefore, a reduction in their abundance or in the amount of calcite in coccoliths may largely influence the global carbonate cycle and reduce the organic carbon export [Meier et al. (2014) and references therein]. *Emiliania huxleyi* (Lohmann 1902) Hay & Mohler *in* Hay et al., (1967) is the most abundant coccolithophore species in the modern oceans (Paasche 2002) and thus, one of the species that contribute the most to

coccolithophore carbon export, with the caveat that in mixed populations, other larger or heavier calcified species may become more important in term of carbon export (Daniels et al. 2014).

Under enhanced pCO_2, photosynthesis and ultimately population growth are thought to be stimulated in species with poorly efficient carbon concentration mechanisms, such as coccolithophores, were photosynthesis is not saturated at present pCO_2 (Paasche 1964, Buitenhuis et al. 1999, Rost et al. 2003, Bach et al. 2013). Low seawater [PO_4^{3-}], precisely 0.009 ± 0.007 μmol L^{-1}, limited coccolithophore growth in the eastern Mediterranean Sea (Kress et al. 2005). How the interaction of high CO2 and P limitation will act upon coccolithophore growth is still an open question. It has been hypothesized (Beardall & Giordano 2002) that increased pCO_2 reduces the need for carbon concentrating mechanisms (CCMs) which consume P, and in turn, it reduces the stress caused by nutrient limitation. So far, the experimental evidence in support of this hypothesis is inconclusive. In the study of Borchard et al. (2011) decreased POP quotas coupled with increased maximum cell densities may indicate less stress from P limitation when the cells are exposed to the combination of P limitation and ocean acidification. This is consistent with the abovementioned hypothesis. On the other hand, in the study of Rouco et al. (2013) high pCO_2 alone caused an increase in POP quotas but the combination of high CO_2 and P limitation caused no change of P requirement. However, no data on maximum cell densities or growth rate are available which makes it impossible to judge whether the stress caused by P limitation was reduced or not.

Most probably, the degree of calcification of a coccolith has biogeochemical implications, because coccolithophores with over-calcified coccoliths are expected to have a higher PIC:POC ratio and this increases the probability of long term carbon burial (Klaas & Archer 2002, Ziveri et al. 2007). On the other hand, coccolith morphology might be more instrumental in evolutionary success of coccolithophores than calcification rate (Langer et al. 2011). The combined effects of phosphorus limitation and ocean acidification on coccolith morphogenesis have not yet been tested in laboratory. However, when tested separately, ocean acidification produces thinner and malformed coccoliths in some cultured strains (Riebesell 2004, Langer et al. 2006, 2009, Rickaby et al. 2010, Bach et al.

2011). On the contrary, P limitation does not result in the malformation of coccoliths in the majority of species and strains tested (Langer et al. 2012, Oviedo et al. 2014) while it increases the degree of calcification in most of the tested strains (Oviedo et al. 2014). Here we tested the effect of seawater acidification and P limitation on population growth, P requirement, and coccoliths morphology of *E. huxleyi*.

3.2. Methods

3.2.1 Strain selection

Emiliania huxleyi strain RCC1827 was obtained from the Roscoff culture collection, isolated during the BOUM cruise in September 2008. RCC1827 was isolated from the south-western Mediterranean (39º 6'N, 5º 21'E). Additional information can be found on: http://www.sb-roscoff.fr/Phyto/RCC/index.php?option=com_dbquery&Itemid=24.

3.2.2 Culture media preparation

The culture media consisted of 68% natural North Sea seawater and 32% artificial seawater (Kester et al. 1967). Replete cultures were enriched to F/2 levels (Guillard & Ryther 1962) while no phosphate was added to the limited ones. In this way, PO_4^{3-} concentrations were ~0.2μM for the limited cultures versus 35.0μM in the replete cultures. The small amount in the limited cultures was calculated from the carryover of the stock cultures at inoculation. Phosphate was measured using an Autoanalyzer Evolution III (Alliance Instruments) with detection limits of 0.1μM. Salinity was adjusted to 38 to mimic Mediterranean surface seawater conditions. All culture media was then sterile-filtered through a 0.2μm pore size cartridge into the culture glass bottles of 2.3 l. A minimum head-space was conserved.

pCO_2 manipulations were done by changing total Alkalinity (TA) with acid (HCl, 1M) and base (NaOH, 1M) additions. Target pCO_2 were: 200 (LGM), 750 (~ year 2100), 1500 (in the upper range of the worst IPCC scenario), and 2150 (extreme value). Measured initial and final carbonate system parameters are shown in Table 1. Alkalinity samples were filtered (Whatman GFF filter, 0.6 μm pore size), stored in 300 ml borosilicate flasks at 4 ºC, and measured in duplicate by potentiometric titration. TA was calculated from linear

Gran plots (Gran 1952). Dissolve inorganic carbon (DIC) samples were sterile-filtered (0.2 μm pore size cellulose-acetate syringe filters) and stored in 13 ml borosilicate flasks free of head space and stored at 4ºC for 1 to 5 days until they were measured using a Shimadzu TOC 5050A. pH was determined potentiometrically (electrode IOline, Schott Instruments, pH meter WTW 340i) on the NBS scale and converted to total scale using Certified Reference Materials (Tris-based pH reference material, Batch No. 2, Scripps Institution of Oceanography, USA). Samples and standards were measured at 20ºC. For each culture bottle, TA, DIC and pH samples were measured in duplicate. The carbonate system was calculated from TA, pH, phosphate, and temperature, using the program CO2Sys (Lewis & Wallace 1998). Equilibrium constants of Mehrbach et al. (1973) refitted by Dickson & Millero (1987) were chosen.

3.2.3 Batch cultures development and harvest

Batch cultures were kept in an incubator (Rubarth Apparate GmbH, Germany) at 20°C on a 16/8 L/D cycle and an irradiance of 300 - 380 μmol photons $s^{-1}m^{-2}$. Cell density at inoculation was ~400 cells ml^{-1}. Limited cultures were allowed to grow to stationary phase, which was reached at cell densities below ~100 x 10^3 cells ml^{-1}. P-replete cultures for each strain were harvest during the exponential phase, trying to match the cell density yielded by the respective limited culture. Cell density and size were monitored, initially every other day and then daily until harvest day, using a coulter counter (Beckman Multisizer III). A small volume of each P-replete culture was grown until cell densities approached 1 x 10^6 cells ml^{-1} or a decrease was observed. Growth rates were calculated by means of exponential regression using all data points until harvest day.

3.2.4 Response variables

3.2.4.1 Element cellular quotas

The protocol for measurements of particulate organic nitrogen (PON), total particulate carbon (TPC), particulate organic carbon (POC) and particulate organic phosphorus (POP) were the same as in Oviedo et al. (2014). Briefly, samples for all cellular quotas were filtered onto pre-combusted (500 ºC; 12 h) GFF filters. Samples for carbon and nitrogen determination were oven dried (60 ºC overnight). Filters for POC were treated with 230 μl

of HCl (0.1 M) to remove all the inorganic carbon and oven-dried again. POC, TPC and PON were measured on a Euro EA Analyser (Euro Vector). PIC was calculated as the difference between TPC and POC. Filters for POP were oven-dried for an hour, dissolved in a mixture of 35 ml Milli-q water and potassium peroxide and autoclaved (120ºC, 30 min). Samples were centrifuged after the addition of ascorbic acid and a mixture of reagents (sulphuric acid, ammonium heptamolybdate-tetrahydrate, potassium antimoyl-tartrate and distilled water). The soluble reactive phosphorus determined photometrically following (Hansen & Koroleff 1999).

3.2.4.2 Coccolith morphology and coccosphere size

A small volume of culture (between 15 and 70 ml depending on yield cell densities) was filtered onto polycarbonate filters (Sartorius, 0.25 μm) and dried at 60ºC for 24 hours. A piece of each filter was placed on aluminum stubs and sputter coated using an EMITECH K550X. Imaging was performed in a ZEISS-EVO MA10 scanning electron microscope (SEM). Between 360 and >1000 coccoliths forming coccospheres were analyzed per sample on its distal view. Coccoliths were classified using captured images in: normal (inner tube circle, external rim and all distal shield elements were well formed and the latter were of the same size and symmetrically distributed around the inner tube circle); malformed (when the coccolith was asymmetrical) or incomplete coccoliths (when all the external rim was absent or only the inner tube circle was present). Te degree of calcification (qualitatively from SEM images) was evaluated in normal coccoliths, which were sub-classified in over-calcified (when distal shield elements were thicker to the point that half or more were fused, usually but not always the inner tube circle was also thicker), normally calcified coccoliths (when individual distal shield elements clearly displayed the space between them and the inner tube circle was wider than distal shield elements) and under-calcified coccoliths (visibly thin coccoliths with a wide space between distal shield elements and thin inner tube circle). See examples in Figure 2.1 of Chapter 2. Coccosphere size was recorded from the Multisizer III coulter counter data.

3.2.5 Statistics

One way ANOVAs followed by Tukey´s post-hoc tests were conducted for each P treatment to examine the differences between the 4 pCO_2 levels. This was done with the software SPSSv19.

3.3. Results

From the beginning to the end of the experiment, pCO_2 changed from to 1% to 25% (the latter in the 1500 pCO_2 - P limitation treatment). Variation in pH was close to ±1%. TA varied between 0,5% and 20%, the latter value in the 750 pCO_2 -P limitation treatment. $\Omega_{calcite}$ at harvest day was always higher than 1.3 (Table 3.1) which is unfavorable for calcite dissolution. On the other hand, phosphorus limitation was evident by the decrease in maximum cell densities, growth rate and POP quotas (Table 3.2).

Table 3.1. Carbonate chemistry in the culture media at the beginning of the experiment (initial) and at harvest day (final). DICc stands for calculated DIC and DICm for measured DIC.

		pCO_2		TA		DICc		DICm				$[CO_2]$		$[HCO_3]$		$[CO_3]$			
	P	(µatm)	SD	(µmol/kg)	SD	(µmol/kg)	SD	(µmol/Kg)	SD	pH	SD	(µmol/kg)	SD	(µmol/kg)	SD	(µmol/kg)	SD	Ωca	SD
Initial	Limited	209	7	2802	8	2279	13	2355	1	8,32	0,01	6,6	0,2	1871	19	387	5	9,0	0,1
Final	Limited	195	1	2301	23	1868	17	1917	8	8,28	0,01	6,2	0,0	1570	11	292	6	6,8	0,1
Initial	Limited	723	39	2482	-	2340	74	2340	0	7,85	0,01	23,0	1,2	2167	71	150	2	3,5	0,0
Final	Limited	714	15	1986	26	1855	20	1892	12	7,76	0,01	22,7	0,5	1735	17	98	4	2,3	0,1
Initial	Limited	1551	20	2358	4	2302	5	2319	5	7,52	0,00	49,3	0,6	2182	5	71	1	1,7	0,0
Final	Limited	1158	90	2094	23	2019	31	2037	13	7,59	0,03	36,8	2,8	1909	31	73	3	1,7	0,1
Initial	Limited	2162	36	2321	2	2313	0	2306	5	7,38	0,01	68,7	1,2	2193	0	51	1	1,2	0,0
Final	Limited	1920	31	2309	18	2286	18	2290	6	7,42	0,01	61,0	1,0	2168	17	57	1	1,3	0,0
Initial	Replete	213	-	2892	3	2321	-	2329		8,33	0,00	7,1	-	1930	-	384	-	9,0	-
Final	Replete	163	1	2560	6	1986	3			8,36	0,00	5,2	0,0	1612	2	368	2	8,6	0,1
Initial	Replete	710	-	2490	3	2266	-	2318	-	7,84	-	22,6	-	2100	-	144	-	3,4	-
Final	Replete	698	16	2303	4	2099	6			7,82	0,01	22,2	0,5	1951	7	126	2	2,9	0,0
Initial	Replete	1538	99	2382	17	2291	7	2295	11	7,52	0,03	48,9	3,1	2171	5	71	5	1,7	0,1
Final	Replete	1218	100	2283	44	2167	50			7,60	0,03	38,7	3,2	2048	49	80	3	1,9	0,1
Initial	Replete	2151	-	2311	-	2270	-	2280	14	7,37	-	68,3	-	2152	-	50	-	1,2	-
Final	Replete	1900	52	2294	5	2237	2			7,42	0,01	60,4	1,6	2122	2	55	2	1,3	0,0

Table 3.2. Average element quotas and cell density in cells exposed to two P regimes and 4 different pCO_2 levels. Standard deviation (SD) of triplicates is shown.

P	pCO_2	TPC (pg/cell)	SD	PON (pg/cell)	SD	POC (pg/cell)	SD	PIC (pg/cell)	SD	POP (pg/cell)	SD	Max. Cell density (cells/ml)	SD
Limited	200	45.73	3.64	2.25	0.06	37.39	1.36	8.34	3.07	0.04	0.00	112380	1733
Limited	750	56.63	3.26	3.02	0.07	50.92	1.01	5.71	3.54	0.05	0.00	990173	5760
Limited	1550	48.97	0.58	2.95	0.07	27.48	1.93	21.49	2.28	0.05	0.01	97207	2510
Limited	2150	21.15	0.81	2.29	0.11	15.02	0.91	6.13	0.30	0.16	0.01	945393	1289
Replete	200	30.72	1.70	2.35	0.17	11.23	1.10	19.50	0.76	0.45	0.03	74067	5605
Replete	750	33.25	4.95	2.60	0.00	15.48	0.86	17.78	4.12	0.49	0.14	458847	1556
Replete	1550	32.22	7.95	2.77	0.39	17.67	3.51	14.55	4.45	0.90	0.12	22980	4933
Replete	2150	27.62	3.77	2.81	0.33	18.48	0.88	9.14	2.94	1.59	0.13	908987	1626

3.3.1 Population growth

Maximum cell densities decreased in one order of magnitude due to phosphorus limitation (Table 3.2). In response to enhanced pCO_2, maximum cell densities of P limited cultures decreased up to 80% (Figure 3.1, A), from ~112 x 10^3 cells ml^{-1} at 200 µatm pCO_2 to ~23 x 10^3 cells ml^{-1} at 2150 µatm pCO_2. On the contrary, Maximum cell densities of P replete cultures reached several thousand cells per ml (Table 3.2) in all pCO_2 treatments. Growth rate was always higher in P replete cultures and decreased with pCO_2 in both nutrient conditions (up to 36% and 47% in limited and replete conditions respectively). At pCO_2 levels between 200 and 1500 µatm P limitation also caused a decrease in growth rate which was less pronounced (23 ± 4 %) than the one caused by increased pCO_2. At 2150 µatm pCO_2, both, P limited cultures and P replete cultures, grew at similar rates (Figure 3.1, B). Nevertheless, P replete cultures at this pCO_2 level could continue growing slowly for 15 days while the limited cultures could not grow beyond day 9, which led to much lower cell densities in P limited cultures (Figure 3.1, A).

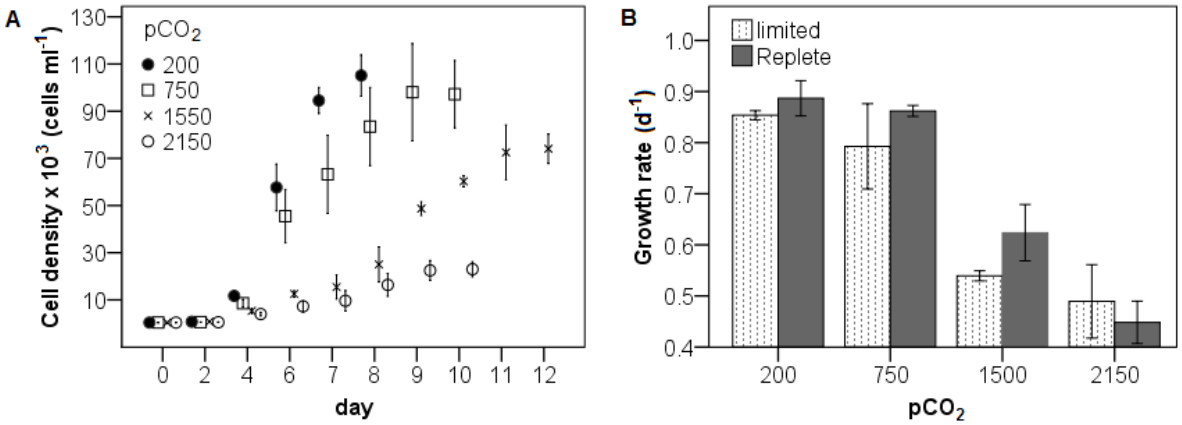

Figure 3.1. Cell density evolution from inoculation (day 0) until stationary phase for *E. huxleyi* strain RCC1827, under P limited conditions (A). Growth rate calculated from the cell density evolution for each strain under P limited and replete conditions (B).

3.3.2 Element quotas

Although a tendency towards increasing POC quota with increased pCO_2 can be observed in P replete cultures, this was only significant between 200 and 1500 µatm pCO2 ($p= 0.015$). In P limited cultures, POC quota initially increased when passing from 200 µatm to 750 µatm pCO_2 ($p<0.001$). Further increase in pCO_2 decreased POC quota with respect to 200µatm ($p<0.001$). POC increased with P limitation but this increase was attenuated at high pCO_2 (Figure 2). Cells were able to produce calcite (i.e. PIC) at all tested pCO_2, under both, P limited and P replete conditions. In P replete cultures, PIC and the PIC:POC ratio showed a tendency to decrease with enhanced pCO_2 (Figure 3.2), however, for PIC quota this was only statistically significant between the extreme treatments ($p= 0.024$ between 200 and 2150 µatm). No linear pattern was observed in P limited cultures. Under both, P replete and P limitation conditions, cells stored more POP at higher pCO_2 (up to 410% in P limited cultures and 350% in P replete cultures, respect to 200 µatm pCO_2). The total PO_4^{3-} assimilated per culture, however, did not change with pCO_2 (Figure 3.2).

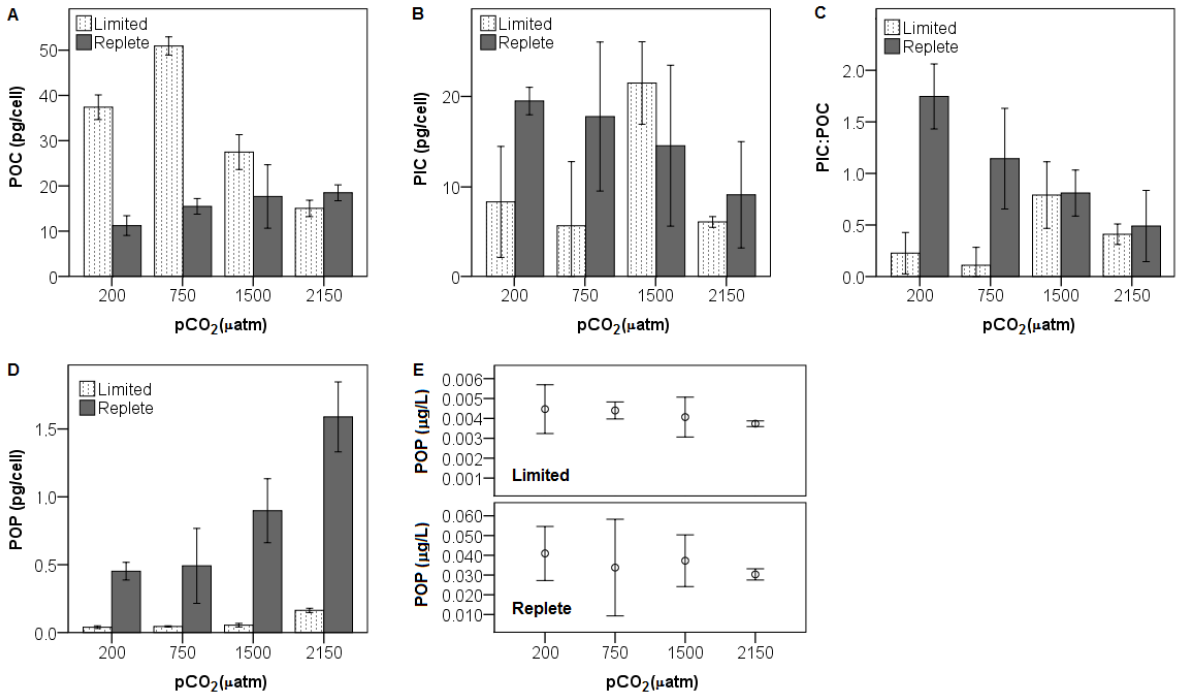

Figure 3.2. Cellular element quotas of: A, particulate organic carbon (POC); B, particulate inorganic carbon (PIC); C, PIC:POC ratio; D, particulate organic phosphorus (POP) and E, the POP assimilated by limited (upper panel) and replete (lower panel) cultures, at different pCO_2 conditions.

From inoculation to harvest day, coccosphere size showed an increasing trend in P limited cultures and decreased or did not change in P replete cultures. In P limited cultures, after 7 days of experiment, the increase in coccosphere size was less pronounced in cultures with enhanced pCO_2 levels (Figure 3.3).

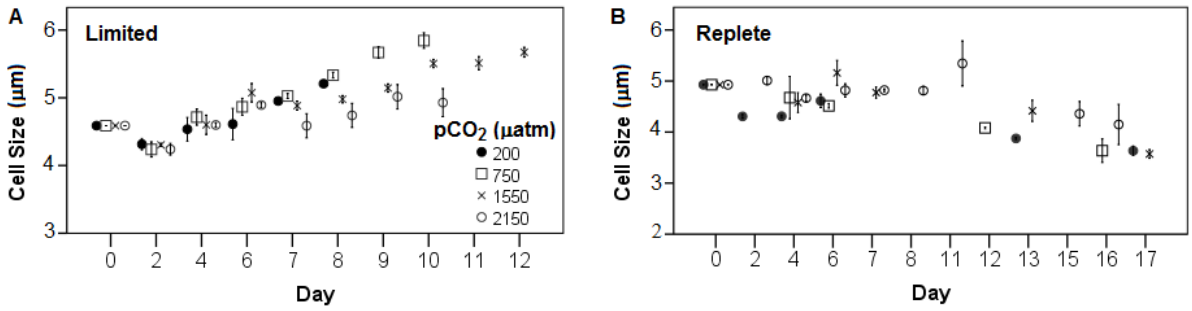

Figure 3.3. Coccosphere size evolution from inoculation (day 0) until stationary phase for *E. huxleyi* strain RCC1827, under P limitation, A; and P replete conditions, B.

3.3.3 Coccolith morphology

The percentage of malformed coccoliths increased significantly in response to increased pCO_2 until 1500 µatm. Further increase in pCO_2 did not augment malformations (Figure

3.4A). The degree of calcification of normal coccoliths did not change with increased pCO_2 (Figure 3.4B-D). The percentage of incomplete coccoliths was neglectible in all treatments (<5%).

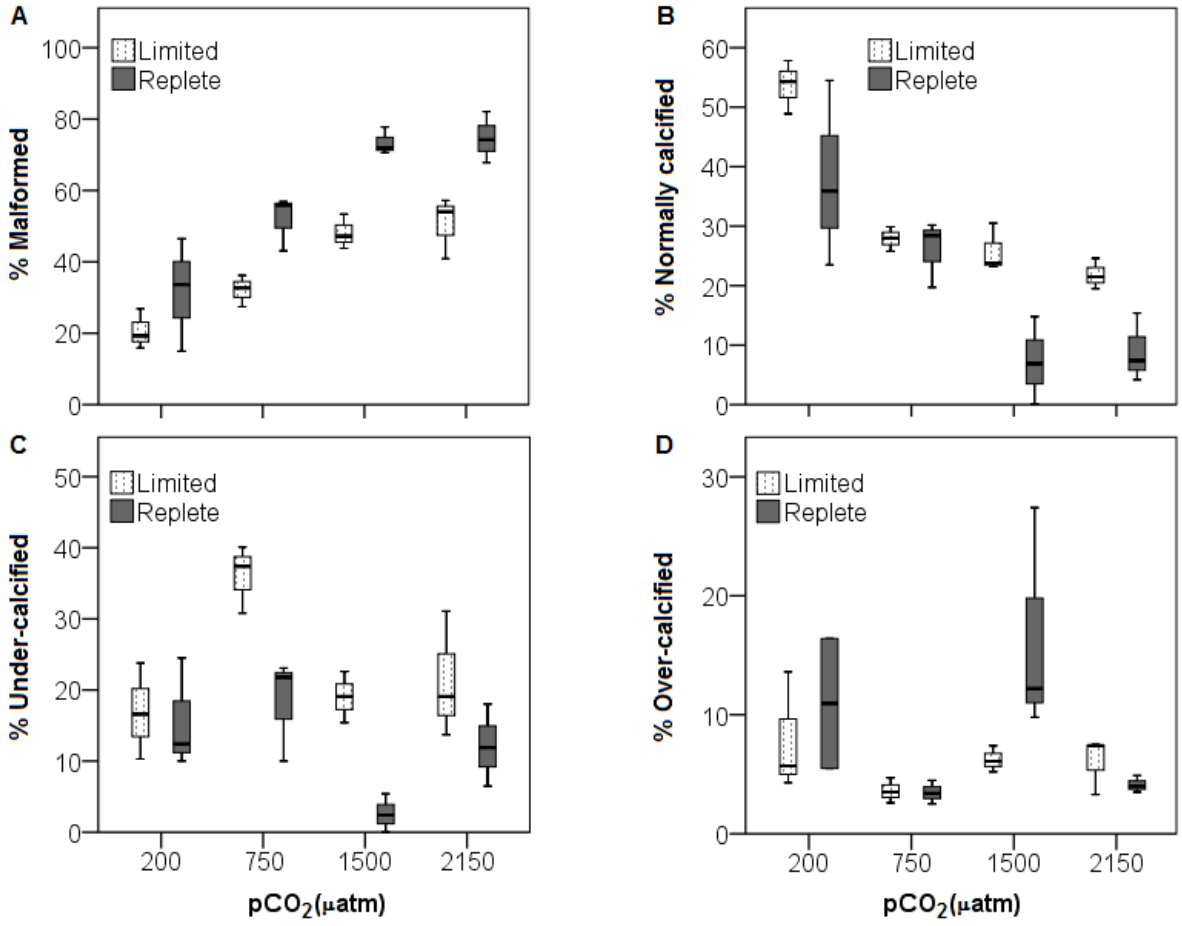

Figure 3.4. A, percentage of malformed coccoliths; and degree of calcification in normal developed coccoliths (B to D), at different pCO_2 conditions.

3.4 Discussion

3.4.1 Population growth

CO_2 assimilation has as constrain that the enzyme mediating carbon fixation, the Rubisco, has a low affinity for its substrate, CO_2 (Morell et al., 1992, Badger et al., 1998). Carbon concentrating mechanisms (CCMs) help then to overcome this constrain by increasing the concentration of CO_2 at the site of carboxylation (Rost *et al.* 2008 and references therein). Thus, it has been hypothesized that species with inefficient CCMs may directly benefit

from the increase in CO_2 (Rost et al., 2008). This seems to be the case of *E. huxleyi*, whose photosynthesis is not saturated at present pCO_2 (Paasche 1964, Buitenhuis et al. 1999, Rost et al. 2003, 2008, Bach et al. 2013). Given that photosynthesis is the starting point of the processes that lead to growth, it is conceivable that if photosynthesis is sensitive to $[CO_2]$, growth will be as well. Nevertheless, at ambient $[CO_2]$, growth of *E. huxleyi* is apparently saturated (Clark & Flynn 2000) and it is not clear how the species growth rate could be affected if pCO_2 further increases.

The decrease in μ and maximum cell densities with increasing pCO_2 in P limited cells indicates that our results cannot be interpreted in terms of carbon limitation. Even further, Blach et al. (2013) suggested that CO_2 is the principal factor responsible for growth inhibition below a $[CO_2]$ of ~ 7.5 μmol/Kg. We tested this strain under $[CO_2]$ as low as ~ 6 μmol/Kg and still inhibition of growth only occurred with increased $[CO_2]$ and not the opposite. The decrease in μ observed in P replete cultures shows that changes in the carbonate chemistry alone are capable to affect *E. huxleyi* physiology, but the potential implication for population size are mostly seen in combination with P limitation.

Regarding the combination of P limitation and OA, the available data suggest that P limited *E. huxleyi* cells can maintain its growth rate when passing from ~360 to 2000 μatm pCO_2 (Leonardos & Geider 2005) and at lower pCO_2 levels (Borchard et al. 2011, Engel et al. 2014). This, however doesn´t mean that maximum cell densities are equally maintained, as an increase, decrease and no change was observed in these experiments respectively. In the Mediterranean *E. huxleyi* strain used here, P limitation and increased pCO_2 decreased μ and the maximum cell densities yield by each culture. The decrease observed in P limited cultures under high pCO_2 points out to a high susceptibility of this strain under the combination of P limitation and ocean acidification. Which is the mechanism by which carbonate system modification (e.g.: pH or other parameter) reduced *E. huxleyi* cell densities in these cultures? What implications would there be for P limited cells? We propose that the effect of pCO_2 on POP quotas caused the decrease in maximum cell densities.

3.4.2 Element quotas and ratios

How P cellular requirement may be affected by the combination of ocean acidification and P limitation is not obvious from previous experiments. Clearly, particulate organic phosphorus production (POP) is expected to decrease with P limitation. However, in relation to ocean acidification this response is less clear. It has been hypothesized (Beardall & Giordano 2002) that increased pCO_2 reduces the need for carbon concentrating mechanisms (CCMs) which consume P. A down-regulation of CCM´s by enhanced pCO_2, would allow the cells to economize P that could help to cope with the effects of P limitation. Some of these effects are carbon overconsumption; low POP quotas and finally decreased reproduction. In a chemostat study by Borchard et al. (2011) enhanced pCO_2 alone or in combination with P limitation, slightly decreased POP quotas. This was probably due to the increased maximum cell densities, which is not observed under P limitation alone. This indicates decreased P requirements in benefice of cell division, which is consisted with the hypothesis of (Beardall & Giordano 2002). In a batch culture experiment (Leonardos & Geider 2005) lowest cell densities were reached under the combination of ocean acidification and P limitation, and it was only under these conditions that all PO_4^{3-} in the media was consumed. The latter results may be indicative of an amplification of the detrimental effects of P limitation when, in addition, cells are exposed to high pCO_2, which opposes the above mentioned hypothesis and the results of Borchard et al. (2011).

The results of our experiment suggest that, if a down-regulation of CCMs occurs at high pCO_2, this one does not attenuate the effects of P limitation. For instance, carbon overconsumption occurred at pCO_2 levels $\leq$ 1500 μatm. and maximum cell densities decreased already when passing from 200 to 750 μatm. How can these responses be explained?

In *E. huxleyi* RCC1827, high pCO_2 increases the cellular P requirement/storage, as evidenced by the increase in POP quotas and decrease in maximum cell densities. Total P-assimilation (i.e.: POP per liter), however, was constant through all pCO_2 levels. This means that ocean acidification does not affect P-uptake, but makes the cells invest in POP quota rather than cell division. If P is a limiting nutrient in their natural environment, their

higher requirement will make them consume the available P faster than at lower pCO_2. This will translate into lower population size, which means that cells under this combination of environmental factors will be less competitive in the field.

While ocean acidification is expected to disrupt calcification (PIC production) through either the decrease in pH or the increase in CO_2 (Langer and Bode 2011, Bach et al. 2012), P limitation apparently enhances calcification (Paasche & Brubak 1994, Paasche 1998). It has been hypothesized that coccolithophores may increase their calcification rates when nutrients become limited. This could be related to calcification generating protons that can be used in exchange for nutrient ions (McConnaughey & Whelan 1997) or to the reduction of cytosolic free Ca^{+} ions that otherwise could precipitate PO_4^{3-} (Degens & Ittekkot 1986). Would that mean that the detrimental effects of enhanced pCO_2 on calcification would be attenuated in P poor waters?. Current evidence suggest that the answer to this question is no. For instance, PIC production in two chemostat experiments running under low [P], decreased at the highest pCO_2 level tested (900 μatm) (Borchard et al. 2011) or did not change within the rage 180 to 750 μatm (Engel et al. 2014), which points towards a stronger effect of pCO_2 on calcification. In our study, PIC quotas and production in P limited cultures had a maximum at ~1500 μatm pCO_2, after which they decreased. Thus, although at CO_2 values predicted for the end of this century calcification may not be negatively affected in this Mediterranean strain growing under P limitation conditions, at extreme CO_2 values the detrimental effect is clear. However, P limited cultures had, generally, lower PIC quota, which means there was no compensatory effect from P limitation.

PIC:POC ratio is > 1 only in P replete cultures ≤ 750 μatm pCO_2. A decrease in calcification rate relative to photosynthesis favors the role of *E. huxleyi* populations as a CO_2 sink in the ocean in a short time scale. Thus, in a P poor environment, at short time scales, the role of *E. huxleyi* populations may be that of a CO_2 sink. This result implies that depending on the nutrient status, the role of some *E. huxleyi* populations can change from source to sink. But that this can also occur if pCO_2 levels go beyond the levels expected for the end of the century.

3.4.3 Coccolith morphology

The earlier hypothesis that macro-nutrient limitation is the main cause for coccolith malformations (Okada & Honjo 1975, Young & Westbroek 1991) could not be confirmed by experimental studies (Langer et al., 2012a, Oviedo et al., 2014). However, high pCO_2 alone is thought to result in thinner and malformed coccoliths in culture experiments (Riebesell et al. 2000, De Bodt et al. 2010, Langer et al. 2011, Bach et al. 2012), with some exceptions depending on the strain used (see Langer et al. 2011). Other exceptions come from mesocosm experiments: Engel et al. (2005) in Norway, and Oviedo et al., (submitted) in the Mediterranean Sea observed no increase in malformations in *E. huxleyi* coccoliths with enhanced pCO_2. The Mediterranean experiment was carried out under P depleted conditions (~10nM) and thus, phytoplankton cells were under similar stressors as those imposed during this study. In the present culture experiment, were the population grew actively from ~400 cell L^{-1} to ~$1x10^5$ cells L^{-1}, high pCO_2 increased the percentage of malformed coccoliths in both nutrient regimes (Figure 3.4). During the mesocosm experiment the population was in decline and no information on the *E. huxleyi* coccolith production rates was achieved. It is possible that the duration of the mesocosm experiment was too short (12 days) in relation to the production of new coccoliths, to allow observing any impact on coccolith morphology. As mentioned above, most experiments performed to test effects of ocean acidification with pCO_2 showed a disruption in the coccolith morphogenesis. Our experiment further confirms this notion. Increased coccolith malformation with enhanced pCO_2 suppose a disruption of the coccolith production process which likely will have a negative impact in the "fitness" of the cell(s) carrying malformed coccoliths.

Regarding the degree of calcification, sediment samples around the globe apparently record a positive correlation between placolith mass (for which the degree of calcification, as observed by SEM, may be an approximation) and $\Omega_{calcite}$ (Beaufort et al. 2011). The degree of calcification of normal coccoliths did not change with increased pCO_2 (Figure 3.4). This does not mean that high pCO_2 did not caused any change in coccolith calcite mass. Indeed, it is possible that the approximation we used (degree of calcification as observations of coccolith SEM images) does not reflect the calcite content of a coccolith (there was no relationship with PIC quotas). Thus, in oligotropic regions the degree of

calcification, as observed by SEM images, is not a good proxy for carbonate chemistry parameters, or for the estimations of PIC quotas.

3.5 Conclusions

i) An important conclusion of this research is that oligothrophy (i.e. P limitation) amplifies the response to ocean acidification in terms of fitness (measured as maximum yield cell densities). The mechanism by which this happens involves an increase in P demand (or storage) with increased pCO_2. Under a P limited supply, accomplishment of these higher quotas decreases maximum yield cell densities. Even if cells living under this combination of environmental conditions may contain more TPC and more POP, the exported material may decrease due to strong limitation of the population growth. Would this mean that the contribution of coccolithophores to the export of carbon will decrease under the combination of P limitation and OCEAN ACIDIFICATION? Or that their role as a sink or source of CO_2 to the atmosphere can change? This depends on the relative abundance of coccolithophores to other phytoplankton groups in the different regions and on changes in the PIC:POC ratio.

ii) The PIC:POC ratio was found > 1 only in P replete cultures under a $pCO_2 \leq 750$ μatm. Thus, our results imply that depending on the nutrient status, the role of some *E. huxleyi* populations can change from source to sink of atmospheric CO_2.

iii) It is also shown that ocean acidification causes coccolith malformation irrespectively of the external nutrient concentration.

Chapter 4.

Coccolithophore community response to increasing pCO_2 in Mediterranean oligotrophic waters

Article submitted: Oviedo A, Ziveri P, Gazeau F (in review) Coccolithophore response to increasing pCO_2 in Mediterranean oligotrophic waters. Estuarine, Coastal and Shelf Science.

Abstract

The effects of elevated partial pressure of CO_2 (pCO_2) on plankton communities in oligotrophic ecosystems were studied during two mesocosm experiments: one during summer 2012 in the Bay of Calvi, France, and another during winter 2013 in the Bay of Villefranche, France. Here we report on the relative abundances of coccolithophores versus siliceous phytoplankton, coccolithophore community structure, *Emiliania huxleyi* coccolith morphology and calcification degree. A pCO_2 mediated succession of phytoplankton groups did not occur. During both experiments, coccolithophore and diatom abundances and the coccolithophore community structure varied with time independently of pCO_2 levels. The abundance and species composition patterns were partly explained by the concentration in phosphate during the winter experiment. During the summer experiment, it could not be related to any of the parameters measured. Day by day analysis showed that while *E. huxleyi*, that dominated the coccolithophore community in winter, was not affected by elevated pCO_2 at any time. In contrast, the abundance of *Rabdosphaera clavigera*, the dominant species in summer, increased with time and this increase was affected at elevated pCO_2. Finally, elevated pCO_2 had no traceable effect on *E. huxleyi* (type A) coccolith morphology or on the degree of coccolith calcification. Our results highlight the possibility that, in oligotrophic regions, nutrient availability might exert

larger constrains on the coccolithophore community structure than high pCO_2 does solely. They also show that a differently coccolithophore community response based on species-specific sensitivities to pCO_2 is likely.

4.1. Introduction

Ocean pH has decreased by 0.1 units since the industrial revolution as a consequence of the absorption by the ocean of CO_2 originating from anthropogenic activities (Feely et al. 2009). If CO_2 emissions continue following the " business as usual" scenario (Representative Concentration Pathway; RCP8.5), the projected further decrease in pH for the end of the century is of 0.43 units and will imply a reduction of 56% in carbonate ion concentration (Gattuso et al. 2014).

Marine phytoplankton fixes nearly half of the total primary productivity on Earth (Field et al., 1998). This carbon accounts for approximately two-thirds of the vertical gradient of carbon in the ocean, the rest is attributed to the "solubility pump" (Passow and Carlson 2012 and references therein). The effects of ocean acidification on phytoplankton would likely depend on the group considered (Rost et al. 2008). On one hand, photosynthesis, and thus particulate organic carbon (POC) production is thought to be stimulated in species with poorly efficient carbon concentration mechanisms, such as coccolithophores (Paasche 1964, Buitenhuis et al. 1999, Rost et al. 2003, Bach et al. 2013), whereas in diatoms, photosynthetic carbon fixation rates are probably close to their maximum at present day CO_2 levels (Rost et al. 2003, Rost & Riebesell 2004). On the other hand, the phytoplanktonic groups producing calcareous crystals and plates covering the cell (e.g. coccolithophores, calcareous dinoflagellates) are expected to be strongly affected by ocean acidification through the decrease in carbonate ions (van de Wall et al. 2013, Meyer and Riebesell 2015).

Calcification is a process that releases CO_2 back to the atmosphere, but also favours the export of carbon as calcium carbonate ($CaCO_3$). Worldwide, coccolithophores (Haptophyta) contribute about half of the modern marine pelagic $CaCO_3$ sedimentation (Broecker & Clark 2009, Frenz et al. 2005) Furthermore, coccolithophore $CaCO_3$ can enhance sinking velocities of biogenic organic aggregates up to 100% (Lombard et al.

2013; Ziveri et al. 2007). Therefore, this important process can favour the export of inorganic and organic carbon to the deep ocean.

The state of knowledge on the impacts of elevated partial pressure of CO_2 (pCO_2) on coccolithophores is mainly derived from laboratory culture experiments on few species (mostly *Emiliania huxleyi*) and few genotypes within these species (see comprehensive review of Meyer & Riebesell 2015). In order to assess the effects of changing seawater carbonate chemistry on natural phytoplankton communities, with different genotypes that co-exist and with intra- and inter-specific competition, pCO_2 manipulations in large seawater volumes entrapping entire communities are necessary if we are to understand the effects on food webs, carbon export and other attributes of the pelagic ecosystem functioning. Mesocosms, that are defined as experimental enclosures from one to several thousands of litres that maintain natural communities under close-to-natural conditions (Riebesell et al. 2008, 2013), have been increasingly used in both aquatic and terrestrial ecology (Stewart et al. 2013). Mesocosms offer the possibility to study the effects of environmental and/or anthropogenic disturbances on a large variety of chemical and biological processes.

Past studies (in ship-board and large mesocosm experiments) have shown increased coccolithophore abundances (mostly *E. huxleyi)* under elevated pCO_2 conditions (Riebesell et al. 2000; Engel et al. 2005; Paulino et al. 2008; Feng et al. 2009) or showed maximum values at present day pCO_2 (Engel et al. 2008). While most studies showed a stimulation of organic growth, calcification has been shown to decrease (Riebesell et al. 2000; Delille et al. 2005) or to remain unchanged (Bellerby et al. 2008, Feng et al. 2009) under elevated pCO_2 conditions.

As shown above, most previous mesocosm experiments agree with the theoretical expectations that account for the effects of CO_2 on photosynthesis and calcification. It must be stressed, that, during these experiments, phytoplankton blooms were induced by nutrient additions. This is a common approach because it allows smaller sample volumes and does not impose nutrient limitation stress to the organisms in a close system. However, more that 60% of the ocean is oligotrophic (Longhurst et al. 1995). In these regions, coccolithophores generally dominate the phytoplankton community (Rost et al. 2003,

Baumann et al. 2004). In addition, it has been hypothesized that coccolithophores may increase their calcification rates when nutrients become limited; this is counterintuitive but could be related to the calcification generating protons that can be used in exchange for nutrient ions (McConnaughey & Whelan 1997). Therefore, some important questions arise, specifically to low nutrient low chlorophyll areas: How will coccolithophore calcification be affected if nutrient limitation and increased pCO_2 have, in theory, opposite effects? Would coccolithophore growth still be enhanced by elevated pCO_2 under oligotrophic conditions? If so, would this lead to a dominance of coccolithophores over other phytoplankton groups?

Among coccolithophores, species-specific sensitivities of calcification and growth rate to ocean acidification exist (Langer et al. 2006). These differences could affect these two processes at the community level. Even further, coccolithophore species have different growth strategies. Some species are typical of oligotrophic conditions while other "opportunistic", bloom according to nutrient inputs (Ziveri et al. 2004, de Vargas 2007). These specific differences raise an additional question: will the responses to elevated pCO_2 at the community level, change according to the initial coccolithophore assemblage?

The semi-enclosed Mediterranean Sea is an ideal place for exploring these questions because, due to its anti-estuarine circulation, nutrients are washed away towards the Atlantic Ocean maintaining a meso- to oligotrophic status in the western basin and an ultra-oligotrophic status in the eastern basin. Coccolithophores are conspicuous all along the Mediterranean Sea (Knappertsbusch 1993; Ignatiades et al. 2009, Oviedo et al. 2015), and in its coastal waters (Dimiza et al. 2008, Garrido et al. 2014). In the Eastern Mediterranean Sea, coccolithophores are the main contributor of biogenic $CaCO_3$ precipitation throughout the year (Knappertsbusch 1993, Ziveri et al. 2000, Malinverno et al. 2003). Its ballasting role (Klaas & Archer 2002, Ziveri et al. 2007) is suggested to explain the high organic matter fluxes in the Ionian Sea (Malinverno et al. 2014).

In the framework of the European Mediterranean Sea Acidification in a changing climate (MedSeA) project (http://medsea-project.eu), the effect of ocean acidification on plankton community has been investigated based on mesocosm experiments conducted in two

different sites of the Northwestern Mediterranean Sea, during two contrasting seasons (summer *vs.* winter). Here we report on the results on coccolithophore community structure, coccolith morphology, apparent degree of calcification in *E. huxleyi*, and the relative abundances of coccolithophores versus siliceous-phytoplankton main groups.

4.2. Methods

4.2.1. Experimental design

Fully described in Gazeau et al. (submitted), the experimental design consisted in a gradient of elevated pCO_2 levels (perturbation treatments; P1 to P6) and a triplicated control under ambient conditions (controls; C1 to C3). Nine mesocosms were deployed in June 2012 in the Bay of Calvi (BC; Corsica, France; 42°34'48" N, 8°43'33" E) and in February 2013 in the Bay of Villefranche (BV; France; 43°41'49" N, 7°18'43" E). Ambient pCO_2 levels in the two sites and seasons were different (i.e., ~ 450 *vs.* 350 µatm in BC and BV, respectively). As a consequence, the targeted elevated pCO_2 levels were also different. In BC, these were P1: 550, P2: 650, P3: 750, P4: 850, P5: 1000 and P6: 1250 µatm. In BV, the levels were P1: 450, P2: 550, P3: 750, P4: 850, P5: 1000 and P6: 1250 µatm.

The mesocosm structure (fully described in Guieu et al. 2014) consisted of large polyethylene-vinyl acetate bags of 0.5 mm thickness (HAIKONENE KY, Finland). They were 2.3 m in diameter and 12.5 m in height for the cylindrical, upper part, and 2.2 m for the conical part at the bottom (total volume of ~50 m^3). The cylindrical bags were ballasted and filled with ambient seawater. A 5 mm mesh screen covering the bottom plates excluded larger organisms. In order to avoid atmospheric deposition, the tops of the mesocosms were covered with UV-transparent ETFE roofs. These covers were elevated to ~10 cm above the top of the structure, allowing air to circulate. They were partially opened during sampling. pCO_2 levels were modified by adding various volumes of filtered (5 mm mesh) CO_2 saturated seawater. A diffusing system was used to ensure a better mixing of this CO_2 saturated seawater inside the mesocosms. In order to minimize the stress induced by the addition of large quantities of acid water, the acidification of the mesocosms was performed over 4 days (for more details see Gazeau et al. submitted). In BC, the

experiment lasted 20 days (June 24th, 2012 = day 0 to July 14th, 2012 = day 20) while, in BV, the experiment was stopped after 12 days (February 21st, 2013 = day 0 to March 5th, 2013 = day 12) as a consequence of bad weather conditions (see Gazeau et al. submitted).

4.2.2. Environmental parameters

Conductivity-temperature-depth (CTD) casts were performed on a daily basis in each mesocosm during both experiments. A Sea-Bird Electronics (SBE) 19plusV2 system, operated with several probes placed in a laminar flow entrained by a pump provided 0.25 m resolution continuous profiles for temperature, salinity, density, dissolved oxygen, fluorometry and irradiance, between 0 and 10 m depth.

Methods used to measure the different parameters of the carbonate chemistry are fully described in Gazeau et al. (submitted). In brief, seawater samples for total alkalinity (A_T) and dissolved inorganic carbon (C_T) measurements were collected daily. A_T was determined potentiometrically (Metrohm© Titrando) according to Dickson et al. (2007) and C_T was determined using an inorganic carbon analyser (AIRICA, Marianda©) coupled to an infrared gas analyser (LI-COR© 6262). All other parameters of the carbonate chemistry were determined from C_T and A_T using the R package seacarb (Lavigne et al. 2014).

Samples for pigments analyses (including total Chl *a* shown here) were taken every day. Two litres of sampled seawater were filtered onto GF/F. Filters were directly frozen with liquid nitrogen and stored at -80 °C pending analysis at the Laboratoire d'Océanographie de Villefranche (France). Filters were extracted at -20 °C in 3 mL methanol (100%), disrupted by sonication and clarified one hour later by vacuum filtration through GF/F filters. The extracts were rapidly analyzed (within 24 h) by high performance liquid chromatography (HPLC) with a complete Agilent Technologies system. The pigments were separated and quantified as described in Ras et al. (2008).

The protocols followed for nutrient analyses are described in Louis et al. (submitted). Briefly, phosphate (PO_4^{3-}) was measured using a Liquid Waveguide Capillary Cell (LWCC) made of a 2.5 quartz capillary tubing and connected to a spectrophotometer. The

limit of detection was 1 nM. Repeatability and reproducibility were ~ 4.8% and 7%, respectively. Nitrate + nitrite (NO_x) was measured spectrophotometrically with a 1 m LWCC. The limit of detection was ~10 nM and the reproducibility was ~6%. Silicate (Si) was measured using a Skalar AutoAnalyser.

4.2.3. Sampling and phytoplankton analyses

Water sampling for taxonomical analyses was conducted from June 25th (day 1) to July 11th (day 17) 2012 at ~8:30am (local time) in BC and from February 21st (day 0) to March 5th (day 12) at ~10:00am (local time) in BV. During both experiments, samples were taken every other day integrating the first 10 m of the mesocosm water column. A 5 L integrated water sampler (IWS; HYDRO-BIOS©) was used for that purpose.

Samples for taxonomical analyses were gently filtered onto acetate cellulose membranes (Millipore, 0.45 μm pore size, 47 mm diameter). Membrane filters were oven-dried at 40 °C for ca. 12 h and stored in sealed Petri dishes. In BC, between 3.6 and 5 L of water were filtered for that purpose. In BV, the volume was lowered to 1 to 3.5 L. A portion of each filter was placed on aluminium stubs and gold-coated using an EMITECH K550X sputter coater. Samples were observed under a ZEISS-EVO MA10 scanning electron microscope (SEM) at 3000x. Phytoplankton groups were quantified as coccolithophores, diatoms, and silicoflagellates. Cell densities (number of cells per L of seawater) were calculated from the counts and the volume of water observed. In samples with very few coccospheres, larger portions of the filter were observed. Nevertheless, due the very low cell densities in BC samples, only day 1 and day 17 were analysed. In BC, the observed portions corresponded to an average of 7.3 mL of seawater (min. 3.2 and max. 11.5 mL). In BV, on average 2.3 mL (min. 1.5 and max. 4.3 mL) were observed. The corresponding detection limits were then calculated from Bollmann et al. (2002). For samples of BC, the detection limit was ~400 cells L^{-1} and for samples from BV it was ~1200 cells L^{-1}. When a small volume was analyzed, a minimum of 100 coccospheres were quantified. In BC, even when looking at larger volumes of seawater, only between 52 and 265 cells were counted. In BV, between 101 and 418 cells were counted. Lower (CL) and upper (CU) confidence intervals at 95% significance were estimated following Bollmann et al. (2002). For a 52-cells count, these were CL= 40 and CU= 68 cells, and for a 418-cell count: CL= 380 and CU= 460

cells. Coccolithophore species were identified to a species level following Young et al. (2003). Diatoms were classified by size (< 20 μm, 20 - 80 μm, > 80 μm) and by taxonomic order (pennales *vs.* centrales). The larger diatom size class was often below detection limits. Thus, for statistical purposes, it was not taken into account by itself, but it was included within "total diatoms".

4.2.3.1. Emiliania huxleyi coccoliths

When attached to coccospheres, *Emiliania huxleyi* coccoliths were classified in: malformed (asymmetrical), incomplete (when the external rim and/or all elements were absent) or normally developed (inner tube circle, external rim and all distal shield elements were well formed and the latter symmetrically distributed around the inner tube circle). In turn, normally developed coccoliths were sub-classified according to their degree of calcification into: over-calcified (when distal shield elements were thicker to the point that half or more were fused, usually but not always the inner tube circle was also thicker), normally-calcified coccoliths (when individual distal shield elements clearly displayed the space between them) and under-calcified (when the space between elements was wider, elements, external rim and inner tube circle were thin). On average, 518 coccoliths per sample (min. 247; max. 919) were classified. The very low *E. huxleyi* cell densities in the samples from BC impeded a robust morphological analysis its coccoliths in these samples.

4.2.4. Statistics

All environmental data used here are available on Pangaea, Bay of Calvi: http://doi.pangaea.de/10.1594/PANGAEA.810331 and Bay of Villefranche: http://doi.pangaea.de/10.1594/PANGAEA.835117.

Stepwise multilinear regression analyses were performed to test for the effects of the carbonate chemistry perturbation treatments and other measured environmental variables on the response variables during the whole course of the experiments and for the first and last sampled days. Percentage data (i.e. coccolith morphology related data) were arcsin transformed prior analysis. Analyses were performed using the SPSS v.18 software.

Additionally, the E-PRIMER v.5 package was used for the following analyses: (1) multidimensional scale ordination (MDS) of coccolithophore species abundances: 2D plots were used to visualize similarities in the community structure among the different samples, (2) the SIMPER routine was run to analyse similarities and dissimilarities in the community structure among the different treatments along time; (3) the BIOENV routine was used to detect the set of environmental variables that yielded the highest Rho–Spearman rank correlation "best fit" with the biological data. The environmental variables used in this routine were: salinity, temperature, oxygen, pCO_2, and the concentrations of bicarbonate ion (HCO_3^-), carbonate ion (CO_3^{2-}), NO_3^-, and PO_4^{3-}. Except for PO_4^{3-} for the BC experiment and oxygen in the BV experiment due to missing data. For running these routines, similarity matrices were generated using the Bray–Curtis similarity coefficient and Euclidean distances for the biological and environmental data respectively.

4.3. Results

The evolution of environmental parameters during the two experiments can be seen in Figures 4.1 and 4.2 (BV and BC respectively). During the BV experiment, pCO_2 declined sharply as a consequence of strong winds and sea surface turbulence that favoured CO_2 degassing at the air-sea interface. After 4 days of experiment (day 4), pCO_2 levels in P1 and P2 were similar and at day 6, P1, P2, P3 and P4 reached similar levels in terms of pCO_2. P5 and P6 remained well separated until the end of the experiment, although pCO_2 levels also declined (see Gazeau et al. submitted, for more details). In BC, pCO_2 levels in P1 and P2 remained relatively constant and well separated from each other during the entire experiment. In contrast, due to CO_2 degassing at the air-sea interface, pCO_2 levels in P5 reached the levels of P4 after 14 days of experiment.

During the winter (BV) experiment, temperature remained more or less stable at ca. 13 °C during all the experiment and salinity increased slightly as a consequence of evaporation (see Gazeau et al. submitted, this issue, for more details). Initial [PO_4^{3-}] was 10.4 ± 2.2 nmol L^{-1}, with no strong variations. [NO_3^-] at day 0 was 0.13 ± 0.03 μmol L^{-1}, stable until day 3. A general increase in [NO_3^-] occurred between day 3 and day 9, after which it

remained constant to be 0.31 ± 0.12 µmol L^{-1} on the last sampled day. [Si] fluctuated between 0.90 µmol L^{-1} and 1.45 µmol L^{-1} with increasing variability towards the end of the experiment. [DFe] was on average 2.5 ± 1.2 nmol L^{-1}. When sampling started (day 0), [chl-*a*] was on average 1.1 ± 0.1 µg L^{-1} and steadily decreased until the end of the experiment (day 12). During the experimental period, O_2 concentrations remained constant close to saturation. All parameters were homogeneous in the water column (data not shown).

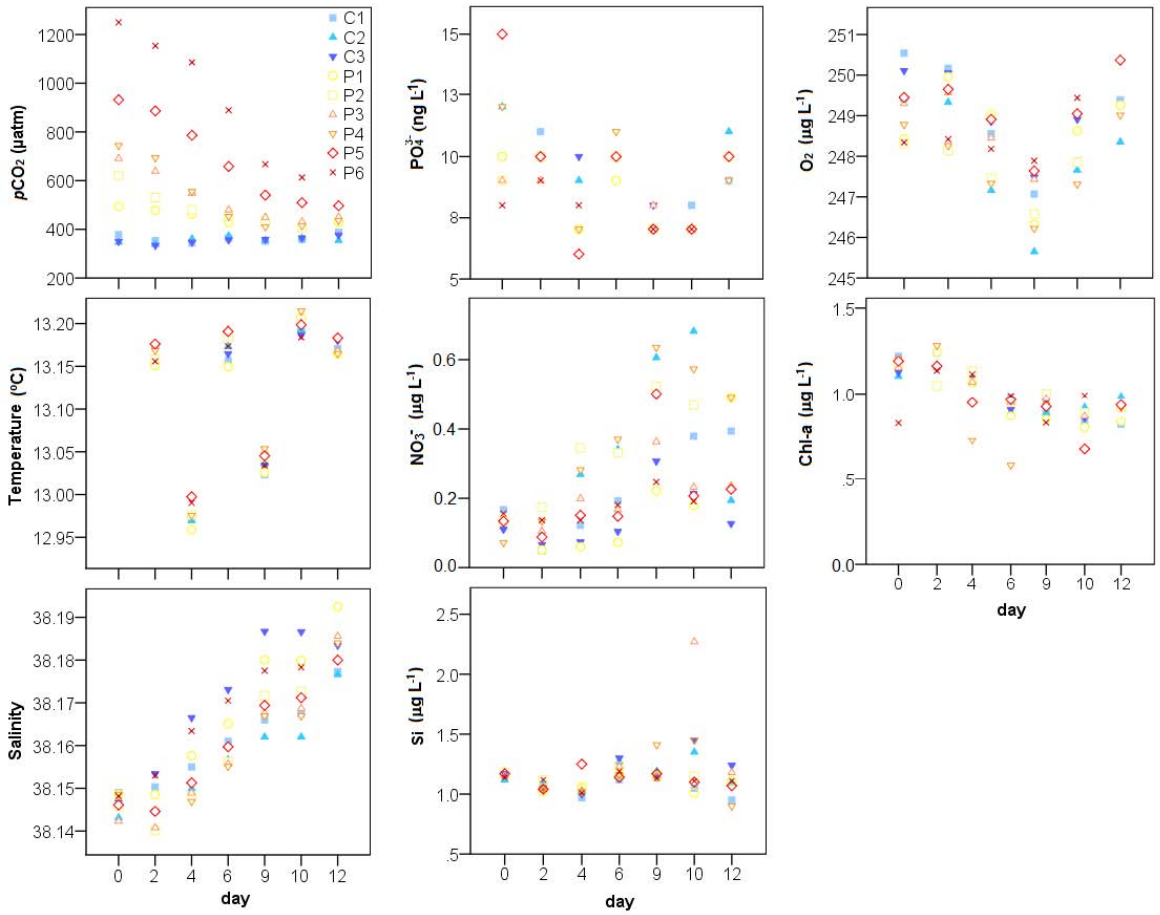

Figure 4.1 Environmental parameters in the different mesocosm bags during the experiment in the Bay of Villefranche (BV). Partial pressure of CO_2 (pCO_2), temperature, salinity, phosphate (PO_4^{3-}), nitrate (NO_3^-), silicate (Si) and dissolved oxygen (O_2) are presented for the 9 mesocosms: C1 to C3 for triplicate controls and P1-6 for increasing levels of CO_2.

The summer experiment performed in BC started with [PO_4^{3-}] of 22.8 ± 4.1 nmol L^{-1}, rapidly (from day 0 to day 1) decreasing to 3 - 12 nmol L^{-1}, [NO_3^-] of 0.097 ± 0.024 µmol L^{-1}, [Si] of 1.68 ± 0.03 µmol L^{-1} and initial [chl-*a*] < 0.06 µg L^{-1}. During the BC experiment, [chl-*a*] increased showing maximal values on day 14 (average between the 9 mesocosms, 0.09 ± 0.01 µg L^{-1}). Temperature levels increased on average from ~22.1 °C

on day 0 to ~24.7 °C on day 17. As in BV, salinity increased as a consequence of evaporation during the experiment. Nevertheless, during all the experiment the water column was homogeneous in terms of salinity.

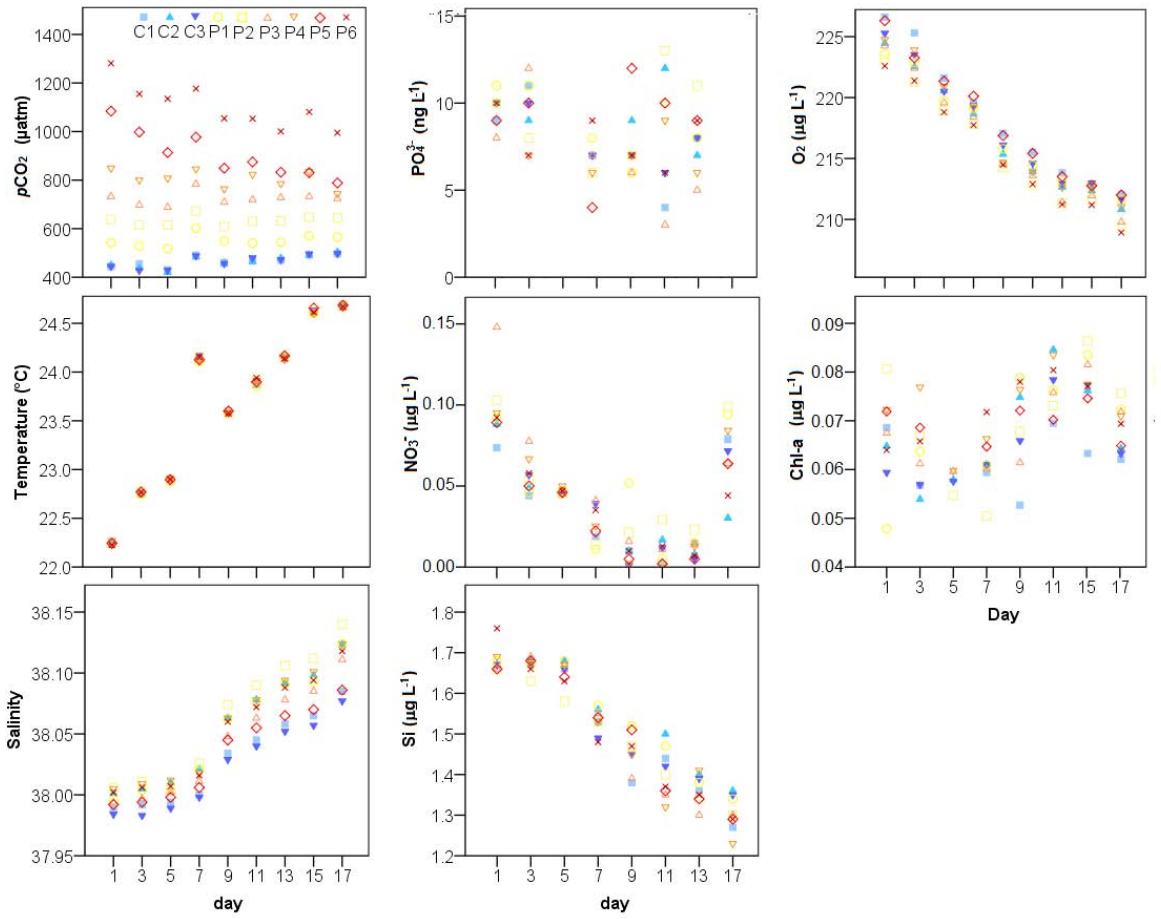

Figure 4.2 Environmental parameters in the different mesocosm bags during the experiment in the Bay of Calvi (BC). Partial pressure of CO_2 (pCO_2), temperature, salinity, phosphate (PO_4^{3-}), nitrate (NO_3^-), silicate (Si) and dissolved oxygen (O_2) are presented for the 9 mesocosms: C1 to C3 for triplicate controls and P1-6 for increasing levels of CO_2.

4.3.1. Coccolithophore, diatom and silicoflagellate communities

In BV, higher cell densities were recorded on day 0, after which a general decrease was observed until the end of the experiment (Figure 4.3). Initial cell densities of coccolithophores, diatoms and silicoflagellates in this experiment ranged from 8.7 x 10^4 to 1.1 x 10^5 cells L^{-1} for coccolithophores, 3.7 x 10^4 to 1.2 x 10^5 cells L^{-1} for diatoms and 1.7 x 10^3 to 4.4 x 10^3 cells L^{-1} for silicoflagellates. This represented a contribution of 28-51%

for diatoms, 48-71% for coccolithophores and 1-2% for silicoflagellates. The temporal dynamics of coccolithophore and diatom cell densities showed the largest decrease in the first three days (Figure 4.3) and few changes during the rest of the experiment. No change with elevated pCO_2 was observed in the abundances of the phytoplankton groups monitored, nor in the coccolithophores:diatoms ratio (Table 4.1). Regarding the species composition, in BV, the coccolithophore assemblage was dominated by *E. huxleyi* (48 to 82%) followed by *Syracosphaera marginoporata* (0 to 29%), *S. ossa* (0 to 24%) and *S. molischii* (0 to 21%). An increase in the species *S. marginoporata* with increasing pCO_2 was significant (Table 4.1) but driven only by an increase of this species abundance in the P6 treatment of day 0, as seen in Figure 4 and confirmed by further day-by-day regression analysis (Table 4.1).

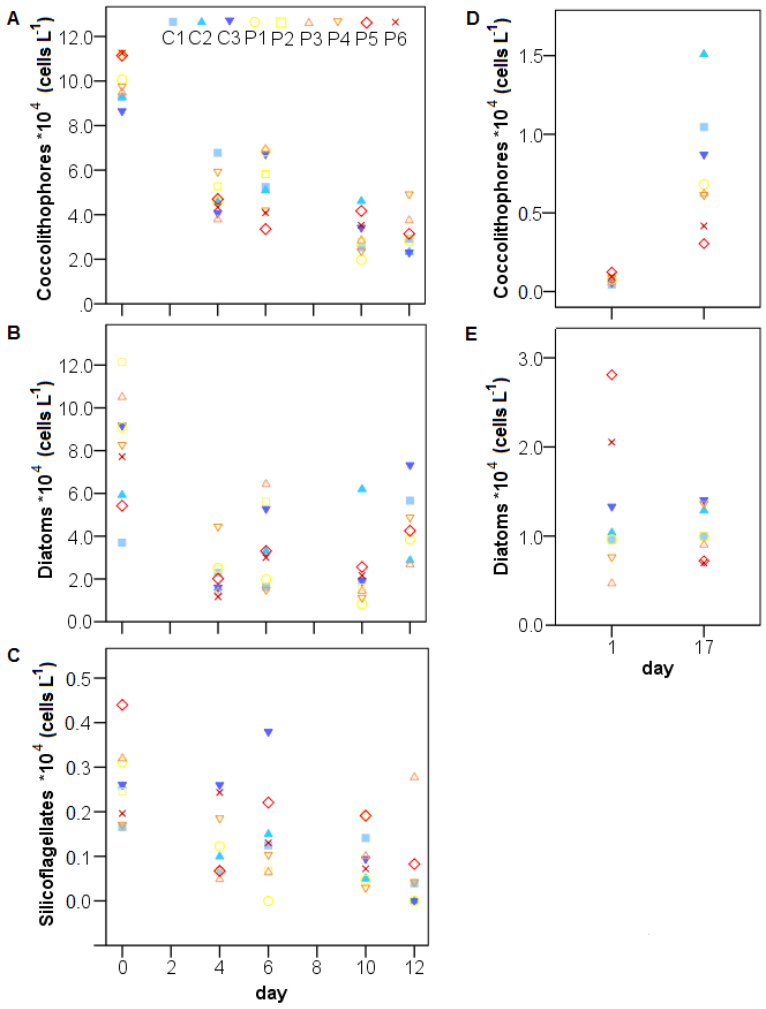

Figure 4.3 Abundances of the dominant phytoplankton groups recorded during the experiment in the Bay of Villefranche (A, B, C) and in the Bay of Calvi (E, F) and comparison with POC concentrations during both experiments (D and G, respectively). In the Bay of Calvi, silicoflagellates were only seen in few samples and are not plotted. C1 to C3 for triplicate controls and P1-6 for increased levels of CO_2.

The best fitting multivariable regression model that explained coccolithophore abundances in BV (Table 4.1) included a negative relationship with salinity and NO_3^- and a positive effect of temperature. Diatom abundances in BV were also positively related to temperature and negatively to salinity. The coccolithophores:diatoms however, showed a decreasing trend with temperature. Silicoflagellate abundances were positively related to $[PO_4^{3-}]$ and negatively with salinity (Table 4.1).

Table 4.1 Results from the stepwise regression analyses performed using data from all days and from the first and last sampled days during the experiment in the Bay of Villefranche. Input variables were: partial pressure of CO_2 (pCO_2), temperature (T), salinity (S), nitrate (NO_3^-), phosphate (PO_4^{3-}) and silicate (Si). βst. values are the standardized coefficients. NS = no statistically significant model (at a risk $\alpha = 0.05$).

Day	Response variable	p	F	Adj. r^2	N	Variables	βst.
All	Coccolithophore abund.	0.000	29.5	0.676	43	S	-0.686
						T	0.395
						NO_3^-	-0.262
All	*E. huxleyi* abund.	0.000	26.4	0.650	43	S	-0.696
						T	0.379
						NO_3^-	-0.226
All	*S. marginoporata* abund.	0.000	24.5	0.632	43	S	-0.518
						T	0.519
						pCO_2	0.327
All	*S. ossa* abund.	0.000	16.9	0.539	43	T	0.472
						PO_4^{3-}	0.365
						S	-0.280
All	Diatom abund.	0.001	8.6	0.285	43	T	0.520
						S	-0.389
All	Diatom (<20μm) abund.	0.001	9.0	0.296	43	T	0.521
						S	-0.407
All	Diatom (20-80μm) abund.	NS					
All	coccolithophore:diatoms	0.002	11.7		43	T	-0.490
All	Silicoflagellates abund.	0.006	5.9	0.204	40	PO_4^{3-}	0.373
						S	-0.317
All	% Under-calcified liths	0.038	4.6	0.081	41	S	0.321
All	% Over-calcified liths	0.026	5.3	0.096	43	T	0.343
All	% Malformed liths	0.000	15.0	0.254	43	S	0.522
0	Coccolithophore abund.	0.018	10.5	0.575	9	pCO_2	0.797
0	*E. huxleyi* abund.	NS					
0	*S. marginoporata* abund.	0.014	11.4	0.748	9	pCO_2	0.777
						PO_4^{3-}	-0.492
0	*S. ossa* abund.	NS					
0	Diatom abund.	NS					
0	Diatom (<20μm) abund.	NS					
0	Diatom (20-80μm) abund.	0.002	497.3	0.996	9	Si	0.981
						NO_3^-	0.278
0	coccolithophore:diatoms	NS					
0	Silicoflagellates abund.	0.032	14.5	0.771	9	PO_4^{3-}	0.910
12	Coccolithophore abund.	NS					
12	*E. huxleyi* abund.	NS					
12	*S. marginoporata* abund.	NS					
12	*S. ossa* abund.	NS					
12	Diatom abund.	NS					
12	Diatom (<20μm) abund.	NS					
12	Diatom (20-80μm) abund.	NS					
12	coccolithophore:diatoms	NS					
12	Silicoflagellates abund.	NS					

In BC, initial cell densities of coccolithophores ranged from 440 cells L^{-1} to 1.2 x 10^3 cells L^{-1} and diatoms densities varied between 1.0 x 10^4 and 2.8 x 10^4 cells L^{-1} (Figure 4.3, D and E). No silicoflagellates were observed at any time. Higher cell densities were recorded at the end of the experiment (day 12). Coccolithophore abundance on this day ranged from 3 x 10^3 to 1.5 x 10^4 cells L^{-1} and for diatoms from 7 x 10^3 to 1.4 x 10^4 cells L^{-1} (Figure 4.3). Diatoms contributed between 86 and 92% of the phytoplankton recorded at the start of the experiment (day 1), but its contribution decreased on day 17 to 46-70%, while coccolithophore contribution increased from an initial 4-10% to 30-54%. At the end of the experiment, higher coccolithophore abundances were related to the species *Rabdosphaera clavigera*, that represented between 60 and 85% of total coccolithophores (Figure 4.4). Together with *E. huxleyi*, these two species represented more than 90% of the coccolithophore assemblage in BC. When analysing the data of the beginning and end of the experiment together, no change with enhanced pCO_2 was observed during BC in any of the variables studied. When analysing the two sampling events separately, a decrease in coccolithophore abundances with increasing pCO_2 on day 17 was evidenced (Table 4.2), concomitantly with a decreasing trend with elevated pCO_2 for the species *R. clavigera* (Table 4.2; Figure 4.4).

Among the environmental variables used as input for the stepwise regressions, temperature was the only significantly related to coccolithophore abundances in BC (Table 4.2). Note that multivariable regression analyses for the whole data set and for day 17 were performed without [PO_4^{3-}] because no data was available for this day. Nevertheless, the data available for day 1 varied little (± 1 nmol L^{-1}) and this variation is below the detection limit. Thus, [PO_4^{3-}] did not significantly relate to coccolithophore abundances when data are available (Table 4.2, day 1). No statistically significant regression model was established for diatom abundances. The ratio coccolithophores:diatoms related positively to temperature (Table 4.2).

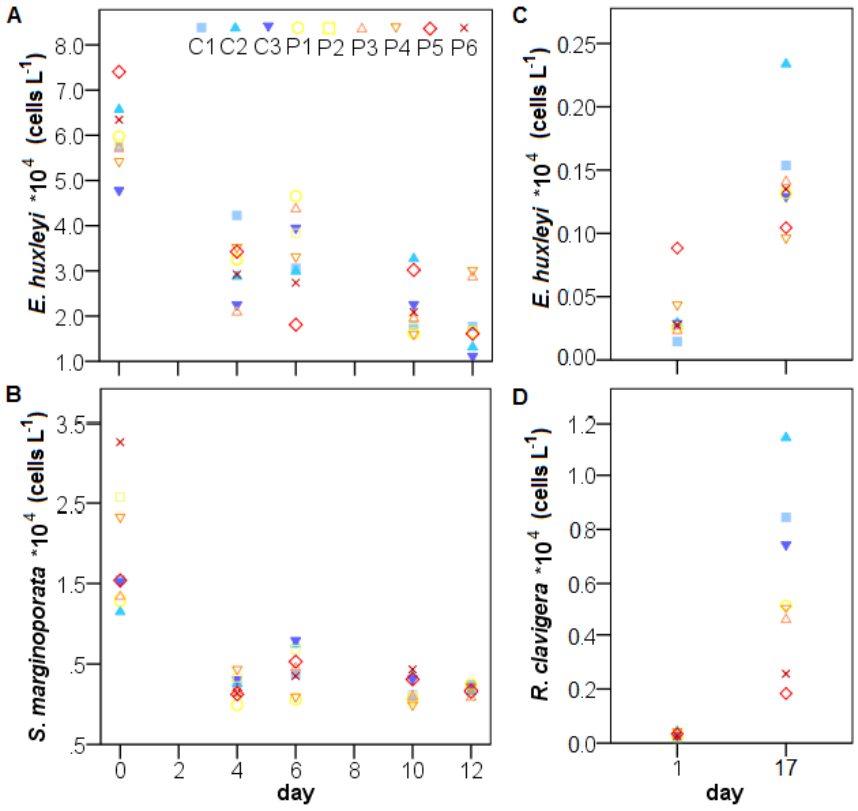

Figure 4.4 Abundances of the two dominant coccolitophore species during the experiment in the Bay of Villefranche (A, B) and in the Bay of Calvi (C, D). C1 to C3 for triplicate controls and P1-6 for increasing levels of CO_2.

Table 4.2 Results from the regression analyses performed using data from all days and from the first and last sampled days during the experiment in the Bay of Calvi. Input variables were: partial pressure of CO_2 (pCO_2), temperature (T), salinity (S), O_2, nitrate (NO_3^-), and silicate (Si). Phosphate (PO_4^{3-}) was used only for day 1. βst. values are the standardized coefficients. NS = no statistically significant model (at a risk $\alpha = 0.05$).

Day	Response variable	p	F	Adj. r^2	N	Variables	βst.
All	Coccolithophore abund.	0.000	21.6	0.596	16	T	0.79
All	*E. huxleyi* abund.	0.000	32.9	0.695	16	T	0.847
All	*R. clavigera* abund.	0.001	20.7	0.585	16	T	0.784
All	Diatom abund.	NS					
All	Diatom (<20µm) abund.	NS					
All	Diatom (20-80µm) abund.	NS					
All	coccolithophore:diatoms	0.000	38.3	0.727	16	T	0.864
1	Coccolithophore abund.	NS					
1	*E. huxleyi* abund.	NS					
1	*R. clavigera* abund.	NS					
1	Diatom abund.	NS					
1	Diatom (<20µm) abund.	NS					
1	Diatom (20-80µm) abund.	NS					
1	coccolithophore:diatoms	NS					
17	Coccolithophore abund.	0.006	16.4	0.814	8	pCO_2	-0.897
						NO_3^-	-0.546
17	*E. huxleyi* abund.	NS					
17	*R. clavigera* abund.	0.007	15.6	0.807	8	pCO_2	-0.925
						NO_3^-	-0.458
17	Diatom abund.	NS					
17	Diatom (<20µm) abund.	NS					
17	Diatom (20-80µm) abund.	NS					
17	coccolithophore:diatoms	NS					

The size distribution of diatoms (< 20, and 20-80) did not change with increasing pCO_2 during any of the two experiments (Tables 4.1 and 4.2). Nano-sized diatoms were the most abundant type of diatoms during the two experiments from the beginning to the end. For instance, during the experiment in BC, small (~15 μm large) diatoms of the order pennales comprised more than 63% of total diatoms. During the experiment in BV, small diatoms (~5-15 μm large) of the order centrales were the most abundant type of diatom, comprising more than 70% of total diatoms.

4.3.2. The coccolithophore community structure

Forty-six coccolithophore species were observed in samples from BV versus 8 recorded in samples from BC (Appendix A). During both experiments, the community structure changed with time, but changes were independent of the pCO_2 treatment (Table 4.3, i.e., pCO_2 was not included within the environmental parameters that best related to patterns in community structure among the sampled treatments). In BV, average similarities in the community structure were higher within samples taken on the same date (71.9-84.4%) than within samples corresponding to the same pCO_2 treatment (55.2-61.4%). Additionally, dissimilarities between the controls and the different perturbed pCO_2 levels were relatively low and almost constant (36.2-39.2%).

Table 4.3 Rho values (ρ) for the best combinations of environmental variables explaining patterns in coccolithophore community structure during the experiment in the Bay of Villefranche (BV) and the one in the Bay of Calvi (BC). Input variables as in tables 1 and 2 respectively, with the addition of carbonate (CO_3^{2-}) and bicarbonate (HCO_3^-) ions concentration.

BV		BC	
Variables	ρ	Variables	ρ
S	0.587	O_2	0.742
S, $[PO_4^{3-}]$	0.585	S, O_2	0.742
T, S	0.584	O_2, $[NO_3^-]$	0.742
T, S, $[PO_4^{3-}]$	0.584	T, O_2	0.742
--	--	S, $[NO_3^-]$	0.738
--	--	S	0.728

MDS of all coccolithophores species also allowed visualizing differences in the community structure with time, but not among the pCO_2 treatments (Figure 4.5A). During

the BV experiment, changes in the community structure were related to salinity (rho = 0.587) and to the combination of salinity and PO_4^{3-} (rho = 0.585), followed by the inclusion of temperature (rho = 0.584; Table 4.3). For BC, the MDS allowed visualising differences in the community structure with time. Changes among the pCO_2 treatments, although insinuated (Figure 4.5B), proved not to be statistically significant (Table 4.3). The BIOENV results suggest that changes in the community structure were related to oxygen, salinity, temperature and $[NO_3^-]$ (rho = 0.742 for different combinations of these parameters; Table 4.3).

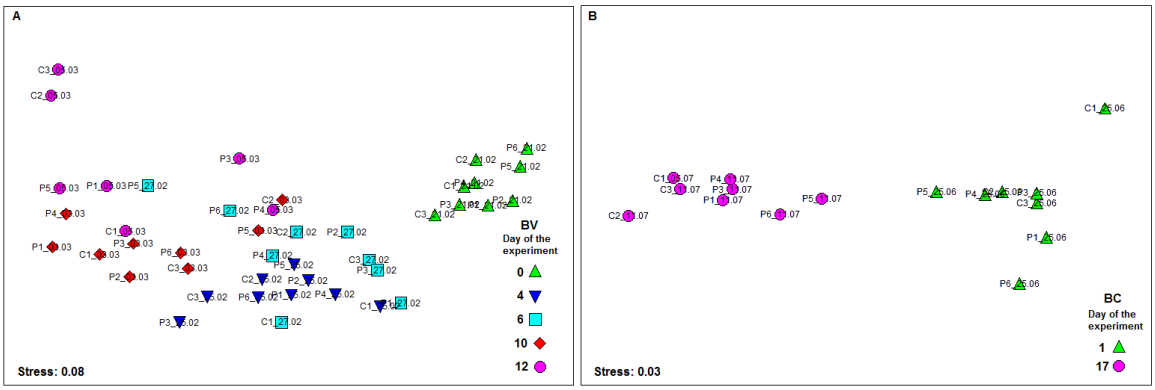

Figure 4.5 MDS plot performed with the similarity coefficients of the species abundance data (biological data) in the Bay of Villefranche (BV; A) and in the Bay of Calvi (BC; B). Sample labels include the treatment and the date of sampling (dd.mm). C1 to C3 for triplicate controls and P1-6 for increasing levels of CO_2.

4.3.3. *Emiliania huxleyi* coccoliths

During the BV experiment, the percentage of malformed coccoliths of *E. huxleyi* did not vary with CO_2 but related to salinity (Table 4.1). Higher percentages of overcalcified coccoliths were related to higher temperatures (Table 4.1). The percentage of malformed coccoliths was initially lower than 5%, but increased with time until maximum values near 20% (in one control and one pCO_2 perturbed mesocosm, Figure 4.6).

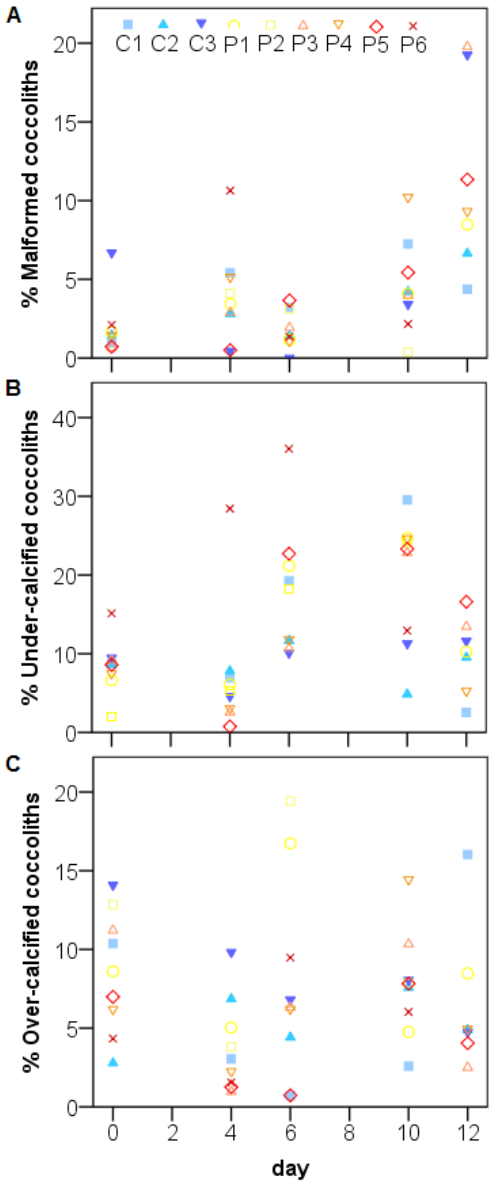

Figure 4.6 Percentage of malformed coccoliths (A), normal developed but under-calcified coccoliths (B) and normal developed but over-calcified coccoliths (C) in the different pCO_2 treatments: C1 to C3 for triplicate controls and P1-6 for increasing levels of CO_2.

4.4. Discussion

4.4.1. Environmental parameters and their dynamics with time

During the BV experiment, initial nutrient concentrations at the time of mesocosm closing and during the acidification phase were higher than in BC. However, inorganic nutrients were rapidly utilized by pico and nano-phytoplankton, causing the rise in Chl-*a* that reached 1.1 ± 0.1 µg L^{-1} on day 0 in BV (Gazeau et al. submitted). The actual mesocosm sampling was performed in low nutrient concentrations, characteristic of mesotrophic

regions. Although chl-*a* values recorded during the BV experiment (0.36 - 1.27 μg L^{-1}) were relatively low, weekly Chl-*a* measurements at the entrance of the Bay of Villefranche (time series Point B; http://somlit-db.epoc.u-bordeaux1.fr/bdd.php) confirmed that the values measured during the experiment were close to the highest recorded for the year 2013 (see Gazeau et al. submitted). Therefore, no real bloom occurred and then, environmental conditions encountered during the BV experiment can be qualified as pre-bloom conditions.

The BC experiment was performed in typical oligotrophic and stratified summer conditions of the Ligurian Sea (see Bosc et al. 2004). Maugendre et al. (in press) suggested the initial plankton community to be in metabolic balance. BC waters represented a source of CO_2 to the atmosphere as a consequence of its trophic state and temperature (Gazeau et al. submitted).

4.4.2. Temporal changes in coccolithophore, diatom and silicoflagellate communities

Coccolithophore cell densities were comparable to previous studies in the open Mediterranean, where a maximum of 2.3 x 10^5 cells L^{-1} (Knappertsbusch 1993) has been reported in the Levantine basin during late winter, though average abundances were ~4.4 x 10^4. In autumn, values of the order of x 10^3 to x 10^4 cells L^{-1} have been reported (Knappertsbusch 1993, Malinverno et al. 2003). During summer and in coastal regions, abundances are below 1 x 10^4 cells L^{-1} (Ignatiades et al. 2009 and Dimiza et al. 2008 respectively).

It has been hypothesized that coccolithophores have a competitive advantage over diatoms under more acidified waters, as predicted from the fact that at actual CO_2 levels, photosynthetic rates of coccolithophores are below CO_2 saturation whereas diatoms efficiently concentrate CO_2 near the carboxilation site and might not benefit from external increases in pCO_2 (Rost et al. 2003, Rost & Riebesell 2004). However, a pCO_2 mediated replacement of phytoplankton groups did not occur in any of the two experiments, where neither the dominance patterns, nor the phytoplankton group abundances changed among

pCO_2 treatments. Instead, temperature, salinity and [NO_3^-] were apparently more predictive of coccolithophore abundances (Table 4.1). Both, salinity and [NO_3^-] increased gradually with time during this experiment. The former within a very small range to affect the euryhaline *E. huxleyi* species (~38.14 to ~38.20, Figure 1). The latter slightly increased from day 3 to day 9 probably due to nitrification (Al-Moosawi et al. in preparation). Thus, the observed relationship with these parameters might just be an artefact of coccolithophores simultaneously decreasing with time (Figure 4.3), with no mechanism functionally connecting the observed trends. Regarding the effect of temperature, although this parameter affects phytoplankton growth rates (Huertas et al. 2011) and among phytoplankton, coccolithophores (Buitenhuis et al. 2008), during the BV experiment, variation in temperature was less than 0.4 ºC. The global distribution of *E. huxleyi* (dominant species during the BV experiment) covers temperatures from about 1 °C to 30 °C (Winter et al. 1994) and in a single strain from the Sargaso Sea a temperature shift of 4 °C (from 20 ºC to 24 ºC) did not cause a significant difference in PIC and POC responses (Feng et al. 2008). Thus, we do not believe temperature to be the sole, nor the main, parameter explaining coccolithophore abundances during the BV experiment. The same holds true for diatom abundance which was related to changes in temperature and salinity by stepwise regression. Correlation analyses suggest that [PO_4^{3-}] stimulated all the phytoplankton groups monitored (at $\alpha = 0.01$ for coccolithophores and $\alpha = 0.05$ for silicolfagellates and diatoms) but its effect was not significant enough, in relation to the effect of the other environmental parameters considered, as [PO_4^{3-}] was not included in the best fitted variables of stepwise regressions. Nevertheless, during the sampled dates the N:P among mesocosms increased from 13 ± 4 to 32 ± 17 which makes PO_4^{3-} limitation likely. Given that the abundances of coccolithophores, diatoms and silicoflagellates clearly changed with time independently of the pCO_2 treatment, it is also possible that: (1) species phenology determined phytoplankton abundance patterns. If this was the case, the phenologycal synchrony was maintained over the course of the experiment, with moderate variations due to [PO_4^{3-}], or (2) a non measured limiting resource caused the observed trends in phytoplankton abundances.

Temperature was also the variable that best explained coccolithophore abundances during BC mesocosm experiment, where coccolithophores were favoured over diatoms at the end of the experiment, which coincided with higher temperature levels. During this experiment,

temperature variability was ca. 2.5 ºC and then, the likelihood that could have had an effect on phytoplankton growth rate is higher than for the BV experiment. However, we cannot exclude the possibility that the relationship mainly describes simultaneous changes with time (Figures 2 and 3), as in the case of salinity during the BV experiment. In general, during the BC experiment, none of the parameters measured could be strongly related to changes in coccolithophore or diatom abundance. For this experiment, again, a phenological synchrony in the phytoplankton species could have determined the abundances patterns.

Shifts between the different phytoplankton groups under elevated pCO_2 conditions have been observed in previous studies and are generally associated to the group's cell size. However, while high pCO_2 on a equatorial pacific community led to the dominance of larger species (i.e. diatoms over nanoflagellates; Tortell et al. 2002), in an Artic community, elevated pCO_2 stimulated pico- and nano- phytoplankton which later led to a decrease in growth and biomass of the diatom community (Brussaard et al. 2013). A similar effect was detected in the Bering Sea, where coccolithophores eventually replaced larger phytoplankton (Hare et al. 2007). In Norwegian waters, no changes in phytoplankton dominance occurred (Paulino et al. 2008) due to increased pCO_2 but nutrient addition caused a shift from small picoplankton to *E. huxleyi* and diatoms. Our two experiments, performed under low nutrient conditions from the beginning to the end, showed no shift between phytoplankton groups. It must be mention that in these Mediterranean experiments, both coccolithophores and diatoms were mostly smaller than 15 μm large and thus, a shift in between them would have not meant a shift cell size. Thus, the initial characteristics of the phytoplankton community size structure, possible linked to the low nutrient levels, may have constrained any shift caused pCO_2 if these occur in relation to cell size. Even if this can be one explanation for the lack of shift during our experiments, it still does not explain why in the few mesocosm experiments performed to date, under nutrient replete conditions, all types of responses have already been observed (i.e. shifts towards larger and towards smaller phytoplankton, and no shift at all).

A similar argument could be used regarding lack of change in the size distribution of diatoms with increasing pCO_2. Feng et al. (2009), Tortell et al. (2008) and Eggers et al. (2014) have observed shifts from small to larger diatoms under elevated pCO_2 and

eutrophic conditions. In the latter study, the occurrence of the shift was dependent on the initial community composition. Contrarily to our experiment, in the above-mentioned mesocosm experiments, there were no nutrient constraints. During our experiments, nutrient availability could have been an external pressure favouring nanoplanktonic diatoms, limiting the build up of biomass associated with larger cell sizes.

4.4.3. Coccolithophore species-specific response

Although the apparent increase of *S. marginoporta* abundance with pCO_2 during the BV experiment is in agreement with previous observations where coccolithophore cell densities have been reported to increase (Engel et al. 2005, Hare et al. 2007, Paulino et al. 2008, Feng et al. 2009) we do not believe this species was actually stimulated by increasing pCO_2 during our experiment, as the increase was led by an extreme value of the highest pCO_2 (P6) in the first sampled day. Although observable only on one sampling event, the species *R. clavigera* during the BC experiment was apparently affected by enhanced pCO_2. Here, the decline in abundance with CO_2 is not the result of an extreme value in one mesocosm unit, but it gradually occurs among the treatments in the last sampled day (Figure 4.3, Table 4.2). This effect was not observed in BV because in this experiment *R. clavigera* cells were rare. Thus, although most changes in coccolithophore species abundance occurred in time and were probably of a phenological character, different sensitivities to elevated pCO_2 of the dominant species have the potential to drive different responses in total coccolithophore abundance. A recent study suggests that in the Mediterranean Sea, *R. clavigera* is preferentially distributed in waters with low nutrients, but may be affected by low [CO_3^{2-}] (Oviedo et al. 2015). Hence, relating its abundance to seawater carbonate chemistry. Overall, this could indicate that coccolithophore communities with different species composition may respond differently to ocean acidification. It implies that the populations of *E. huxleyi* present during our experiments were less affected (if at all) by elevated pCO_2 than *R. clavigera*. Nevertheless, it should be noticed that *R. clavigera* is not a bloom forming species and its absolute abundance in samples from the Atlantic, Pacific and Mediterranean oceans rarely pass the 10 $x10^3$ cells L^{-1}, which is reflected in a poor contribution of *R. clavigera* coccoliths to biogenic calcite in surface sediments (Kleijne 1992). Therefore, it is likely that even if a decrease in *R.*

clavigera abundance occurs due to enhanced pCO_2, the geochemical effects of this change may be small.

4.4.4. The coccolithophore community structure

To the best of our knowledge, this is the first study that analyses changes in the coccolithophore community structure (i.e. species composition, total and relative abundances) when manipulating pCO_2 in naturally occurring communities. Thus, direct comparisons are not yet possible. Nevertheless, employing the same analytical approach in a set of samples collected along a E-W transect in the Mediterranean Sea, Oviedo et al. (2015) observed that heterococcolithophores distribution patterns were highly related to carbonate chemistry and salinity. [PO_4^{3-}] also seemed to play an important role in unravelling the distribution of this coccolithophore life phase. In a similar approach, Charalampopoulou et al. (2011) associated changes in coccolithophore assemblage composition with the combination of irradiance and pH. Results from our two mesocosm experiments are not consistent with these previous findings in that carbonate chemistry was not found to be a structuring variable. Instead, nutrients (with PO_4^{3-} being important during the BV experiment and NO_3^- during BC), salinity (in both) and oxygen and temperature (in BC) appeared co-related variables. Salinity is not known to affect coccolithophore growth, and in both experiments it could just indicate that major changes occurred with time (as discussed in section 4.2). The same is true for temperature and oxygen during the BC experiment, which changed gradually on time. By contrast, nutrient availability is fundamental for phytoplankton growth and stoichiometry (Sverdrup 1953, Klausmeier et al. 2004). In specific, a [PO_4^{3-}] of 0.009 ± 0.007 μmol L^{-1} has proven to be limiting for coccolithophore growth in the Eastern Mediterranean Sea (Kress et al. 2005). This concentration was often reached during the two experiments. During the BV experiment, N/P ratio increased from 13 ± 4 to 32 ± 17, being below Redfield's ratio in one control only (C3). Therefore, some of the coccolithophore species present during BV could have been limited by PO_4^{3-}, which, in turn, could determine the species composition of the community. Nitrification during the BC experiment makes the relationship between [NO_3^-] and the coccolithophore community difficult to interpret (discussed in section 4.4.2).

4.4.5. *Emiliania huxleyi* coccoliths

Adverse effects of ocean acidification on coccolith morphology and calcite production were first suggested by Riebesell et al. (2000). Further culture experiments showed species-specific (Langer et al. 2006; Rickaby et al. 2010) and even strain-specific (Langer et al. 2011) sensitivity to increased pCO_2, which likely has a genetic basis. Increased coccolith malformation was observed in only two *E. huxleyi* strains out of the 4 tested by Langer et al. (2011) at > 900 μatm pCO_2 (note that our category of "malformed" includes Langer et al. categories "malformed" and "malformed and incomplete"). Bach et al. (2012) showed that in this common species, malformations are related to $[H^+]$, starting at a pH form ~8 down to 7.1. In naturally occurring populations, from ocean acidification mesocosm experiments and field studies, signs of harmed coccolith morphogenesis seem rare and ambiguous. For instance, an increase in *E. huxleyi* malformed coccoliths was recorded in a natural pH gradient near CO_2 vents off Vulcano Island, Italy (Meier et al. 2014). However, high pCO_2 and low pH were not fully linked to high proportion of malformed coccoliths. In fact, key factors such as the levels of exposure to elevated CO_2 at volcanic vents and small-scale hydrological/atmospheric factors (i.e. wind-driven currents) might have determined the effects on coccolith morphogenesis. During a mesocosm experiment in Norway, Engel et al. (2005) did not observe an increase in malformation in *E. huxleyi* coccoliths, consistently to observations made during our experiments. Towards the end of the BV experiment, we observed increased proportion of malformed coccoliths (e.g. in C3 and P3), probably indicating other disturbances affecting *E. huxleyi* coccolith morphogenesis. The outcome of the multivariable regression analysis suggests that increased percentage of malformed coccoliths was linked to increased salinity. However, in a culture experiment (Green et al. 1998), decreased salinity of the medium led to increased coccolith malformation, which opposes the results of the regression analysis and supports the idea that the relationship with salinity is not functional (as previously discussed).

Regarding the degree of calcification, although several previous studies on naturally occurring *E. huxleyi* populations suggest that its coccolith´s calcite decreases at elevated pCO_2 (Cubillos et al. 2007, Beaufort et al. 2011, Meier et al. 2014), others have observed no effect (Young et al. 2014) as in this study (Figure 4.6). It is important to note that our samples, as well as in Young´s et al. study, consisted almost entirely of *E. huxleyi*

morphotype A. Thus, if the previously observed decrease in *E. huxleyi* coccolith´s calcite associated to high pCO_2 is based on morphotypes sorting, our samples could not record it. In fact, Cubillos et al. (2007) claimed that, for *E. huxleyi* in the Southern Ocean, changes in calcite saturation states rather lead to shifts in dominance from the heavier calcified morphotype A to the poorly calcified morphotype B/C. On the same line, Beaufort et al. (2011) suggested that the association between calcification (i.e. calcite mass per coccolith), pCO_2 and the co-varying carbonate ion reflected the distribution of differentially calcified species and morphotypes according to carbonate chemistry. The decrease in the coccolith mass of *E. huxleyi* in sediment trap time series (from 1993 to 2005) observed by Meier et al. (2014) and related to changes in surface ocean carbonate chemistry can also reflect the distribution of differentially calcifying morphotype strains.

4.5. Conclusions

Overall, our results highlight the possibility that nutrient limitation in oligotrophic regions might exert larger constrains on coccolithophores than high pCO_2 does and prevail on determining the coccolithophore community structure. We did not detect any negative effect on *Emiliania huxleyi* abundance, coccolith morphology and degree of calcification of its coccoliths that could be attributed to elevated pCO_2. However, we cannot rule out the possibility that carbonate chemistry affects the distribution of *E. huxleyi* morphotypes whose coccoliths degree of calcification differs.

Given that most changes in phytoplankton abundances and community structure were time-dependent, and possibly linked to the initial community (i.e. composition and size structure), mesocosm studies ideally should be performed in different initial community conditions and covering different stages of a seasonal cycle. This will also allow studying the effects of increased pCO_2 on species phenology, which could have drove most of the observed changes. The influence of nutrient availability (i.e. phosphate) in Mediterranean coccolithophore responses to on-going environmental changes should be approached in multiple stressors studies.

Please note that Appendix A (Coccolithophore species list) is derived from this Chapter.

Chapter 5.

Is coccolithophore distribution in the Mediterranean Sea related to seawater carbonate chemistry?

Published as: Oviedo A, Ziveri P, Alvarez M, Tanhua T (2015) Is coccolithophore distribution in the Mediterranean Sea related to seawater carbonate chemistry?. Ocean Sci 11:13-32

Abstract

The Mediterranean Sea is considered a "hot-spot" for climate change, being characterized by oligotrophic to ultra-oligotrophic waters and rapidly changing carbonate chemistry. Coccolithophores are considered a dominant phytoplankton group in these waters. As marine calcifying organisms they are expected to respond to the ongoing changes in seawater carbonate chemistry. However, very few studies have covered the entire Mediterranean physicochemical gradients from the Strait of Gibraltar to the Eastern Mediterranean Levantine Basin. We provide here a description of the springtime coccolithophore distribution in the Mediterranean Sea and relate this to a broad set of *in situ* measured environmental variables. Samples were taken during the Meteor (M84/3) oceanographic cruise in April 2011, between 0 – 100 m water depth from 28 stations. Total diatom, and silicoflagellate cell concentrations are also presented. Our results highlight the importance of seawater carbonate chemistry, especially [CO_3^{2-}], and [PO_4^{3-}] in unraveling the distribution of heterococcolithophores, the most abundant coccolithophore life phase. Holo- and hetero-coccolithophores respond differently to environmental factors. For instance, changes in heterococcolithophore assemblages were best linked to the combination of [CO_3^{2-}], pH, and salinity (ρ = 0.57) although salinity might be not functionally related to coccolithophore assemblage distribution. Holococcolithophores, on the other hand, showed higher abundances and species diversity in oligotrophic areas (Best

fit, ρ = 0.32 for nutrients), thriving in nutrient depleted waters. Clustering of heterococcolithophores revealed three groups of species sharing more than 65% similarities. These clusters could be assigned to the eastern and western basins, and deeper layers (below 50 m), respectively. In addition, the species *Gephyrocapsa oceanica, G. muellerae* and *Emiliania huxleyi* morphotype B/C are spatially distributed together and trace the influx of Atlantic waters into the Mediterranean Sea. The results of the present work emphasize the importance of considering holo- and hetero-coccolithophores separately when analyzing changes in species assemblages and diversity. Our findings suggest that coccolithophores are a main phytoplankton group in the entire Mediterranean Sea and can dominate over siliceous phytoplankton. They have life stages that are expected to respond differently to the variability in seawater carbonate chemistry and nutrient concentrations.

5.1 Introduction

Marine phytoplankton constitutes about 1–2 % of the global biomass among primary producers (Falkowski 1994); however, it contributes to ~ 46 % of the primary production in a global scale (Field et al. 1998). Coccolithophores represent ~ 10 % of global phytoplankton biomass (Tyrrell & Young 2009). They play an important role in biogeochemical cycles, contributing to both the organic and inorganic carbon pumps through photosynthesis and calcification. The latter is the main process controlling PIC : POC (rain ratio). For instance, in the eastern Mediterranean Sea, they are the main contributor to the inorganic carbon pump ($CaCO_3$ production and flux) throughout the year (Knappertsbusch 1993, Ziveri et al. 2000, Malinverno et al. 2003).

Most studies looking at coccolithophore assemblages and distribution take into account parameters such as nutrients, photosynthetically active radiation (PAR), temperature, salinity and oxygen (e.g., Young 1994, Ziveri et al. 1995, Hagino et al. 2000, Takahashi & Okada 2000, Haidar & Thierstein 2001, Cortés et al. 2001, Ignatiades et al. 2009). Parameters related to the seawater carbonate system have only recently been considered due to their importance for calcification and the ongoing and projected changes directly related to the rapidly increasing atmospheric pCO_2. Carbonate chemistry parameters have

been suggested as drivers of coccosphere morphology modification in field samples (Beaufort et al. 2008, 2011, Meier et al. 2014, Triantaphyllou et al. 2010), *Emiliania huxleyi* blooms (Merico et al. 2006, Tyrrell et al. 2008), and changes in coccolithophore assemblage composition (Charalampopoulou et al. 2011). Although it is not clear why coccolithophores calcify, calcification is an energy-consuming process for coccolithophores (Brand 1994, Balch 2004), maintained by natural selection over millions of years, that changes the carbonate chemistry of their surrounding media. It is therefore plausible that the availability of the necessary resources for carrying out calcification (i.e. HCO_3^- and CO_3^{2-}) should facilitate coccolithophore´s growth in the ocean. In this context, it is important to understand how marine calcifying organisms could respond to the rapidly accumulation of atmospheric CO_2 and their interaction with ocean´s carbonate chemistry (Kroeker et al. 2013).

The Mediterranean Sea provides an ideal ground to explore the factors controlling coccolithophore distribution because of the well known large gradient in physicochemical parameters. It has a negative fresh-water balance with evaporation exceeding precipitation. Surface water temperature, salinity, total alkalinity (TA), [CO_3^{2-}] increase towards the eastern basin. The Mediterranean Sea is one of the most nutrient-poor regions of the global ocean (Dugdale & Wilkerson 1988), with a trophic status ranging from mesotrophic in the northwest to extremely oligotrophic in the east (Krom et al. 1991, Berman et al. 1984, Berland et al. 1988, Yacobi et al. 1995, Psarra et al. 2000). The spatial distribution of the phytoplankton community along an east–west transect shows that coccolithophores can dominate along the Mediterranean Sea; trough the Levantine, Ionian and Tyrrhenian basins (Ignatiades et al. 2009). Ocean acidification, warming and changes in nutrient availability are expected to significantly alter primary production rates, as well as the overall plankton community structure. Studies on coccolithophores distribution in the Mediterranean Sea are mostly regional (Dimiza et al. 2008, Malinverno et al. 2003), loosing part of the above-mentioned gradients. Additionally, carbonate chemistry parameters were not available in older studies focussed on the distribution of coccolithophores in the Mediterranean Sea. Thus comparisons between the different basins are scarce and the influence of carbonate chemistry parameters on actual coccolithophore assemblages remains therefore uncertain.

The present work investigates the regional and vertical distribution of living coccolithophores in the Mediterranean Sea with respect to *in situ* measured environmental parameters and with focus on those of the carbonate chemistry. It provides a description of the late springtime coccolithophore assemblage's composition and distribution in the Mediterranean Sea, with a basin resolution that has not been assessed before, and along physical and chemical gradients.

5.2. Methods

5.2.1 Sampling

A detailed water sampling was conducted during the M84-3 cruise from 6 to 28 April 2011 on board the R/V Meteor (Tanhua 2013, Tanhua et al. 2013a). Here we investigate a subset of 81 samples from 28 stations collected between 0 and 100 m water depth. Samples were taken using a carousel of 24 Niskin bottles and interfaced with the SBE911 CTD system (SeaBird) that provided the hydrographical data for in situ temperature, salinity and dissolved oxygen of the seawater samples. Samples collected at <1 m water depth were obtained by filling a 5 L plastic container with surface water. Between 1.5 and 4.5 liters of water were gently filtered onto acetate cellulose membranes (Millipore, 0.45μm pore size, 47mm diameter). Membrane filters were oven dried at 40ºC for ~ 12 hours and stored in sealed Petri dishes. Figure 5.1 shows the location of all sampled stations during the cruise trajectory. Table 5.1 shows the stations coordinates, dates and sampled depths. The bottle data can be found at: http://cdiac.ornl.gov/ftp/oceans/CLIVAR/Met_84_3_Med_Sea/.

Table 5.1: Location, date, and water depth from which the samples were collected.

.

Station	Month/day/year	Longitude (° E)	Latitude (° N)	Bot. depth (m)	Sampled depth (m) 100	50	25	5	0
287	4/6/2011	25.60	37.67	829	X*		X	X	
288	4/7/2011	26.22	35.65	2293			X	X	
291	4/8/2011	33.00	34.07	2474	X	X	X	X	
292	4/9/2011	35.17	33.99	1681				X	
293	4/9/2011	34.42	34.00	2034				X	
294	4/10/2011	31.00	33.70	2437	X	X	X	X	X
296	4/11/2011	28.77	33.58	2934			X		
297	4/11/2011	26.02	34.40	4210	X		X	X	
298	4/12/2011	24.33	34.50	3287			X	X	
299	4/12/2011	22.50	35.00	3117				X	
302	4/13/2011	20.35	35.07	2968	X	X	X	X	X
305	4/14/2011	17.25	35.60	4440			X	X	
306	4/15/2011	19.00	36.50	3445		X	X	X	
307	4/15/2011	19.30	37.90	3305				X	X
308	4/15/2011	19.00	38.50	3462	X	X		X	X
309	4/16/2011	18.80	39.50	805	X	X	X		
313	4/16/2011	18.00	41.25	1105			X	X	
316	4/19/2011	11.50	38.60	1665			X	X	
319	4/20/2011	11.30	40.30	2880				X	X
320	4/20/2011	10.61	38.75	2490	X			X	
321	4/20/2011	9.40	38.25	1565	X	X	X	X	
324	4/21/2011	5.60	38.65	2845	X	X	X	X	X
329	4/23/2011	2.00	37.90	2730	X	X	X	X	X
331	4/23/2011	0.00	37.05	2704	X	X	X	X	X
332	4/24/2011	−1.40	36.50	2340			X	X	
334	4/24/2011	−4.40	36.10	1228	X	X	X	X	
337	4/25/2011	−5.36	36.00	935	X	X	X	X	X
338	4/25/2011	−5.75	35.95	337				X	

* 75 m

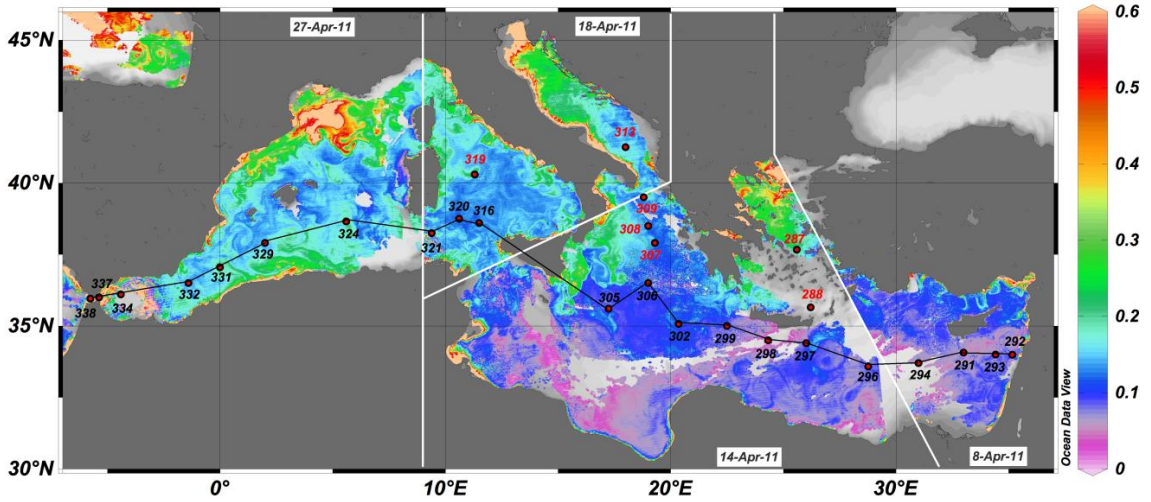

Figure 5.1. Sampling stations presented in this study collected during the M84-3 research cruise. Superimposed a composite image showing the surface chlorophyll concentration (mg/m^3) at an approximate date of the sampling period in the different basins. The transect shown in the following figures includes the stations labeled in black.

5.2.2 Phytoplankton analyses

A portion of each filter was placed on aluminum stubs and gold coated using an EMITECH K550X sputter coater. The quantification and identification of the main phytoplankton groups and coccolithophore species were performed by JEOL-JSM 6300 and ZEISS-EVO MA10 scanning electron microscopes (SEMs). Transects of 5 - 15mm on the filter, corresponding to an average of 2.3 ml of seawater were observed at 3000X and phytoplankton groups quantified as coccolithophores, diatoms, and silicoflagellates (*Dictyocha spp*.). A subset of five random samples was analysed under light microscope for estimation of coccolithophore and diatom cell abundance at 1000X. This was done in order to check if counts at higher magnification were biased towards smaller cells. This comparison showed that relative abundances of diatoms were similar in the two methods. They comprised between 1.7 and 3.3% (SD= 0.85) of cells counted by optical microscopy and between 0.8 and 4.1% (SD= 1.6) of cells by counted SEM. Coccolithophore species were identified, and their absolute and relative abundances counted. In samples with very few coccospheres a larger filter portion was observed in order to quantify a minimum of 100 cells (a maximum number of 420 cells were counted). Lower (C_L) and upper (C_U) confidence intervals at 95% significance were estimated following Bollmann et al. (2002). For a 100 cell count these were: C_L=82, C_U=102 and for a 420 cell count: C_L=382, C_U=422. Cell densities (number of cell L^{-1} seawater) were calculated. *Emiliania huxleyi* was sub-classified into morphotypes according to Young et al. (2003). For each sample the Shannon-Wiener diversity index (H´) was calculated for heterococcolithophores and holococcolithophores. These two groups were treated separately because they represent two different stages of a coccolithophore´s life cycle, and taxonomy between the two does not always account for it.

5.2.3 Environmental parameters

A detailed protocol of all measured environmental variables can be found in Tanhua et al. (2013a). *In situ* salinity, temperature and oxygen data were measured by CTD (described in section 2.1). Overall data accuracies were: 0.002 ºC for temperature and 0.003 for salinity. Macronutrients (phosphate, nitrate and silicate concentrations) were measured on-board with a QuAAtro auto-analyzer from SEAL analytics. The following protocols from SEAL analytics were followed: Nitrate (NO_3) (Method No. Q-068-05 Rev. 4), phosphate

(PO_4^{3-}) (Method No. Q-031-04 Rev. 2) and Silicium (Si) (Method No. Q-066-05 Rev. 3). The nutrient analytical error was determined on 5-7 sample replicates taken at selected stations. The error is: for nitrate 0.08 μmol kg^{-1}, phosphate 0.007 μmol kg^{-1} and silicate 0.10 μmol kg^{-1}.

The carbonate system was characterized by measuring dissolved inorganic carbon (DIC), pH and total alkalinity (TA). DIC content was measured coulometrically using a SOMMA (Single-Operator Multi-Metabolic Analyzer) system. The precision of the analysis is ±0.6 μmol kg^{-1} and the accuracy is 2.5 μmol kg^{-1}. pH was measured by double-wavelength spectrophotometry , and it is reported at 25ºC on the total scale. The reproducibility of the pH measurements was 0.0012. TA was analyzed following a double end point potentiometric technique. The precision of the TA measurements was 0.1 μmol kg^{-1}. More details about the DIC, TA and pH measurements and quality control are presented in Álvarez et al. (2013). *In situ* conditions for other CO_2 –related variables were calculated from in situ pH and TA for the first 100 m water column. Calculations were performed using the program CO2Sys (Lewis & Wallace 1998). Equilibrium constants of Mehrbach et al. (1973) refitted by Dickson & Millero (1987) were chosen (Álvarez et al. 2014).

A characterization of the upper 100 m environmental parameters is shown in Figure 5.2; the profiles for the complete water column at a higher spatial horizontal resolution and a full description of the physicochemical setting are presented in Tanhua et al. (2013b); Álvarez et al. (2014).

5.2.4 Statistical analyses

The E-PRIMERv.5 package was used for the following analyses: 1) The BIOENV routine, which computes a rank correlation between the elements of similarity matrices for environmental parameters and biological data, was run to detect the combined changes in environmental parameters and species distribution among stations. The routine examines all possible combinations of environmental variables and gives the "best fit" (higher Rho – Spearman rank correlation) of environmental variables explaining changes in biological communities. This test was performed for all heterococcolithophore and holococcolithophore species contributing > 2% to the total assemblage of each group.

Before running the routine, we checked for mutual correlation among environmental variables and selected a subset of them for this routine. These were: salinity, temperature, oxygen, pH, partial pressure of carbon dioxide (pCO_2), and the concentrations of bicarbonate ion (HCO_3^-), carbonate ion (CO_3^{-2}), $NO_3 + NO_2$ and PO_4^{3-}.

2) Hierarchical Cluster Analyses by group average. These were performed for heterococcolithophore and holococcolithophore species. *Emiliania huxleyi* morphotype A was removed of the data set used to run the cluster analyses. This was done to emphasize our results on overall community composition and not on *E. huxleyi* that largely dominated the assemblages in our samples. When clusters among species were detected, pair wise Spearman correlations were performed using the software SPSSv18 to assess the environmental parameters influencing changes in each species´ abundance.

For the analyses performed by E-PRIMER software, the biological data was transformed in logarithmic scale log(1+x) to avoid overemphasizing the dominant species. Environmental data were standardized (-mean*STD) to bring data into a comparable scale. Similarity matrices were created for biological and environmental data. For the biological data the Bray-Curtis similarity coefficient was used to examine similarity between each sample´s pair. Euclidean distances were used to create the environmental data matrix. Pair wise Spearman correlations were performed on the basis of non-transformed non-standardized data.

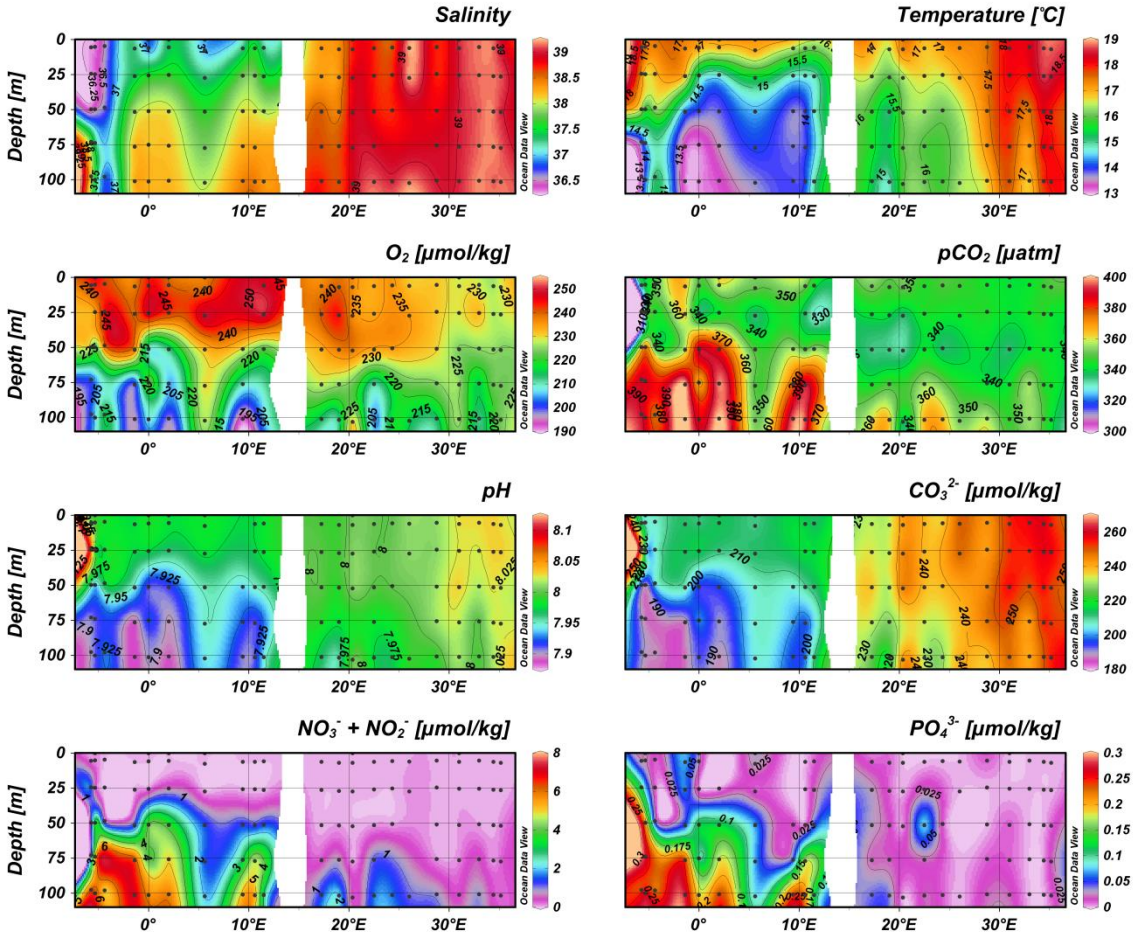

Figure 5.2. Environmental parameters at sampling stations for surface waters during the M84-3 cruise. The west to east transect along the Mediterranean Sea does not take into account the stations in the Aegean, Adriatic, the northernmost Ionian, or northern Tyrrhenian regions. It includes the stations labeled in black (west-east transect) in Figure 5.1.

5. 3 Regional settings

The Mediterranean Sea can be divided into two basins with a general counterclockwise circulation: the western and eastern basins. The Strait of Sicily prevents deep-water exchange between the two. The upper layer (from the surface down to 150–200 m, according to the basin and the season) is occupied by the Atlantic Water (AW) (Ribera d'Alcalà et al. 2003). In the western Mediterranean, AW flows along the eastern part of the Alboran Sea in an anticyclonic fashion, and moves to the western Alboran in a more variable pattern (Robinson et al. 2001). Further east, the AW is transported along the Algerian slope until the Sardinia Channel. Part of the flow then proceeds to the eastern basin along the Tunisian slope, while the other part reaches northern Sicily and circulates along Italy. In the north, the Liguro–Provenco–Catalan current, is form by AW

surrounding Corsica. AW closes its western gyre southeast of Spain, where it encounters the newly entered AW (see Robinson et al. 2001, for more details). In the eastern basin, a jet of Atlantic Water enters through the Strait of Sicily, meanders through the interior of the Ionian Sea and continues to flow through the central Levantine all the way to the shores of Israel (Robinson et al. 2001). Convection occurs when the water approaches the Rhodos gyre. Another part of the AW flow moves to the Ionian and a part of it goes further into the Adriatic Sea. Deep-water formation also occurs in the Adriatic gyre (Pinardi & Masetti 2000).

During the M84-3 cruise, the surface layer in the western basin was filled by the inflow of relatively low-salinity AW through the Strait of Gibraltar. The salinity minimum, in the surface layer of the strait, shows the entrance of this water into the Mediterranean. Once it reaches the Sicily Channel (close to stations 304/305), the salinity minimum was found at ~100 m depth. (Hainbucher et al. 2014). In terms of carbonate chemistry AW from the surface western Mediterranean were characterized by TA below 2560 μmol Kg^{-1}, DIC near 2250 μmol Kg^{-1} and pH of 8 (Àlvarez et al. 2014). In the surface layer, AW with salinity lower than 38 was detected in all the Tyrrhenian stations except 319 in the centre of the basin where salinity was higher. There, Álvarez et al. (2014) suggest that the upper ~50dbars were occupied by probably AW affected by evaporation or mixed with the salty intermediate water entering through the Strait of Sicily. During the M84-3 cruise modified AW and Levantine Surface Water (LSW) dominated the Eastern Mediterranean, approximately down to 100m water depth. The LSW, formed by intensive heating and evaporation, has the largest salinity and temperature of the entire Mediterranean (>17°C, > 38.9), and TA values around 2610 μmol Kg^{-1}, DIC around 2270 μmol Kg^{-1} and pH25T around 8.03 (Álvarez et al. 2014). Levantine Intermediate Water (LIW) were detected at ~ 50–100 m in the Levantine Sea, in its spreading way from the northeastern Levantine Sea and Rhodes cyclonic gyre (Hainbucher et al. 2013 and references therein). Close to the M84/3 trajectory, wind induced upwellings and downwellings zones are found in different seasons (see Bakun & Agostini 2001). For instance: 1) downwelling along the southern coastal boundary during winter, reversing to coastal upwelling off Libya in spring and off Algeria in summer and fall; 2) strong upwelling in the eastern Aegean Sea throughout the year, becoming remarkably intense in the summer and fall seasons; and 3) strong summer and fall upwelling in the eastern Ionian Sea.

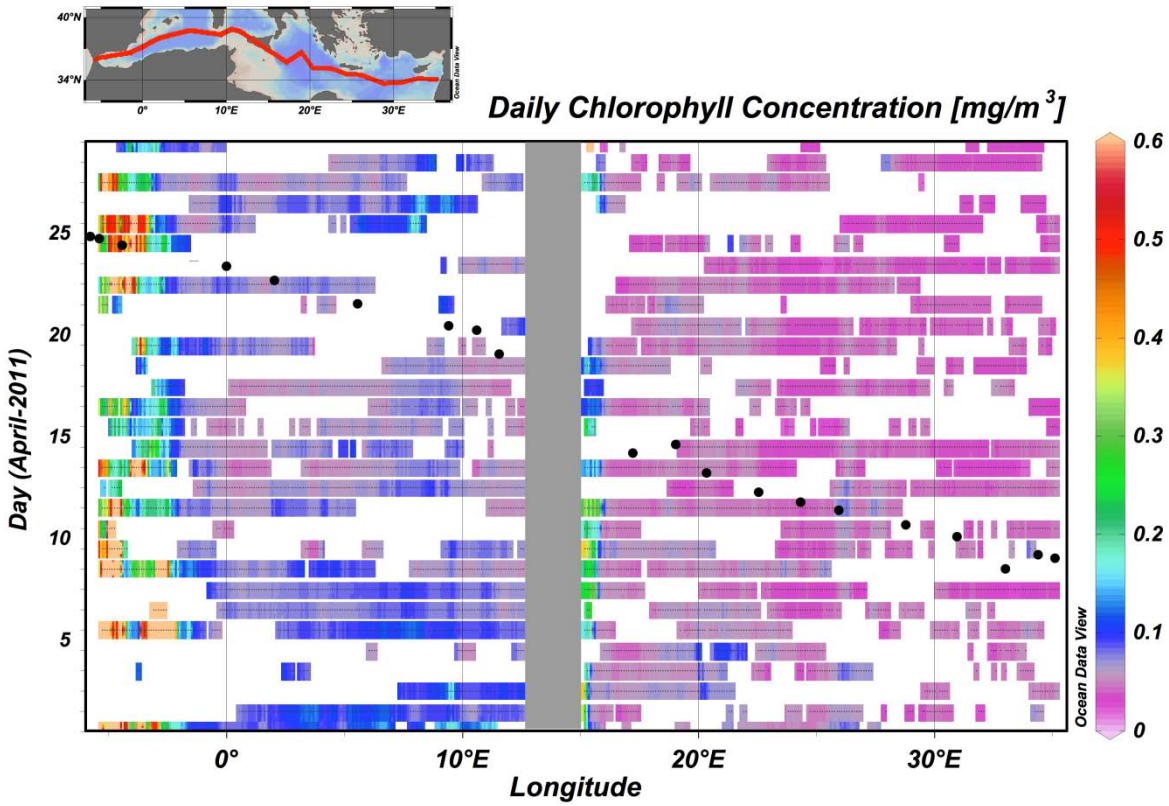

Figure 3. Daily mean chlorophyll-a concentration from satellite data (Volpe et al., 2012) along the transect of the M84/3 cruise, plotted for the month of April 2011. In this figure, gaps correspond to cloud covered observations and the temporal-spatial location of the samplings during our study is indicated by black dots. The transect is representative of 18Km in latitude, (two pixels at 9Km resolution).

Figure 5.3 shows daily variations in cloud coverage during the month of April (from satellite observations). It provides an overlook of the meteorological situation and possible short-term variability that may mask any relationship with long-term average oceanographic gradients. Approximately half of the satellite observations were cloud covered, with a minimum in cloud coverage (~40% of observations) at about 25°E (south of Crete). This minimum corresponds to the only segment of the transect directly influenced by northern wind regimes. Such approximation can be compared with the meteorological reports during the M84-3 (data not shown), which shows that ~58% of the sampling days were cloudy (at the time of recording) with a majority of sunny days from south Crete towards the Adriatic. Therefore, the sampled days were representative, in terms of cloud coverage, of the conditions during April 2011.

5.4 Results

5.4.1 Main phytoplankton community

Overall, phytoplankton cell density was highest in the western Mediterranean Sea, in the Strait of Gibraltar and in the Alboran Sea. For coccolithophores, the pattern was not one of gradual increase towards the west but rather of localized spots of higher cell densities close to Gibraltar and a continuous presence, at lower cell densities, in the rest of the Mediterranean. The satellite-derived chlorophyll-a concentration during April 2011 (Fig. 3) shows a similar pattern. Coccolithophores were the most abundant phytoplankton group during the sampling, relative to siliceous phytoplankton. They were present in great numbers in all the main Mediterranean basins and accounted for 68 to 99 % of counted phytoplankton. Diatoms, although present in all studied basins, displayed low concentrations in the eastern Mediterranean, increasing towards the west. They were on average 6 % (maximum 25 %) of total phytoplankton. Silicoflagellates (*Dictyocha* spp.) accounted on average for 1 % of phytoplankton (maximum 9 %). Figure 5.4 shows the distribution of these different phytoplankton groups in the Mediterranean transect. A species present mostly at low cell densities was the xanthophyte *Meringosphaera mediterranea*.

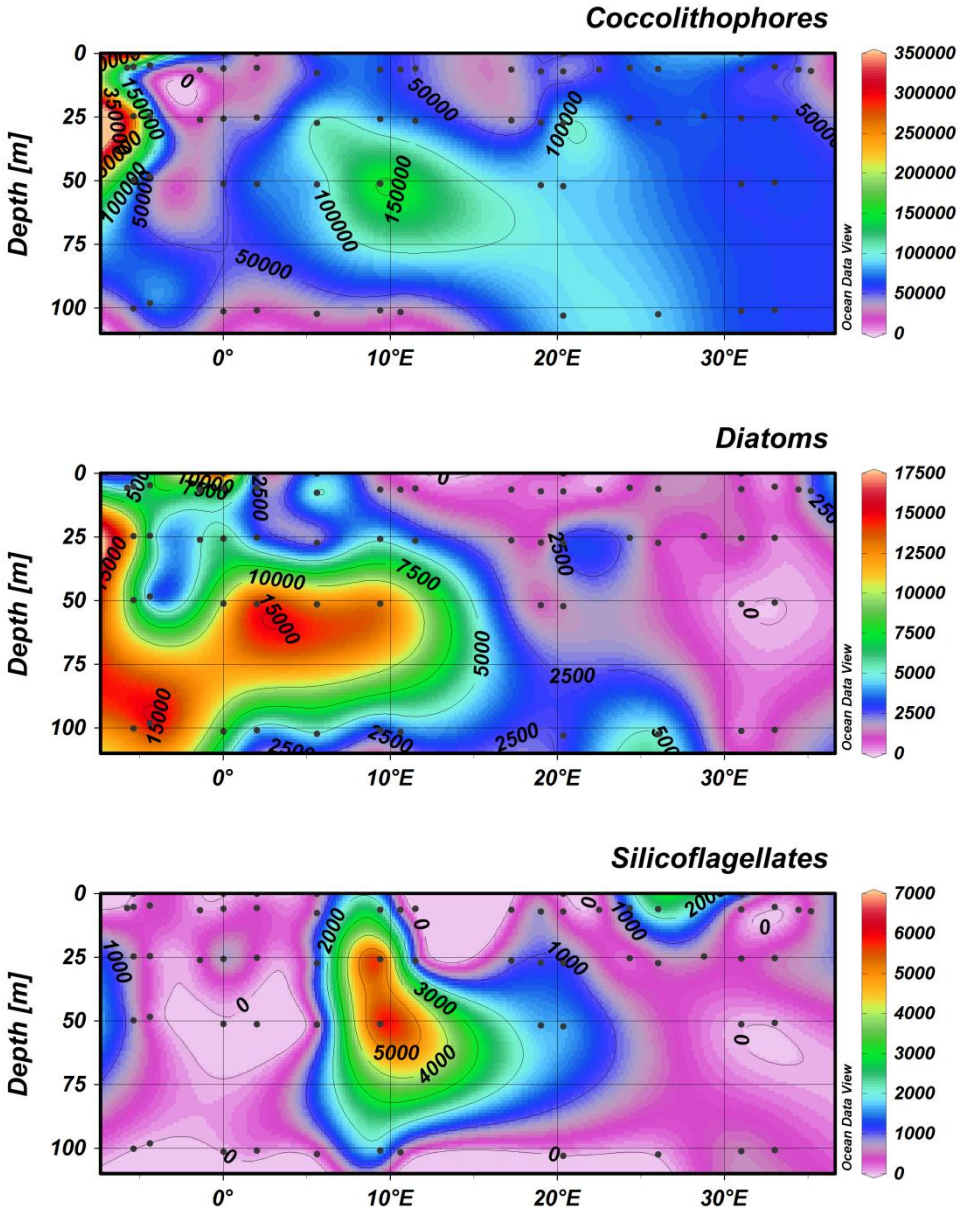

Figure 5.4. Distribution of coccolithophores (upper panel), diatoms (middle panel) and silicoflagellates (lower panel) in a west to east transect along the Mediterranean Sea (the transect includes the stations labeled in black in Figure 5.1).

5.4.2 Environmental factors controlling coccolithophore community distribution

A total of 70 coccolithophore species in heterococcolithophore life stage and 45 in the holococcolithophore stage were recorded (see Appendix B). The majority of the quantified cells were in the heterococcolithophore phase. The species *Emiliania huxleyi* largely dominated the coccolithophore counts in all stations except for station 319 (at the center of the Tyrrhenian Basin), where *Corisphaera gracilis* and *Rabdosphaera clavigera* were the dominant species.

The results from the Spearman`s rank correlation based routine (BIOENV) suggest that holococcolithophores were preferentially distributed in low nutrient - high pH seawaters. (ρ=0.328, Table 5.2). They were almost absent at 100 m. Heterococcolithophore distribution was best linked to a combination of [CO_3^{2-}], pH, and Salinity with ρ=0.566 as well as to [PO_4^{3-}] (Table 5.3).

5.4.3 Species assemblages

When clustering all the species within the heterococcolithophore life stage, three groups or assemblages were identified that shared more than 65 % similarities. Figure 5.5 presents the results of further clustering of the species with high similarities. The distribution of these species along the east–west transect (stations with black labels in Fig. 5.1) that includes the stations in the Levantine, Ionian (excluding 307–309), Tyrrhenian (excluding 319), Algerian, Alboran, and Gibraltar regions shows that the three groups are distinctively distributed in the Mediterranean Sea (Figs. 5.5 – 5.8). The first group comprises species that were more abundant in the eastern stations: *U. tenuis*, *D. tubifera*, *P. vandelii*, *S. pulchra*, *R. clavigera*, and *S. protrudens* (*R. xyphos* was very close to this cluster, with similarity > 50 %). *P. vandelii*, however, was patchily distributed all along the transect. The second group includes *E. huxleyi* Type B/C and the Gephyrocapsa species: *G. ericsonii*, *G. muellerae* and *G. oceanica*. These species were almost exclusive of the western basin. A third group was formed by *Florisphaera profunda* and *Gladiolithus flabellatus*, being closely related to *A. robusta* and *H. carteri* (the last two with similarities between 40 and 60 %). The species in the latter group were almost restricted to depths below 50 m, with higher abundances at 100 m, and were patchily present from the Algerian to the Levantine basins. Clustering analysis for the holococcolith phase did not reveal any pattern in the species composition among the different samples.

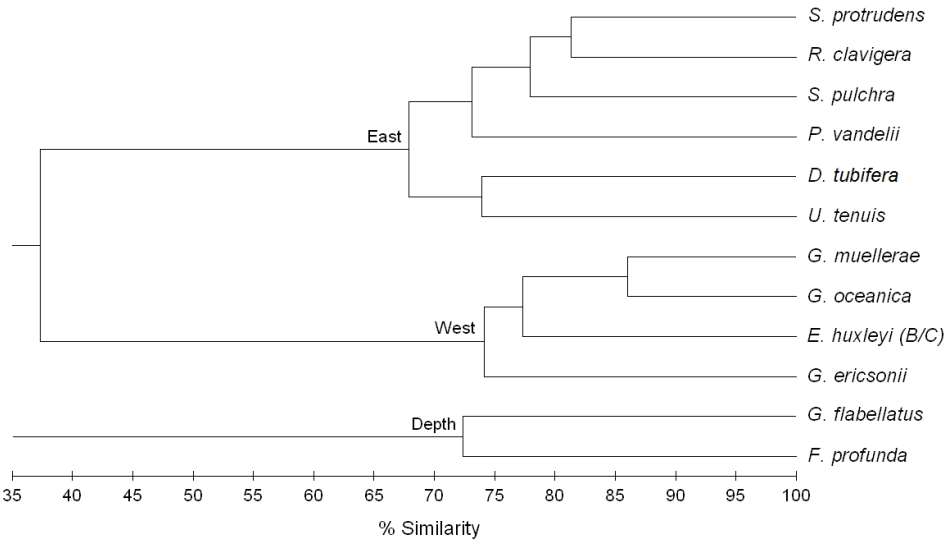

Figure 5.5. Hierarchical cluster for the heterococcolithophores species that shared more than 65% similarity in their abundance and distribution patterns.

Single Spearman correlations for the species that were clustered together reveal that their distribution can be better explained by seawater carbonate chemistry parameters; for instance, species that were mostly abundant at eastern stations thrived in waters with higher [CO_3^{2-}] and pH and in the surface. Among these species, *U. tenuis*, *R. clavigera*, *S. pulchra*, and *S. protrudens* were negatively correlated to phosphate concentrations and only *D. tubifera* showed a high positive correlation with temperature. Finally, *F. profunda* and *G. flabellatus* were correlated to [NO_3 + NO_2] and negatively with temperature. Table 5.4 shows these results.

Table 5.2. Rho values (ρ) for the best Spearman`s rank correlations for all possible combinations between the environmental parameters explaining patterns in holococcolithophores assemblages. Only ρ> 0.2 are shown. Description as in Table 5.1. On the left, the number of variables taken into account; on the right, description of the variables and the highest ρ values at a given number of variables. In the first row, the ρ value for each variable is shown in decreasing order of contribution.

Number of variables	Variables (ρ)							
1	$NO_3^- + NO_2^-$	(0.275);	PO_4^{3-}	(0.236);	pH	(0.214);	pCO_2	(0.204);
2	$NO_3^- + NO_2^-$	pH	(0.327)					
3	$NO_3^- + NO_2^-$	PO_4^{3-},	pH	(0.328)				
4	$NO_3^- + NO_2^-$	pH, O_2,	Salinity	(0.311)				
5	$NO_3^- + NO_2^-$	PO_4^{3-},	pH, O_2,	salinity	(0.311)			
6	$NO_3^- + NO_2^-$	PO_4^{3-},	pH, pCO_2, O_2, salinity				(0.299)	
7	$NO_3^- + NO_2^-$	PO_4^{3-},	pH, pCO_2, O_2, salinity,		Temperature			(0.283)
8	All	(0.275)						

Table 5.3. Rho values (ρ) for the best Spearman`s rank correlations for all possible combinations between the environmental parameters explaining patterns in heterococcolithophores assemblages. Description as for Table 5.2.

Number of variables	Variables (ρ)
1	CO_3^{2-} (0.551); pH (0.498); pCO_2 (0.397); PO_4^{3-} (0.358); $NO_3^- + NO_2^-$ (0.328); salinity (0.310); O_2 (0.226);
2	CO_3^{2-} salinity (0.563)
3	CO_3^{2-} pH, salinity (0.566)
4	CO_3^{2-} pH, PO_4^{3-}, salinity (0.565)
5	CO_3^{2-} pH, pCO_2, PO_4^{3-}, salinity (0.539)
6	CO_3^{2-} pH, pCO_2, PO_4^{3-}, salinity, temperature (0.517)
7	CO_3^{2-} pH, pCO_2, PO_4^{3-}, salinity, O_2, temperature (0.507)
8	All (0.491)

5.4.4 Species diversity (H')

Hetero- and holococcolithophore species diversity index (H') changed slightly in the W–E transect. Although correlations between H' and the longitude of the sample sites (°E) in the first 50m water column were rather weak, the trend was opposite for the two life stages. For instance, heterococcolithophores diversity tended to decrease towards the east (ρ= -0.419, p =0.000), while holococcolithophore species diversity tended to increase W–E (ρ =0.310; p =0.005) (Fig. 5.9). H' index at 100m was often zero for both groups, being on average 0.3 for holococcolithophores, which are mostly present at surface, and 1.3 for heterococcolithophores.

5.5. Discussion

5.5.1 Main phytoplankton community

Although picoplankton can seasonally dominate phytoplankton assemblages in the Mediterranean Sea (Decembrini et al. 2009; Yacobi et al. 1995), previous studies have often suggested that coccolithophores are one of the most abundant phytoplankton groups in this sea, in both, eastern (e.g. Gotsis-Skretas et al. 1999; Malinverno et al. 2003; Ignatiades et al. 1995, 2009; Rabitti et al 1994; Ziveri et al., 2000), and western basins (e.g Barlow et al. 1997; Barcena et al. 2004, Ignatiades et al. 2009). Our findings suggest that coccolithophores are a main phytoplankton group in the entire Mediterranean Sea that dominated over siliceous phytoplankton for the period under study (Figure 5.4). Silicoflagellates were almost absent at 100m and more abundant at surface waters of the Tyrrhenian Sea, with cell densities up to $6.7x10^3$ cells l^{-1}. Diatoms were preferentially

distributed in the higher nutrients, colder, less saline and with lower [CO_3^{2-}] waters of the western Mediterranean Sea at maximum cell density of 1.6 $x10^4$ cells l^{-1} (Figure 5.4). Diatom cell densities in the Mediterranean have ranged from few individuals, in the Ionian Sea-surface to ~ $3.5x10^4$ in the Tyrrhenian Sea (June 1999, Ignatiades et al. 2009); from 0.8 $x10^3$ to 2 $x10^4$ (July 2005, Decembrini et al. 2009); from $0.2x10^3$ to 5 $x10^3$ (September-October 2004, Lasternas et al. 2011) and from 0.7 $x10^3$ to 2.6 $x10^3$ cells l^{-1} (December 2005, Decembrini et al. 2009) in the Tyrrhenian Sea. With out taking into account inter-annual variability, this suggests a pattern of enhanced diatom abundances in the first part of the year and a decrease after July.

Since decades, many attempts to explain the temporal and spatial phytoplankton distribution based in few key environmental factors have been done. Some of the most discussed are the hypothesis of Sverdrup (1953), stating that changes in phytoplankton abundances are light – nutrients controlled features; and the so called Margalef´s Mandala (Margalef 1978), that proposes phytoplankton succession to depend on nutrients concentration and turbulence. Regarding the possible role of light in the relative success of coccolithophores over siliceous phytoplankton, we recorded global and UV radiation at surface, at the time of sampling in some of the stations but lack light data at every depth. No significant correlation was observed for any of the phytoplankton groups with radiation data ($p>0.05$, $N=21$). Most likely, a response to changes in radiation will not be immediate (specially because the variable that we recorded – cell densities – relates to cell division). In such a case the short temporal extension of our data (by minute during the sampling) could mask a correlation. Large variations in light are also observed on the vertical profile. Holococcolithophores and diatoms correlated with depth (negative and positive correlations, respectively), although for diatoms this correlation was rather weak ($\rho = 0.240$; $p = 0.031$). This could indicate that the two groups are more sensitive to light conditions than heterococcolithophores, but it might also be an artefact of the co-correlation between depth and nutrients. Additionally, light attenuation can differ between stations and therefore this comparison is only approximate.

In the case of nutrients, it is important to notice that the dominance of coccolithophores over siliceous phytoplankton was clear in all the basins, including the Gibraltar strait, where nitrate and phosphate were available and silicate concentrations were above the half-

saturation constant for diatoms (Ks_Si: c.a. 3.5μM Merico et al. 2006; Leblanc et al. 2003; Sarthou et al. 2005 or 0.8–2.3 μM Nelson et al. 1976) and we could have expected the community to be dominated by fast growing phytoplankton. In the interior of the Mediterranean [Si] was probably too low (often below 1.0 μmol/Kg) to support large diatom populations, except for the deeper layers (100m) of the Ionian and Levantine basin which ranged from 0.8 -1.4 μmol/Kg. Egge & Aksnes (1992) observed that at Si values lower than 0.6μM *Emiliania huxleyi* outcompeted the otherwise dominant *Skeletonema costatum*. For the dataset here presented, nutrients variability alone does not explain the dominance of coccolithophores during April 2011, at least not directly. A possible phosphate limitation for other phytoplankton groups (notice the high N:P ratios in both the eastern and western basins as well as in the Gibraltar Strait) cannot be ruled out of explaining coccolithophore dominance over other groups. Turbulence does not account for it neither, since coccolithophores dominated in regions were water density was homogeneous thought the first 100m as well as in regions where isoclines can be distinguished (e.g. see salinity and temperature profiles from Fig. 5.2). Overall, the reason for the dominance of coccolithophores over siliceous phytoplankton remains unclear.

Table 5.4. Three highest Spearman´s correlation (ρ) results for: 1) the dominant species *Emiliania huxleyi*, 2) each of the species belonging to the observed clusters with the environmental parameters, 3) the holo-hetero- life phases of the same species and 4) hetero- and holo- coccolithophore abundances and diversity (H`) and abundances of siliceous phytoplankton groups. Preferential depth and distribution along the west to east transect is described. Number of samples taken into account for the analysis is also shown (N). Significance level was 0.05.

Species/group	Varible (r, N)			Pref. depth	Pref. Distribution
E. huxleyi Type A	pH (0.468; 73)	CO_2 (-0.448; 73),	CO_3^{2-} (0.444; 73),	0 - 100 m	W-E
E. huxleyi Type B/C	Salinity (-0.691; 81),	CO_3^{2-} (-0.685;73),	pH (-0.616; 73)	0 - 100 m	W
G. ericsonii	Salinity (-0.805; 81),	CO_3^{2-} (-0690; 73),	pH (-0.576; 73)	Above 50 m	W
G. oceanica	CO_3^{2-} (-0.833; 73),	Salinity (-0.803; 81),	pH (-0.731; 73)	0 - 100 m	W
G. muellerae	CO_3^{2-} (-0.835; 73),	Salinity (-0.830; 81),	pH (-0.707; 73)	0 - 100 m	W
U. tenuis	CO_3^{2-} (0.626; 73),	pH (0.605; 73),	PO_4^{3-} (-0.551; 74)	Above 50 m	E
R. clavigera	CO_3^{2-} (0.727; 73),	pH (0.701; 73),	PO_4^{3-} (-0.546; 74)	Above 50 m	E
D. tubifera	pH (0.600; 73),	Temp. (0.597; 81),	CO_3^{2-} (0.541; 73)	Above 50 m	E
S. pulchra	pH (0.551; 73),	CO_3^{2-} (0.528; 73),	PO_4^{3-} (-0.399; 74)	0 - 100 m	E
S. protrudens	pH (0.557; 73),	CO_3^{2-} (0.489; 73),	PO_4^{3-} (-0.450; 74)	Above 50 m	E
F. profunda	$NO_3^- + NO_2^-$ (0.637; 81),	Temp. (-0.553; 81),	pH (-0.468; 73)	Below 50 m	W-E
G. flabellatus	$NO_3^- + NO_2^-$ (0.583; 81),	Temp. (-0.522; 81),	O_2 (-0.481; 73)	Below 50 m	W-E
S. pulchra HOL	PO_4^{3-} (-0.308; 74)	CO_2 (-0.261; 73),	O_2 (0.260; 73)	Above 50 m	W-E
C. mediterranea	HCO_3^- (-0.294; 73)	-	-	Above 50 m	W-E
C. mediterranea HOL	O_2 (0.240; 73)	-	-	Above 50 m	W-E
H. carteri	CO_2 (0.341; 73),	pH (-0.339; 73),	-	0 - 100 m	W-E
H. carteri HOL	$NO_3^- + NO_2^-$ (-0.284; 81),	-	-	Above 50 m	W-E
Hetero- abund.	CO_2 (-0.278; 73),	-	-	0 - 100 m	W-E
Holo- abund.	Depth (-0.427; 81),	$NO_3^- + NO_2^-$ (-0.391; 81),	CO_2 (0.339; 73)	Above 50 m	E
Hetero- diversity (H´)	CO_3^{2-} (-0.486; 73),	Salinity (-0.426; 81),	pH (-0.413; 73)	-	-
Holo- diversity (H´)	HCO_3^- (-0.460; 74)	CO_3^{2-} (0.446; 73),	pH (0.388; 73)	-	-
Diatoms	CO_3^{2-} (-0.617; 73),	pH (-0.602; 73),	PO_4^{3-} (0.534; 74)	Below 25 m	W
Silicoflagellates	Si (0.254; 76)	-	-	0 - 100 m	W-E

We suggest that the relative success of coccolithophores over siliceous phytoplankton during April 2011 in all Mediterranean Sea basins can be due to a parameter(s) not measured during this study or to a threshold concentration in a resource that limits the growth of the other phytoplankton groups, but that covers the requirements of coccolithophores. The last hypothesis would be better tested experimentally than by correlation analysis.

5.5.2 Environmental factors controlling coccolithophore distribution

Concerning the coccolithophore community, the study of Knappertsbusch (1993) suggests the occurrence of seasonal variability. His sampling was divided in two periods: late winter (February–March 1988) and late summer (September–October 1986). Knappertsbusch observed higher cell densities during late winter and increasing towards the eastern Mediterranean, reaching 230 000 cells per liter in the Levantine Basin. During September–October this pattern was reversed. Our results resemble those corresponding to September–October in Knappertsbusch work. However, there was no gradual increase towards the west but rather localized higher cell densities close to Gibraltar and a continuous presence, at lower cell densities, in the rest of the Mediterranean (Fig. 5.4). This is in agreement with the relatively low satellite-derived chlorophyll a values in most the surface Mediterranean Sea during the month of April, ~0 mg m^{-3}, and the increased values approaching the Strait of Gibraltar, ~0.5–0.6 mg m^{-3} (Fig. 5.3), and measured data from Rahav et al. (2013) ranging from ~0.03 to ~0.1 μg L^{-1} in most of the Mediterranean and rising to 0.31 μg L^{-1} near the Strait of Gibraltar. It also agrees with the suggested modulation of pH by primary production in the western basin during the cruise (Álvarez et al. 2014). In the study by Ignatiades et al. (2009), the increase in coccolithophore cell densities in the western Mediterranean is mainly due to the significantly higher values at one station (close to the Balearic Islands).

5.5.2.1 Holococcolithophores

Our findings documented that during the time of the M84-3 cruise holococcolithophore distribution was best explained by changes in nutrients ($[NO_3+NO_2]$ and $[PO_4^{3-}]$) and pH (ρ=0.328, Table 5.3). They were more abundant in low nutrient-high pH seawaters typical of the surface (upper 50 m) Mediterranean waters. Holococcolithophores were, in general

present in all samples collected in Mediterranean surface waters but almost absent at deeper depths (~100m). Higher abundances in very oligotrophic waters of the Mediterranean Sea have been reported before (Kleijne 1991,1992). Cros & Estrada (2013), reported holococcolithophores being more abundant at the upper photic zone, nutrient depleted waters. They linked the observed segregation to a differentiation of ecological niches. Dimiza et al. (2008) observed that holococcolithophores around the Andros Island were more abundant in surface waters together with some heterococcolithophore species such as *Rabdosphaera clavigera*. The lower ρ obtained in the BIOENV analysis for holococcolithophores (Table 5.2) might be due to the lack, in the statistical analysis, of an important parameter (e.g. irradiance, zooplankton grazing) not measured during this study.

5.5.2.2 Heterococcolithophores

Heterococcolithophore distribution was best linked to a combination of [CO_3^{2-}], pH, and salinity (ρ= 0.566; Table 5.3) The ρ value for the 4 variables combination: [CO_3^{2-}], pH, salinity, and [PO_4^{3-}] was not so much lower than the "best fit" ([CO_3^{2-}], pH, salinity). This might indicate that apart from seawater carbonate chemistry, [PO_4^{3-}] is also important in explaining heterococcolithophore distribution. It is worth noticing that [PO_4^{3-}] correlated to the heterococcolithophore species diversity (H`) (ρ: 0.322, $p<0.05$) but not to the abundance. Thus, the availability of PO_4^{3-} might co-determine the assemblage composition. Differences in PO_4^{3-} usage have been reported between strains of the same species (Oviedo et al. 2014). It is therefore likely that different species show different sensitivities to [PO_4^{3-}], which could induce differences in community composition upon environmental [PO_4^{3-}]. Overall, we suggest [CO_3^{2-}], pH and probably [PO_4^{3-}] as functionally related important variables in explaining heterococcolithophore distribution in the Mediterranean Sea.

Although heterococcolithophores preferentially use HCO_3^- for their intracellular calcification within a calcifying vesicle (Mackinder et al. 2010) at alkaline pH values CO_3^{2-} is the major carbon source for $CaCO_3$ and we can assume the uptake of both $HCO_3^-$and CO_3^{2-} (Ziveri et al. 2012). In the Mediterranean Sea, [CO_3^{2-}] increases gradually towards the east. Thus, it is possible that those species thriving in the eastern basins utilize

comparatively more CO_3^{2-} than those that prosper in the western Mediterranean. Using a compilation from world-wide plankton samples and sediments spanning the last 40k years, Beaufort et al., (2011) recorded significant correlations between coccolith mass belonging to the family Noelaerhabdaceae (genera *Emiliania, Gephyrocapsa* and *Reticulofenestra*) with [CO_3^{2-}] and [HCO_3^-]. They argue that differentially calcified species are distributed in the ocean according to the ocean´s carbonate chemistry. Modeling studies also highlighted the importance of [CO_3^{2-}] for coccolithophore distribution, as observed by Merico et al. (2006). Tyrell et al. (2008) observed that *Emiliania huxleyi* blooms in the Baltic Sea coincide with periods of high [CO_3^{2-}].

Changes in pH are concomitant with changes in the ratio between bicarbonate and carbonate ions. This makes difficult to disentangle which parameter of the carbonate system could affect coccolithophore populations. Under laboratory culture conditions, *Emiliania huxleyi* calcification is sensitive to low pH and bicarbonate, while photosynthesis and growth is sensitive to low pCO_2 (Balch et al., 2013) and the coccolith morphogenesis in *Calcidiscus leptoporus* is hampered by pCO_2 and no other parameter of the carbonate chemistry (Langer & Bode 2011). How will these responses translate to a community scale in the ocean? Charalampopoulou et al. (2011) found that the coccolithophore species distribution between the North Sea and the Atlantic Ocean related to pH and irradiance. In this study, pCO_2, one of the parameters considered to run the BIOENV routine, was not part of the best fitting variables to explain coccolithophore distribution patterns. This might be an indication that, during the time of the study there was no evident pCO_2 limitation of photosynthesis in the observed species or that coccolithophore sensitivity to CO_2 among species, even if different (Langer et al. 2006; Langer et al. 2009) do not have major effects on coccolithophore species assemblages in the Mediterranean. Mimicking the experimental design of the above mentioned culture experiments into a mesocosm scale could help elucidating how will the different effects of carbonate chemistry modification on coccolithophore`s physiology and morphology shape of the community.

Salinity, even if one of the environmental variables that optimized the best-fitting combination of variables explaining the biological data, might not be crucial in controlling heterococcolithophores distribution. Experimental evidence (Brand 1984) indicates strain-

specific differences that allow *Emiliania huxleyi* to survive at a wide salinity range. *E. huxleyi* has been found in oceanographic regions characterized by very different salinities (reviewed by Tyrrell et al., 2008). Furthermore, heterococcolithophores isolated from the Mediterranean Sea (CODENET collection) were maintained at salinities of 32–33 with non-observed adverse effects (Probert and Houdan, 2004).

5.5.3 Species assemblages

Another feature that was different between the coccolithophore life stages is the development of species assemblages. Holococcolithophore species did not form different assemblages along the Mediterranean Sea (no species clustering with high similarities in abundance and distribution). Holococccolithophores seem to behave as a homogeneous group, exploiting a similar ecological niche. On the contrary, three heterococcolith clusters were identified whose species shared more than 65% similarities (Figure 5.5). The first group comprises species that were more abundant in the eastern stations: *U. tenuis, D. tubifera, P. vandelii, S. pulchra, R. clavigera,* and *S. protrudens*. The second group includes *E. huxleyi* Type B/C and the *Gephyrocapsa* species*: G. ericsonii, G. muellerae* and *G. oceanica* that were almost exclusive of the western Mediterranean. A third group was formed by *Florisphaera profunda* and *Gladiolithus flabellatus,* found with higher abundances below 50m. Most of the species in these clusters have been found to share an ecological niche in other studies: *U. tenuis, D. tubifera, S. pulchra and R. clavigera* have been considered typical in oligotrophic warm waters and/or surface water species (Okada & Honjo 1973; Okada & McIntyre 1977; 1979; Nishida 1979; Ziveri et al. 2000; Haidar & Thierstein 2001; Malinverno et al. 2003; Ziveri et al. 2004 for *Syracosphaera* spp.; Triantaphyllou et al. 2004). The gephyrocapside species have been considered typical of eutrophic areas (Kleijne 1989; Broerse et al. 2000) with lower density, lower salinity and higher temperature (Takahashi & Okada 2000; Knappertsbusch 1993). Finally, *F. profunda* and *G. flabellatus* are widely recognized depth euphotic zone species, often living below the 100 m depth (Okada & Honjo 1973; Boeckel et al. 2006); and are controlled by the dynamics of the nutricline and thermocline (Molfino & McIntyre 1990; Triantaphyllou et al. 2004). Both species were an important component below the 50m; with highest abundances around 100m, where fluorescence data (not shown) locate the deep chlorophyll maximum. The positive correlation with [NO_3 + NO_2] support the previous observations.

The negative correlation with temperature reflects the fact that nutrients are generally linked to deep mixing and colder waters. For instance, higher abundances of *F. profunda* have been observed in sediments underneath relatively warmer and stratified surface waters with a deep nutricline (Boeckel et al. 2006).

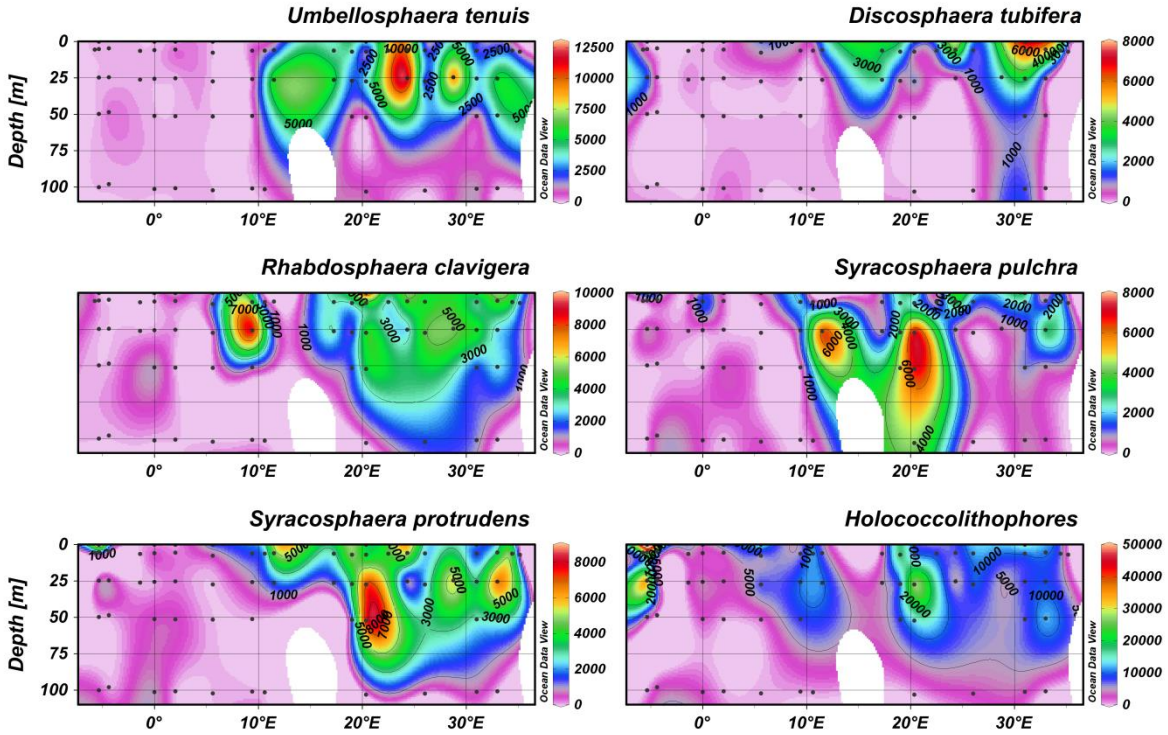

Figure 5.6. Distribution, along a west to east transect, of the heterococcolithophore species forming the cluster comprised mainly by "eastern Mediterranean species". Holococcolithophores as a group is added in the bottom right panel (the transect includes the stations labeled in black in Figure 5.1).

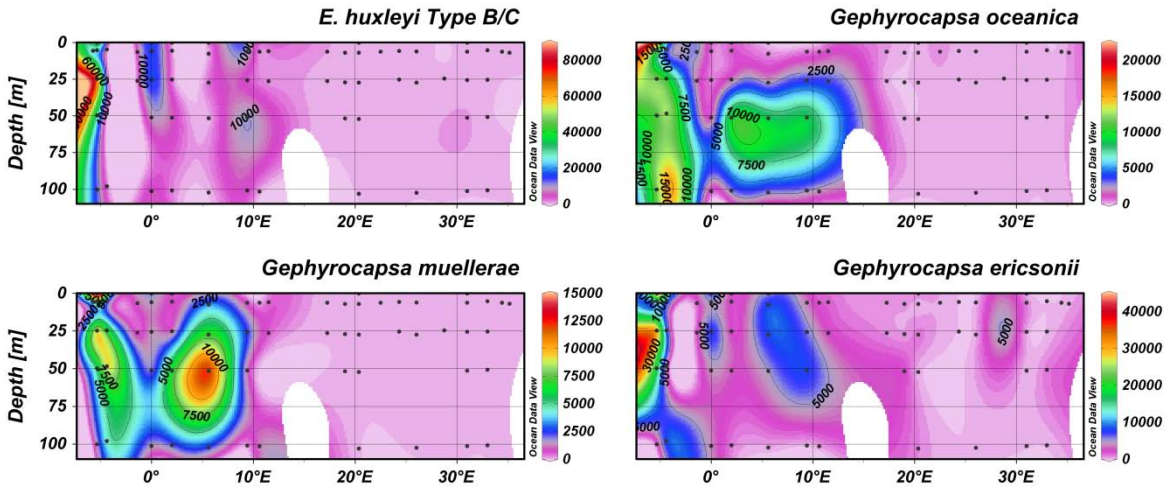

Figure 5.7. Distribution, along a west to east transect, of the heterococcolithophore species forming the cluster comprised mainly by "western Mediterranean species" (the transect includes the stations labeled in black in Figure 5.1).

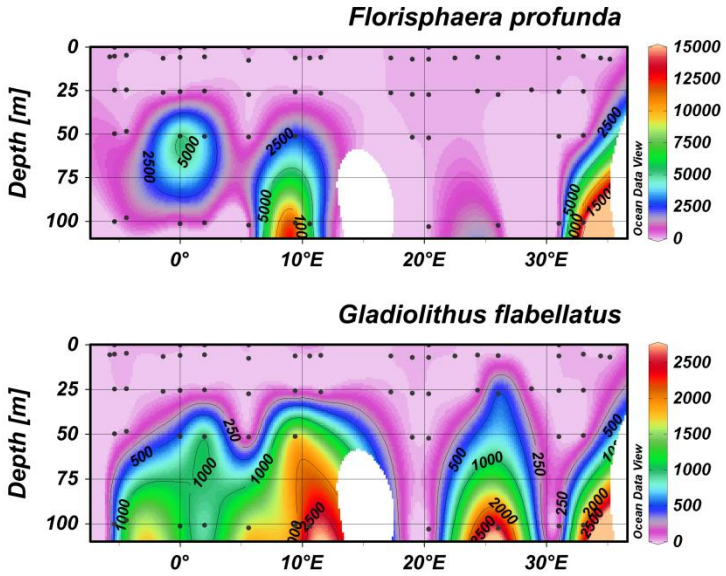

Figure 5.8. Distribution, along a west to east transect, of the heterococcolithophore species forming the smallest of the observed clusters comprised by 2 deep photic zone species (the transect includes the stations labeled in black in Figure 5.1).

The clustering of coccolithophore species resembles those proposed by Young (1994): umbelliform group such as *Umbellosphaera tenuis*, found in nutrient-depleted waters; a second group of placolith-bearing cells such as *Emiliania huxleyi* or *Gephyrocapsa* spp. found in coastal or mid-ocean upwelling regions and a last group, composed of floriform cells, such as *Florisphaera profunda*, associated with deep photic-zone assemblages in low to mid-latitudes. We would add in his first group the Rabdolith bearing species as well as some *syracosphaera* species widely associated to oligotrophic (Ziveri et al. 2004) surface waters (Malinverno et al. 2003) and cluster them together in our study. As Balch (2004) suggested when referring to this species grouping proposed by Young, "it is likely that the three groups of coccolithophores show differences in their growth strategies which ultimately would relate to their natural abundance".

Heterococcolithophores and holococcolithophores also displayed opposite trends in species diversity (Fig. 5.9). However the weak correlation obtained between the diversity index H' and the longitude of the sample site should be taken into account. Given the taxonomical problems between the two life stages (see Section 5.2.1) when considering the two as a single group would lead to the overestimation of the number of species, affecting H'.

Future work on the topic of discriminating between the two life stages would be necessary in order to clarify the trends suggested here.

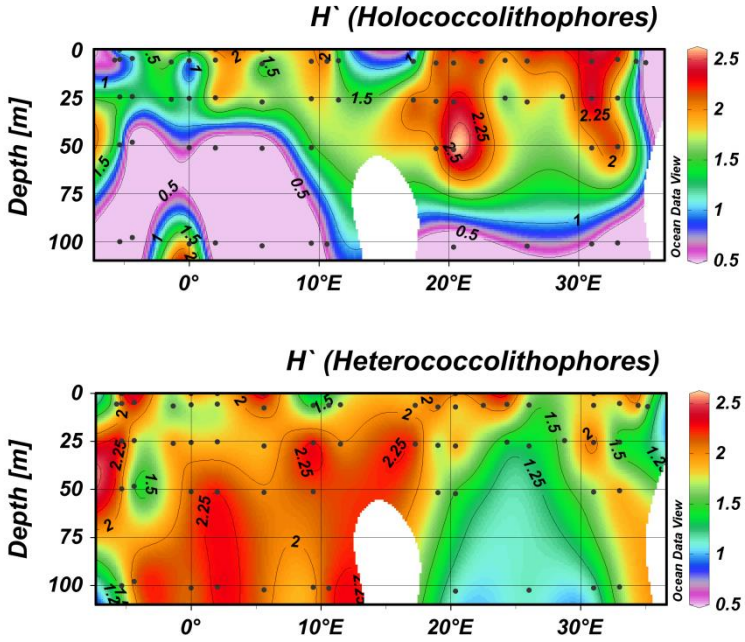

Figure 5.9. Shannon-Weiner diversity index for holococcolithophores and heterococcolithophores. A higher index, or higher uncertainty in correctly guessing the "next species" that would be sampled, is representative of a more diverse community.

Overall, distribution patterns and their relation to environmental parameters are different between the holo- and heterococcolithophores life phases. This is probably the result of a different physiology and reveals that the two phases are ex exploiting different ecological niches. Differences in the morphology and ecology of the two life phases enable the species to survive under a wider range of environmental conditions and could result in a wider distribution range in space and/or time. For instance, blooms of *Emiliania huxleyi* in heterococcolith phase can end due to viral attacks (Martínez et al. 2007; Vardi et al. 2012) which the haploid phase (i.e., holococcolithophores) can resist (Frada et al. 2008, 2012): Therefore, the occurrence of haploid individuals would serve as new starting point in the case of viral attack in the heterococcolith phase. Another factor that could have affected the results presented here is zooplankton grazing: although generally zooplankton grazing does not cause *E. huxleyi* blooms to end (Nejstgaard et al. 1997), their effect on smaller populations could be more important. Possibly important factors that were not addressed in our study are zooplankton grazing and irradiance. Therefore, their contribution to the

control of the observed distribution of holo- and heterococcolith life phases cannot be ruled out.

5.5.3.1 *Gephyrocapsa oceanica, G. muellerae* and *Emiliania huxleyi* morphotype B/C as tracers of Atlantic waters influx

Atlantic waters (AW), with a winter salinity around 36.5 (Rohling 2009), enter the Mediterranean Sea through the Gibraltar Strait. In its eastwards pathway following a cyclonic circulation, the surface water increases in salinity, TA, temperature and decreases in nutrient concentrations. A main part of this AW flows into the Tyrrhenian Sea (Tanhua et al. 2013b and references therein). Therefore, if there are species that arrive within this water mass (but whose optimal environment is not typical of eastern Mediterranean waters), the Tyrrhenian Sea could still host them.

During April 2011, the distribution of the species *Gephyrocapsa oceanica* and *G. muellerae* and morphotype B/C of the species *Emiliania huxleyi* was highly and negatively correlated with salinity. We have argued that salinity constrain to coccolithophore distribution is not critical. A high correlation with this parameter might just reflect the carry-over of a different species assemblage in a different water mass. *Gephyrocapsa oceanica*, *G. muellerae*, and morphotype B/C of the species *Emiliania huxleyi* were mostly present until ~10° E after the Sardinia Channel and in the Tyrrhenian Sea. They are all present in AW (Ziveri et al. 2004; McIntyre & Bé 1967) and have been reported before for western Mediterranean waters (e.g., Cross 2002, Knappertsbusch 1993; the latter only for *Gephyrocapsa* spp). The morphotype B/C of *E. huxleyi* has been associated with cold (Hagino et al. 2005; Mohan et al. 2008), nutrient rich waters (> 10 μmol kg^{-1} nitrate) with low calcite saturation states. These characteristics can be found in AW but are lost very soon in the Mediterranean Sea. Knappertsbusch (1993) related *G. oceanica* to surface AW's influence given the highly negative correlation with salinity. Here we propose *Gephyrocapsa oceanica*, *G. muellerae*, and *Emiliania huxleyi* morphotype B/C as tracers for AW influx into the Mediterranean.

5.6. Conclusions

Our results highlight the importance of seawater carbonate chemistry and $[PO_4^{3-}]$ in unraveling the distribution of heterococcolithophores, the most abundant coccolithophore life stage. Thus, carbonate system parameters might be critical, but under-looked, to solve the coccolithophore distribution patterns. In contrast, holococcolithophore distribution was mainly linked to oligotrophic conditions. This correlation can be due to competitive advantages under such conditions, but this hypothesis remains to be tested.

Environmental parameters that drive the observed patterns in distribution and assemblage composition of the haploid and diploid life phases of coccolithophores (holo- and heterococcolithophore) differ. Our results emphasize the importance of considering holo- and heterococcolithophores separately when analyzing changes in species assemblages and diversity, and the impacts of acidification on coccolithophores. Changes in the biogeographic distribution of hetero- and holococcolithophores can be expected along with the changes in carbonate chemistry and nutrient concentrations that are projected for the next century.

Please note that one Appendix is derived from this Chapter: Appendix B which contains the Coccolithophore species list.

Chapter 6

Synrhesis and conclusions

6.1 Effects of P limitation and ocean acidification in *E. huxleyi* populations and its contribution to biogeochemical cycles

The extremely low PO_4^{3-} concentrations in the Mediterranean Sea already impose limits for coccolithophore growth (as shown by Kress et al. 2005 for the eastern basin). If the predicted decrease in the concentrations of this nutrient (see section 1.1) would occur alone, further decline in cell abundances is to be expected. These cells would be larger, contain less POP, and more carbon (TPC) than those thriving in nutrient replete waters (Chapter 2). As a result, they will show increased C:N ratios, likely containing more carbohydrates and lipids. Since coccolithophores are at the base of the food web, these changes could alter the trophic webs by changing the nutritional values for grazers. It could also alter the C:P ratios in exported biological material. However, other factors have to be taken in consideration, all of which complicate the predictive power of unifactorial-single-strain experiments:

i) Environmental changes in the next decades will include ocean acidification and global warming as well as the likely intensification of other environmental stressors linked with human activities (e.g. eutrophication, overfishing) in some Mediterranean areas.

ii) Coccolithophores "compete" with other phytoplankton groups for different resources.

iii) Within coccolithophores, strain specific responses to P limitation were observed (results of Chapter 2) and species specific responses also exist. As confirmed by the disparate results of carbon quotas between *E. huxleyi* (Chapter 2), *Calcidiscus leptoporus* (Langer et al. 2012) and *Coccolithus pelagicus* (Gerecht et al. 2015)

i) This thesis studied the possible changes linked to the future parallel decrease in [P] in ocean pH expected from global climate change projection scenarios. One very important conclusion of this research is that oligothrophy (i.e. P limitation) amplifies the response to

ocean acidification in terms of maximum cell densities. The mechanism by which this happens involves an increase in P demand (POPq) with increased pCO_2. Accomplishment of these higher POP quotas decreases maximum cell densities (Chapter 3). Even if cells living under this combination of environmental conditions may contain more TPC and more POP, the total mass of exported material may decrease due to lower cell abundances (results from Chapter 3). Would this mean that the contribution of coccolithophores to the export of carbon will decrease under the combination of P limitation and ocean acidification? Judging from Chapter 3 only, that seems indeed likely, but the relative abundance of coccolithophores to other phytoplankton groups depends, of course, on the response of the other groups to P limitation and ocean acidification. Not only that, but if the response within coccolithophores is species specific, it also depends on the dominant coccolithophore species.

ii) The coccolithophore fraction of the total carbon sinking flux is of special interest because, as opposed to e.g. diatoms, coccolithophores contain organic as well as inorganic carbon. The ratio of inorganic to organic carbon (PIC:POC) in exported matter has a great influence on long term carbon burial and seawater carbonate chemistry . Changes in the PIC:POC in response to P-limitation were strain-specific (results of Chapter 2), which holds also with respect to seawater carbonate chemistry changes (Langer et al. 2009). Nevertheless, considering that the data set presented here (Chapter 2) is the most comprehensive published to date, comparing six *E. huxleyi* strains under P limitation, and that the PIC:POC decreased in five strains and remained constant in one, we can hypothesize that in Mediterranean *E. huxleyi* populations, P limitation most likely decreases PIC:POC. Similarly, in the majority of the strains studied, this ratio decreases with ocean acidification (Meyer & Riebesell 2015). Hence *E. huxleyi* might, in a future P-poor and acidified ocean, contribute relatively little inorganic carbon to exported matter, which would in turn favour remineralization over long term burial at depth. This effect will be of particular importance in areas where *E. huxleyi* dominates the coccolithophore community (e.g. English Channel). There are, however, vast expanses of ocean dominated by other species. In the South Atlantic *C. leptoporus* is the key species, and in the high latitude North Atlantic, *C. pelagicus* dominates (Baumann et al. 2004, Daniels et al. 2014). These species do not react to P-limitation and ocean acidification as *E. huxleyi* does. *C. leptoporus* decreases PIC:POC in response to ocean acidification, but is insensitive to P-

limitation (Langer et al. 2006, Langer et al. 2012). *C. pelagicus* is insensitive to OA (up to worst case IPCC year 2100 scenarios), and might increase the PIC/POC in response to P-limitation (although sub-species *braarudii* shows a decrease, Langer et al. 2006, Gerecht et al. 2014, 2015).

iii) Scaling the results of experiments focused on genotypes to the community and ecosystem levels is recognized as a challenge, but a necessity for OA studies (Riebesell et al. 2010). In order to get a broader picture, Chapters 4 and 5 were dedicated to the analysis of samples coming from two *in situ* perturbation experiments of a mesocosm scale and an *in situ* observational study respectively. In both, the coccolithophore community and their abundance relative to siliceous phytoplankton was addressed.

As coccolithophores have higher affinities for P (Riegman et al. 2000) and their photosynthesis is not saturated under present day pCO_2 [reviewed in Rost et al. (2008)] they could dominate over diatoms in the future ocean. Regarding the higher affinities for P, this seems to be supported by evidence from the field. For instance, Cermeño et al. (2008) observed that in areas with a deep nutricline, and thus highly stratified oligotrophic conditions as in the eastern Mediterranean Sea, the ratio of coccolithophores to diatoms is higher than in shallow nutricline areas. On the other hand, Chapter 4 does not provide evidence to support the hypothesis that coccolithophore growth will be enhanced by elevated pCO_2 under oligotrophic (i.e.: P poor) conditions, as coccolithophore cell densities did not vary in response to the pCO_2 treatments imposed in any of the two mesocosm perturbations. As a result, a pCO_2 driven phytoplankton succession did not occur in these oligotrophic areas and if coccolithophores turned to dominate over other phytoplankton groups it was probably due to phenological changes in the phytoplankton community.

The data derived from the Meteor cruise (M84/3, Chapter 5) show a higher coccolithophore to diatom ratio in the eastern basin (Figure 6.1), which is consistent with lower $[PO_4^{3-}]$ in this area, but is not consistent with the lower pCO_2 measured in the eastern basin. Three non-excluding explanations can be given: First, increased pCO_2 may not favour all species in the coccolithophore community or any species at all. Even further, it can cause deleterious effects such as malformations (Chapter 3). Second, the competitive interactions between these two groups in the Mediterranean Sea may be more constrained

by nutrient availability than by pCO_2. Third, the rage of the pCO_2 gradient in the Mediterranean Sea is too small to see the effects on the phytoplankton community (~340 to ~500 µatm) (Gemayel et al., 2015).

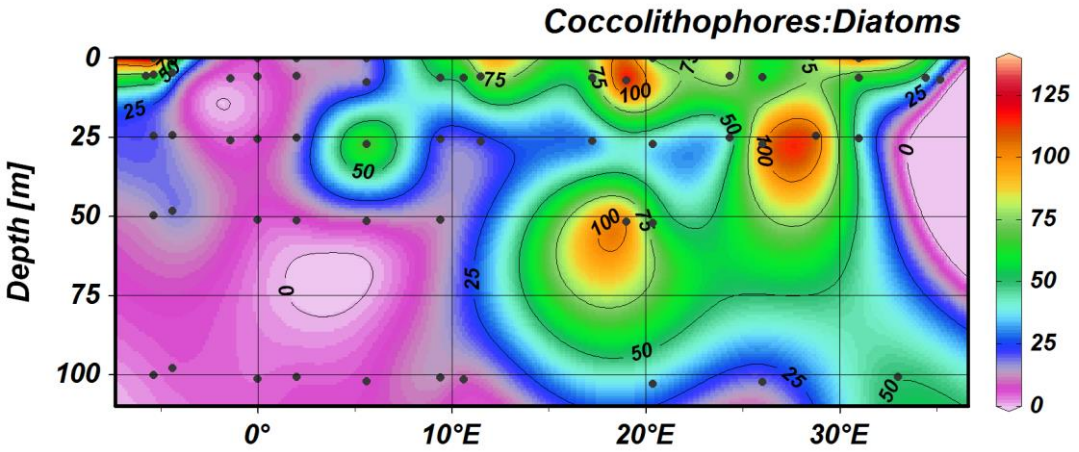

Figure 6.1 Ratio of coccolithophores to diatoms along a west to east transect in the Mediterranean Sea (data as used for Chapter 5).

As mentioned above, it was shown in Chapter 3 that increased pCO_2 decreased µ and maximum yield cell densities in the Mediterranean strain tested. Other experiments have also shown decreased µ [see review in Raven and Crawfurd (2012)] although most strains at a global scale seem to be favoured by the increase in pCO_2. It is concluded that a detrimental effect of high pCO_2 on coccolithophore populations will be possible.

Whether, in oligothrophic regions, nutrients affect the coccolithophore community structure stronger than pCO_2 does was discussed in Chapter 4 (mesocosm experiments). Coccolithophore community structure did not change with pCO_2 in either of the two mesocosm experiments (summer and winter-spring). In Chapter 5, however, a different coccolithophore assemblage could be assigned to the eastern and the western basin. Even further, changes in heterococcolithophore assemblages were best linked to $[CO_3^{2-}]$ and pH, but $[PO_4^{3-}]$ also seemed important. The fact that gradients in these parameters overlap in the Mediterranean makes it difficult to distinguish which one could contribute the most to explain changes in coccolithophore community. These different results could also indicate that some of the species present in the Mediterranean are negatively affected by increased pCO_2, while others are not.

6.2 *E. huxleyi* coccolith morphology in relation to ocean acidification and P-limitation

6.2.1 Hampered morphogenesis

Contrary to a previous hypothesis (Okada & Honjo 1975, Young & Westbroek 1991), P limitation does not induce coccolith malformations in *E. huxleyi* (Chapters 2 and 3). While this is true for *C. leptoporus* as well (Langer et al 2012), the case of *C. pelagicus* shows that this finding cannot be generalized (Gerecht et al 2014, 2015). Whether the occasional occurrence of a high percentage of malformed coccoliths in field samples can be explained by nutrient limitation remains to be investigated, but seems rather unlikely in the light of available experimental data. Stand-alone experimental data, however, are on no account sufficient to analyse the complex situation in the field. This is illustrated when considering the effect of carbonate chemistry on coccolith morphology. Experimental results suggest that the majority of coccolithophores is sensitive to seawater acidification (Riebesell et al. 2000; De Bodt et al. 2010; Langer et al. 2006, 2011; Langer and Bode 2011, Bach et al. 2012). This was confirmed in the present study (Chapter 3). In natural populations of *E. huxleyi*, however, manipulated carbonate chemistry (Chapter 4) had no effect on morphology. Technical reasons can not be ruled out. Given that the population size of *E. huxleyi* was decreasing during the spring time mesocosm experiment (Chapter 4), and its duration was relatively short (12 days), it is not surprising that no increase in malformations due to acidification could be observed. However, in a mesocosm experiment where the population size of *E. huxleyi* was increasing and that lasted 19 days (Engel et al. 2005), high pCO_2 did not caused malformations either. Apart from this technical issue, there is also the influence of clone selection in mesocosm or field samples, which is not existent in monoclonal culture experiments. An increase in *E. huxleyi* malformed coccoliths was recorded in a natural pH gradient near CO_2 vents off Vulcano Island, Italy (Meier et al. 2014). However, a hypothetical larger time of exposure to elevated CO_2 at volcanic vents (not quantified in the study of Meier et al.) might have determined the effects on coccolith morphogenesis. It is then probable that a short time exposure to enhanced pCO_2 together with a likely clone selection resulted in a weak signal of the effects of ocean acidification during the mesocosm experiments.

6.3.2 Degree of calcification

The results obtained from the culture and mesocosm experiments seem to differ with the *in situ* observations. Briefly the results were: i) Under P limitation (Chapter 2) the majority of strains showed an increased percentage of over calcified coccoliths. ii) Under P limitation and ocean acidification (Chapter 3) there was no relationship between the treatments and the degree of calcification. iii) Similarly, in the mesocosm experiments (Chapter 4) no effect was observed. iiii) In the west to east transect along the Mediterranean, the percentage of under-calcified coccoliths decreased while the percentage of over-calcified coccoliths increased (Figure 6.2).

Two non-exclusive explanations are proposed:

1. In the west to east transect, most changes in the degree of calcification are due to different distribution of *E. huxleyi* morphotypes. In particular, type A *versus* type B/C. The latter characteristic of Atlantic water influx and observed almost exclusively in the western Mediterranean basin. Since the B/C morphotype has thin coccoliths, the percentage of under–calcified coccoliths is higher in the west. On the contrary, in the culture and mesocosm experiments there was only *E. huxleyi* morphotype A, which displays all degrees of calcification but tends to be normally calcified. It would then be important to experimentally confirm whether the morphyotype B/C, or any other morphotype featuring under-calcified coccoliths would be favoured over the morphotype A in more acidified waters.
2. The observed patterns along the Mediterranean transect are better explained by changes in $[PO_4^{3-}]$ or by other environmental parameters that differed between the western and eastern basins. Again, please note that in the P limitation experiment (Chapter 2) the majority of the tested strains had a higher percentage of over-calcified coccoliths under P limitation. In the eastern Mediterranean *E. huxleyi* can be P-limited (Kress et al. 2005) while is not confirmed for the western Mediterranean.

The degree of calcification was proposed as a proxy for PICp (Beaufort et al. 2011, Bach et al 2012). Given the reliability of this putative proxy, this could be a promising way of reconstructing past changes in PICp over various timescales, because individual coccoliths

can be obtained in sufficient numbers from sediments. A caveat here is the above mentioned morphotype/clone selection issue.

In any case, judging from the P limitation experiment and the ocean acidification and P limitation experiment the degree of calcification does not seem to be a good proxy for calcite production or PIC:POC. In these experiments the degree of calcification was no correlated to PICq, PICp or the PIC:POC.

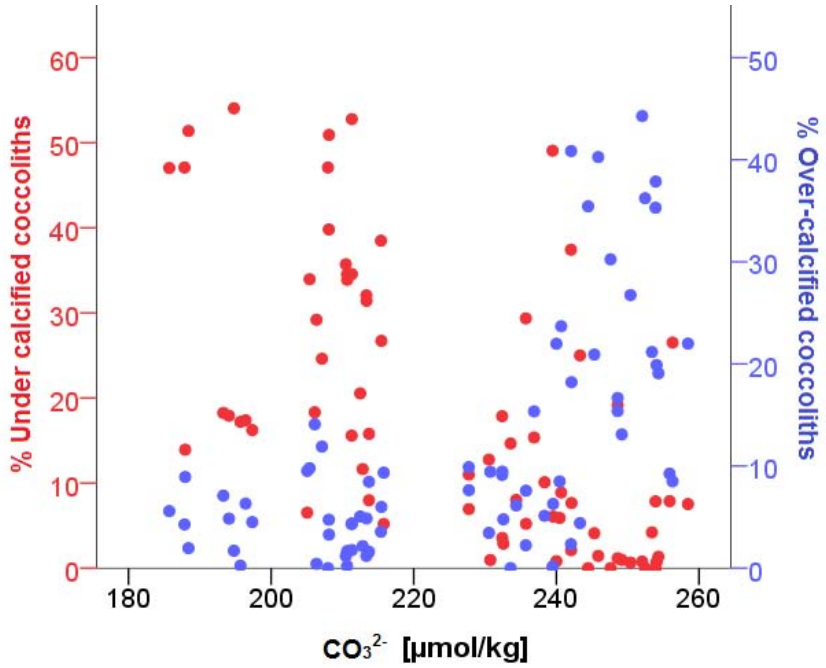

Figure 6.2. Percentage of under-calcified and over-calcified coccoliths of *Emiliania huxleyi* along a carbonate chemistry gradient in the Mediterranean Sea. The data is derived from the M84-3 cruise on board of the Meteor R.V. as detailed in Chapter 5.

6.3 Research perspectives and recommendations

- The dynamics (i.e.: frequency of pulsed nutrient supply) can control competitive interaction between phytoplankton groups (Cermeño et al. 2008). This limits the inferences that can be drawn from "snap-shot" *in situ* observations on the relationship between phytoplankton and nutrient concentration.
- In all *in situ* observations, whether coming from manipulative approaches or not, the phenological dynamics of the phytoplankton community is an important factor that should be addressed in further studies. As noted in Chapter 4, it is possible that in oligothrophic regions with pulsed input of macro- and micro- nutrients, phenological dynamics mask the effects of pCO_2.

- Finally, if pCO_2 is to select upon *E. huxleyi* morphotypes, and if this is to be evident over a wide range of pCO_2, it will be then more useful to use the relative abundances of the different morphotypes as a proxy for ancient pCO_2 than to use the presence of coccolith malformation in coccoliths.

Appendix A. Species list from Chapter 4

	Coccolithophore species	BV	BC
	Family Calciosoleniaceae Kamptner		
1	*Calciosolenia brasiliensi*s (Lohmann) Young	X	
	Family Coccolithaceae Poche		
2	*Calcidiscus leptoporus* (Murray et Blackman) Loeblich et Tappan	X	
3	*Umbilicosphaera sibogae* var. *sibogae* (Weber-Van Bosse) Gaarder	X	
	Family Helicosphaeraceae Black		
4	*Helicosphaera carteri* (Wallich) Kamptner	X	
	Family Noelaerhabdaceae Jerkovic		
5	*Emiliania huxleyi* (Lohmann) Hay et Mohler	X	X
6	*Gephyrocapsa ericsonii* McIntire et Bé	X	
7	*Reticulofenestra parvula* (Okada et McIntyre) Biekart	X	
	Family Pontosphaeraceae Lemmermann		
8	*Scyphosphaera apsteinii* Lohmann	X	
	Family Rhabdoaphaeraceae Ostenfeld		
9	*Acanthoica quattrospina* Lohmann	X	
10	*A. acanthifera* Lohmann ex Lohmann	X	
11	*Anacanthoica cidaris* (Schlauder) Kleijne	X	
12	*Algiropsphaera robusta* (Lohmann) Norris	X	
13	*Cyrtosphaera lecaliae* Kleijne	X	
14	*Discosphaera tubifera* (Murray et Blackman) Ostenfeld	X	
15	*Palusphaera vandeli* Lecal emend. Norris	X	X
16	*Rhabdosphaera clavigera* Murray et Blackman	X	X
	Family Alisphaeraceae Young, Kleijne et Cros		
17	*Alisphaera extenta* (Kamptner) Kleijne, Jordan, Heimdal, and others	X	
	Family Syracosphaeraceae Lemmermann		
18	*C. mediterranea* (Lohmann) Gaarder	X	X
19	*Ophiaster formosus* Gran	X	
20	*O. hydroideus* Gran	X	
21	*Syracosphaera anthos* (Lohmann) Janin	X	X
22	*S. bannockii* (Borsetti et Cati) Cros, Kleijne, Zeltner, Billard et Young	X	
23	*S. borealis* Okada et McIntire	X	
24	*S. corolla* Lecal	X	
25	*S. delicata* Cros, Kleijne, Zeltner, Billard et Young	X	
26	*S.dilatata* Jordan, Kleijne et Heimdal	X	
27	*S. histrica* Kamptner	X	
28	*S. lamina* Lecal-Schlauder	X	
29	*S. marginoporata* Knappertsbusch	X	
30	*S. molischii* Schiller	X	
31	*S. nana* (Kamptner) Okada et McIntyre	X	

32	*S. nodosa* Kamptner	X	X
33	*S. noroitica* Knappertsbusch	X	
34	*S. orbiculus* Okada et McIntyre	X	
35	*S. ossa* (Lecal) Loeblich et Tappan	X	X
36	*S. protrudens* Okada et McIntyre	X	
37	*S. pulchra* Lohmann	X	
38	*S. rotula* Okada et McIntire	X	
39	*S. tumularis* Sánchez- Suárez	X	
40	*Syracosphaera sp*. type D, sensu Kleijne	X	
	Family Umbellosphaeraceae Young et Kleijne		
41	*Umbellosphaera tenuis* (Kamptner) Paasche	X	
42	*Gladiolithus flabellatus* (Halldal et Markali) Jordan et Green	X	
43	*Ceratolithus cristatus* Norris	X	
	Holococcolithophores		
44	*Anthosphaera fragaria* Kamptner emend. Kleijne	X	
45	*C. leptoporus* ssp. *quadriperforatus*HOL (Kamptner) Geisen, Billard, Broerse, and others	X	
46	*Syracolithus dalmaticus*(Kamptner) Loeblich et Tappan	X	
47	*Syracosphaera anthos* HOL (Lohmann) Janin		X

Appendix B. Species list from Chapter 5

B.1. Heterococcolithophores.
Family Calciosoleniaceae Kamptner, 1937
[1] *Anoplosolenia brasiliensis* (Lohmann, 1919) Deflandre, 1952
[2] *Calciosolenia murrayi* Gran, 1912
Family Coccolithaceae Poche, 1913
[3] *Calcidiscus leptoporus* (Murray and Blackman, 1898) Loeblich and Tappan, 1978
[4] *Hayaster perplexus* (Bramlette and Riedel, 1954) Bukry, 1973
[5] *Pleurochrysis carterae* (Braarud and Fagerland, 1946) Christensen, 1978
[6] *Umbilicosphaera sibogae* var. sibogae (Weber-Van Bosse, 1901) Gaarder, 1970
[7] *U. sibogae* var. foliosa (Kamptner, 1963; ex Kleijne, 1993) in Sáez et al., 2003
[8] *U. hulburtiana* Gaarder, 1970
Family Helicosphaeraceae Black, 1971
[9] *Helicosphaera carteri* (Wallich, 1877) Kamptner, 1954
[10] *H. pavimentum* Okada and McIntire, 1977
Family Noelaerhabdaceae Jerkovic, 1970
[11] *Emiliania huxleyi* (Lohmann, 1902) Hay and Mohler, in Hay et al., 1967
[12] *Gephyrocapsa ericsonii* McIntire and Bé, 1967
[13] *G. ornata* Heimdal, 1973
[14] *G. oceanica* Kamptner, 1943
[15] *G. muellerae* Bréhéret, 1978
[16] *Reticulofenestra parvula* (Okada & McIntyre, 1977) Biekart, 1989
Family Papposphaeraceae Jordan and Joung, 1990
[17] *Papposphaera lepida* Tangen, 1972
Family Pontosphaeraceae Lemmermann, 1908
[18] *Pontosphaera japonica* (Takayama, 1967) Nishida, 1971
[19] *Scyphosphaera apsteinii* Lohmann, 1902
Family Rhabdoaphaeraceae Ostenfeld, 1899
[20] *Acanthoica biscayensis* Kleijne, 1992
[21] *A. quattrospina* Lohmann, 1903
[22] *Algirosphaera cucullata* (Lecal-Schlauder, 1951) Young, Probert and Kleijne, 2003
[23] *Algiropsphaera robusta* (Lohmann, 1902) Norris, 1984
[24] *Anacanthoica acanthos* (Schiller, 1925) Deflandre, 1952
[25] *Cyrtosphaera lecaliae* Kleijne, 1992
[26] *Discosphaera tubifera* (Murray and Blackman, 1898) Ostenfeld, 1900
[27] *Palusphaera vandeli* Lecal, 1965
[28] *Rhabdosphaera clavigera* var. *clavigera* Murray and Blackman, 1898
[29] *R. clavigera var. stylifera* (Lohmann, 1902) Kleijne and Jordan, 1990
[30] *R. xiphos* (Deflandre and Fert, 1954) Norris, 1984
Family Syracosphaeraceae Lemmermann, 1908
[31] *Alisphaera capulata* Heimdal, 1981
[32] *A. extentata* (Kamptner, 1941) Kleijne, Jordan, Heimdal, Samtleben, Chamberlain and Cros, 2002
[33] *A. gaudi* (Kamptner, 1941) Kleijne, Jordan, Heimdal, Samtleben, Chamberlain and Cros, 2002
[34] *A. unicornis* Okada and McIntire, 1977

[35] *Calciopappus caudatus* Gaarder and Ramsfjell, 1954
[36] *C. rigidus* Heimdal, 1981
[37] *Coronosphaera binodata* (Kamptner, 1927) Gaarder, in Gaarder and Heimdal, 1977
[38] *C. mediterranea* (Lohmann, 1902) Gaarder, in Gaarder and Heimdal, 1977
[39] *Michaelsarsia adriaticus* (Schiller, 1914) Manton, Bremer and Oates, 1984
[40] *M. elegans* Gran, 1912, emend. Manton, Bremer and Oates, 1984
[41] *Ophiaster formosus* Gran, 1912
[42] *Ophiaster hydroideus* Gran, 1912
[43] *Syracosphaera ampliora* Okada and McIntire, 1977
[44] *S. anthos* (Lohmann, 1912) Jordan and Young, 1990
[45] *S. bannockii* (Borsetti and Cati, 1976) Cros, Kleijne, Zeltner, Billard and Young, 2000
[46] *S. borealis* Okada and McIntire, 1977
[47] *S. corolla* (Lecal, 1966)
[48] *S. delicata* Cros, Kleijne, Zeltner, Billard and Young, 2000
[49] *S.dilatata* Jordan, Kleijne and Heimdal, 1993
[50] *S. histrica* Kamptner, 1941
[51] *S. lamina* Lecal-Schlauder, 1951
[52] *S. marginoporata* Knappertsbusch, 1993
[53] *S. molischii* Schiller, 1925
[54] *S. nana* (Kamptner) Okada & McIntyre, 1977
[55] *S. nodosa* Kamptner, 1941
[56] *S. noroitica* Knappertsbusch, 1993
[57] *S. ossa* (Lecal, 1966) Loeblich and Tappan, 1968
[58] *S. pirus* Halldal and Markali, 1955
[59] *S. prolongata* Gran, 1912, ex Lohmann, 1913
[60] *S. protrudens* Okada and McIntyre, 1977
[61] *S. pulchra* Lohmann, 1902
[62] *S. rotula* Okada & McIntire, 1977
[63] *Syracosphaera sp. type D*, sensu Kleijne, 1993
[64] *S. tumularis* Sánchez- Suárez, 1990
[65] *Syracospahaera* sp.
Sub-Family Umbellosphaeroideae Kleijne, 1993
[66] *Umbellosphaera tenuis* (Kamptner, 1937) Paasche, in Markali & Paasche, 1955
[67] *F. profunda* Okada and Honjo, 1973
[68] *Gladiolithus flabellatus* (Halldal and Markali, 1955) Jordan and Green, 1994
[69] *Polycrater galapagensis* Manton and Oates, 1980
[70] *Ceratolithus cristatus* Norris, 1965

B2. Holococcolithophores.
[1] *Acanthoica quattrospina* HOL = sp. aff Sphaerocalyptra Cros et al. 2000
[2] *Anthosphaera fragaria* Kamptner, 1937, emend. Kleijne, 1991
[3] *A. lafourcadii* (Lecal, 1967); Kleijne, 1991
[4] *A. periperforata* Kleijne, 1991
[5] *Anthosphaera sp*. Type A Cros and Fortuno, 2002
[6] *Anthosphaera* sp. Type C Cros and Fortuno, 2002
[7] *Calcidiscus leptoporus* HOL (Murray and Blackman, 1898) Loeblich and Tappan, 1978
[8] *C. leptoporus* ssp. quadriperforatus HOL (Kamptner,1937) Geisen et al., 2002
[9] *Calicasphaera concava* Kleijne, 1991

[10] *Calyptrolithina divergens* (Halldal and Markali, 1955) Heimdal, 1982
[11] *C. divergens f. tuberosa* (Heimdal, in Heimdal and Gaarder, 1980) Heimdal, 1982
[12] *C. multipora* (Gaarder, in Heimdal and Gaarder, 1980) Norris, 1985
[13] *Calyptrolithophora papillifera* (Halldal, 1953) Heimdal, in Heimdal & Gaarder, 1980
[14] *Calyptrosphaera cialdii* Borsetti and Cati, 1976
[15] *C. dentata* Kleijne, 1991
[16] *C. heimdalae* Norris, 1985
[17] *C. sphaeroidea* Schiller, 1913
[18] *Coccolithus pelagicus* ssp. braarudii HOL = *Crystallolithus braarudii* (Gaarder, 1962) Geisen et al., 2002
[19] *Corisphaera gracilis* Kamptner, 1937
[20] *C. strigilis* Gaarder, 1962
[21] *C. tyrrheniensis* Kleijne, 1991
[22] *Corisphaera* sp. Kleijne, 1991
[23] *Coronosphaera mediterranea* HOL gracillima-type = *Calyptrolithophora gracillima* (Kamptner 1941) Heimdal in Heimdal and Gaarder 1980
[24] *Coronosphaera mediterranea* HOL hellenica type = *Zygosphaera hellenica* Kamptner, 1937
[25] *Gliskolithus amitakarenae* Norris, 1985, orthog. emend., Jordan and Green, 1994
[26] *Helicosphaera carteri* HOL = *Syracolithus catilliferus* (Kamptner, 1937) Deflandre, 1952
[27] *Helladosphaera cornifera* (Schiller, 1913) Kamptner, 1937
[28] *Homozygosphaera arethusae* (Kamptner, 1941) Kleijne, 1991
[29] *H. spinosa* (Kamptner, 1941) Deflandre, 1952
[30] *H. triarcha* Halldal and Markalii, 1955
[31] *Homozygosphaera vercellii* Borsetti and Cati, 1979
[32] *Poricalyptra gaarderae* (Borsetti and Cati, 1967) Kleijne, 1991
[33] *Poritectolithus* sp. 2 in Cros and Fortuño, 2002
[34] *Sphaerocalyptra adenensis* Kleijne, 1991
[35] *S. quadridentata* (Schiller, 1913) Deflandre, 1952
[36] *Sphaerocalyptra* sp. 1 in Cros and Fortuño, 2002
[37] *Sphaerocalyptra* sp. 3 in Cros and Fortuño, 2002
[38] *Sphaerocalyptra* sp. 6 in Cros and Fortuño, 2002
[39] *Syracolithus schilleri* (Kamptner, 1927) Loeblich and Tappan, 1963
[40] *Syracolithus sp*. type A of Kleijne, (1991)
[41] *Syracosphaera anthos* HOL = *Periphyllophora mirabilis* (Schiller, 1925) Kamptner, 1937
[42] *Syracosphaera bannockii* HOL = *Zygosphaera bannockii* (Borsetti and Cati, 1976) Heimdal, 1982
[43] *Syracosphaera pulchra* HOL oblonga type = Calyptrosphaera oblonga Lohmann, 1902
[44] *Syracosphaera pulchra* HOL pirus type = Calyptrosphaera pirus Kamptner, 1937
[45] *Zygosphaera amoena* Kamptner, 1937

References

Al-Moosawi L, Rees AP, Clark DR, Gazeau F, Guieu C, Louis J, Vincent A (in Prep.) The impact of ocean acidification on the pelagic nitrogen cycle in the western Mediterranean Sea. Estuarine, Coastal and Shelf Science.

Álvarez M, Sanleón-Bartolomé H, Tanhua T, Mintrop L, Luchetta A, Cantoni C, Schroeder K, Civitarese G (2014) The CO_2 system in the Mediterranean Sea: a basin wide perspective. Ocean Sci 10:69–92

Ammerman JW, Hood RR, Case DA, Cotner JB (2003) Phosphorus deficiency in the Atlantic: An emerging paradigm in oceanography. Eos 84:165

Anderson TR (2005) Plankton functional type modelling: running before we can walk? J Plankton Res 27:1073–1081

Augustin L, Barbante C, Barnes PR, Barnola JM, Bigler M, Castellano E, Cattani O, Chappellaz J, Dahl-Jensen D, Delmonte B, others (2004) Eight glacial cycles from an Antarctic ice core. Nature 429:623–628

Bach LT, Mackinder LCM, Schulz KG, Wheeler G, Schroeder DC, Brownlee C, Riebesell U (2013) Dissecting the impact of CO_2 and pH on the mechanisms of photosynthesis and calcification in the coccolithophore *Emiliania huxleyi*. New Phytol 199:121–134

Bach LT, Bauke C, Meier KJS, Riebesell U, Schulz KG (2012) Influence of changing carbonate chemistry on morphology and weight of coccoliths formed by *Emiliania huxleyi*. Biogeosciences 9 (8):3449–3463

Bach LT, Riebesell U, Schulz KG (2011) Distinguishing between the effects of ocean acidification and ocean carbonation in the coccolithophore *Emiliania huxleyi*. Limnol Oceanogr 56:2040–2050

Bakun A, Agostini VN (2001) Seasonal patterns of wind-induced up- welling/downwelling in the Mediterranean Sea. Sciencia Marina 65:243–257

Balch WM (2004) Re-evaluation of the physiological ecology of coccolithophores. In: Thierstein H, Young JR (eds) Coccolithophores – From Molecular Processes to Global Impact. Springer, Berlin. pp. 165–190

Barcena MA, Flores JA, Sierro FJ, Pérez-Folgado M, Fabres J, Calafat A, Canals M (2004) Planktonic response to main oceanographic changes in the Alboran Sea (Western Mediterranean) as documented in sediment traps and surface sediments. Mar Micropaleontol 53:423–445

Barlow RG, Mantoura RFC, Cummings DG, Fileman TW (1997) Pigment chemotaxonomic distributions of phytoplankton during summer in the western Mediterranean. Deep-Sea Res. Part II 44:833–850.

Bates NR, Peters AJ (2007) The contribution of atmospheric acid deposition to ocean acidification in the subtropical North Atlantic Ocean. Mar Chem 107:547–558

Båtvik H, Heimdal BR, Fagerbakke KM, Green JC (1997) Effects of unbalanced nutrient regime on coccolith morphology and size in Emiliania huxleyi (Prymnesiophyceae). Eur J Phycol 32(2):155–165

Baumann K-H, Bockel B, Frenz M (2004) Coccolith contribution in the South Atlantic carbonate sedimentation. In: Thierstein HR, Young JR (eds.) Coccolithophores: From Molecular Processes to the Global Impact. Springer, 367–402 pp.

Beardall J, Giordano M (2002) Ecological implications of microalgal and cyanobacterial CO_2 concentrating mechanisms, and their regulation. Funct Plant Biol 29:335–347

Beaufort L, Couapel M, Buchet N, Claustre H, Goyet C (2008) Calcite production by coccolithophores in the south east Pacific Ocean. Biogeosciences 5:1101–1117

Beaufort L, Probert I, Garidel-Thoron T de, Bendif EM, Ruiz-Pino D, Metzl N, Goyet C, Buchet N, Coupel P, Grelaud M, Rost B, Rickaby REM, Vargas C de (2011) Sensitivity of coccolithophores to carbonate chemistry and ocean acidification. Nature 476:80–83

Behrenfeld MJ, O'Malley RT, Siegel DA, McClain CR, Sarmiento JL, Feldman GC, Milligan AJ, Falkowski PG, Letelier RM, Boss ES (2006) Climate-driven trends in contemporary ocean productivity. Nature 444:752–755

Bellerby RGJ, Schulz KG, Riebesell U, Neill C, Nondal G, Heegaard E, Johannessen T, Brown KR (2008) Marine ecosystem community carbon and nutrient uptake stoichiometry under varying ocean acidification during the PeECE III experiment. Biogeosciences 5: 1517–1527

Berland BR, Benzhitski AG, Burlakova ZP, Georgieva LV, Izmestieva MA, Kholodov V I, Maestrini SY (1988) Conditions hydrologiques estivales en Mediterranee, repartition du phytoplankton et de la matiere organique. Oceanol Acta 9:163–177

Berman T, Townsend DW, El Sayed SZ, Trees GC, Azov Y (1984) Optical transparency, chlorophyll and primary productivity in the Eastern Mediterranean near the Israeli Coast. Oceanol Acta 7:367–372

Béthoux J., Morin P, Chaumery C, Connan O, Gentili B, Ruiz-Pino D (1998) Nutrients in the Mediterranean Sea, mass balance and statistical analysis of concentrations with respect to environmental change. Mar Chem 63:155–169

Boeckel B, Baumann KH, Henrich R, Kinkel H (2006) Coccolith distribution patterns in South Atlantic and Southern Ocean surface sediments in relation to environmental gradients. Deep-Sea Res Part I 53:1073–1099

Bopp L, Resplandy L, Orr JC, Doney SC, Dunne JP, Gehlen M, Halloran P, Heinze C, Ilyina T, Séférian R, Tjiputra J, Vichi M (2013) Multiple stressors of ocean ecosystems in the 21st century: projections with CMIP5 models. Biogeosciences 10:6225–6245

Bollmann J, Cortes MY, Haidar AT, Brabec B, Close A, Hofmann R, Palma S, Tupas L, Thierstein HR (2002) Techniques for quantitative analyses of calcareous marine phytoplankton. Mar Micropaleontol 44(3-4):163−185

Borchard C, Borges AV, Händel N, Engel A (2011) Biogeochemical response of *Emiliania huxleyi* (PML B92/11) to elevated CO_2 and temperature under phosphorous limitation: A chemostat study. J Exp Mar Biol Ecol 410:61–71

Bosc E, Bricaud A, Antoine D (2004) Seasonal and interannual variability in algal biomass and primary production in the Mediterranean Sea, as derived from 4 years of SeaWiFS observations. Global Biogeochemical Cycles. 18, GB1005.

Brand LE (1984) The salinity tolerance of forty-six marine phytoplankton isolates. Estuar Coast Shelf Sci 18:543–556

Brand LE (1994) Physiological ecology of marine coccolithophores. In: Winter A, Siesser WG (eds.) Coccolithophores. Cambridge University Press, UK. pp. 39–49

Broecker W, Clark E (2009) Ratio of coccolith $CaCO_3$ to foraminifera $CaCO_3$ in late Holocene deep sea sediments: Coccolith to forams in deep sea sediment. Paleoceanography 24: PA3205

Broerse ATC, Brummer G-J A, Van Hinte JE (2000) Coccolithophore export production in response to monsoonal upwelling off Somalia (northwestern Indian Ocean). Deep-Sea Res Part II 47:2179–2205

Brownlee C, Taylor A (2004) Calcification in coccolithophores: a cellular perspective. In: Thierstein HR, Young JR (eds.), Coccolithophores, from Molecular Processes to Global Impact. Springer, Berlin, pp. 31–49

Brussaard CPD, Noordeloos AAM, Witte H, Collenteur MCJ, Schulz K, Ludwig A, Riebesell U (2013) Arctic microbial community dynamics influenced by elevated CO_2 levels. Biogeosciences 10:719–731

Buitenhuis ET, Pangerc T, Franklin DJ, Le Quéré C, Malin G (2008) Growth rates of six coccolithophorid strains as a function of temperature. Limnol Oceanogr 53(3):1181–1185

Buitenhuis ET, de Baar H, Veldhuis M (1999) Photosynthesis and calcification by *Emiliania huxleyi* (Prymnesiophyceae) as a function of inorganic carbon species. J Phycol 35:949–959

Cermeño P, Dutkiewicz S, Harris RP, Follows M, Schofield O, Falkowski PG (2008) The role of nutricline depth in regulating the ocean carbon cycle. Proc Natl Acad Sci 105:20344–20349

Charalampopoulou A, Poulton AJ, Tyrrell T, Lucas MI (2011) Irradiance and pH affect coccolithophore community composition on a transect between the North Sea and the Arctic Ocean. Mar Ecol Progr Ser 431:25–43

Ciais P, Sabine C, Bala G, Bopp L, Brovkin V, Canadell J, Chhabra A, DeFries R, Galloway J, Heimann M, others (2013) Carbon and other biogeochemical cycles. In: Stocker TF, Qin D, Plattner G-K, Tignor M, Boschung J, Nauels A, Xia Y, Bex V, Midgley PM (eds) Climate change 2013: the physical science basis. Contribution of Working Group I to the Fifth Assessment Report of the Intergovernmental Panel on Climate Change. Cambridge University Press, p 465–570

Clark DR, Flynn KJ (2000) The relationship between the dissolved inorganic carbon concentration and growth rate in marine phytoplankton. Proc R Soc Lond B Biol Sci 267:953–959

Cortès MY, Bollman J, Thierstein HR (2001) Coccolithophore ecology at the HOT station Aloha, Hawaii. Deep-Sea Res Part II 48:1957–1981

Cros L (2002) Planktonic coccolithophores of the NW Mediterranean. PhD Thesis, Universitat de Barcelona, Barcelona, 181 pp.

Cros L, Estrada M (2013) Holo-heterococcolithophore life cycles: ecological implications. Mar Ecol Progr Ser 492:57–68

Cros L, Fortuno J-M (2002) Atlas of northwestern Mediterranean coccolithophores. Sci Mar 66:7–182

Cubillos J, Wright S, Nash G, Salas M de, Griffiths B, Tilbrook B, Poisson A, Hallegraeff G (2007) Calcification morphotypes of the coccolithophorid *Emiliania huxleyi* in the Southern Ocean: changes in 2001 to 2006 compared to historical data. Mar Ecol Progr Ser 348:47–54

Daniels C J, Sheward RM, Poulton AJ (2014) Biogeochemical implications of comparative growth rates of *Emiliania huxleyi* and *Coccolithus* species. Biogeosciences 11:6915–6925

de Vargas C, Aubry MP, Probert I, Young J (2007) Origin and Evolution of Coccolithophores: From Coastal Hunters to Oceanic Farmers. In: Falkowski PG, Knoll AH (eds.) Evolution of Primary Producers in the Sea. Elsevier Academic Press, New York

Decembrini F, Caroppo C, Azzaro M (2009) Size structure and production of phytoplankton community and carbon pathways channelling in the Southern Tyrrhenian Sea (Western Mediterranean). Deep-Sea Res Part II 56:687–699

Degens ET, Ittekkot V (1986) Ca2+-stress, biological response and particle aggregation in the aquatic habitat. Neth J Sea Res 20:109–116

Delille B, Harlay J, Zondervan I, Jacquet S, Chou L, Wollast R, Bellerby RGJ, Frankignoulle M, Borges AV, Riebesell U, Gattuso JP (2005) Response of primary production and calcification to changes of pCO_2 during experimental blooms of the coccolithophorid *Emiliania huxleyi*. Global Biogeochemical Cycles. 19. GB2023.

Dickson AG, Millero FJ (1987) A comparison of the equilibrium constants for the dissociation of carbonic acid in seawater media. Deep Sea Res Part I. 34:1733–1743

Dimiza MD, Triantaphyllou MV, Dermitzakis MD (2008) Vertical distribution and ecology of living coccolithophores in the marine ecosystems of Andros Island (Middle Aegean Sea) during late summer 2001. Hell J Geosci 43:7–20

Doney SC, Fabry VJ, Feely RA, Kleypas JA (2009) Ocean Acidification: The Other CO_2 Problem. Annu Rev Mar Sci 1:169–192

Doney SC, Mahowald N, Lima I, Feely RA, Mackenzie FT, Lamarque J-F, Rasch PJ (2007) Impact of anthropogenic atmospheric nitrogen and sulfur deposition on ocean acidification and the inorganic carbon system. Proc Natl Acad Sci 104:14580–14585

Dugdale RC, Wilkerson FP (1988) Nutrient sources and primary production in the Eastern Mediterranean. Oceanol Acta 9:179–184

Egge JK, Aksnes DL (1992) Silicate as regulating nutrient in phytoplankton competition. Mar Ecol Progr Ser 83:281–289

Eggers SL, Lewandowska AM, Barcelos e Ramos J, Blanco-Ameijeiras S, Gallo F, Matthiessen B (2014) Community composition has greater impact on the functioning of marine phytoplankton communities than ocean acidification. Global Change Biology. 20:713–723

Engel A, Cisternas Novoa C, Wurst M, Endres S, Tang T, Schartau M, Lee C (2014) No detectable effect of CO_2 on elemental stoichiometry of *Emiliania huxleyi* in nutrient-limited, acclimated continuous cultures. Mar Ecol Progr Ser 507:15–30

Engel A, Schulz KG, Riebesell U, Bellerby R, Delille B, Schartau M (2008) Effects of CO_2 on particle size distribution and phytoplankton abundance during a mesocosm bloom experiment (PeECE II). Biogeosciences 5:509–521

Engel A, Zondervan I, Aerts K, Beaufort L, Benthien A, Chou L, Delille B, Gattuso JP, Harlay J, Heemann C, Hoffmann L, Jacquet S, Nejstgaard J, Pizay MD, Rochelle-Newall E, Schneider U, Terbrueggen A, Riebesell U (2005) Testing the direct effect of CO_2 concentration on a bloom of the coccolithophorid *Emiliania huxleyi* in mesocosm experiments. Limnol Oceanogr 50:493-507

Fabry VJ (1989) Aragonite production by pteropod molluscs in the subarctic Pacific. Deep Sea Res Part Oceanogr Res Pap 36:1735–1751

Falkowski PG (1994) The role of phytoplankton photosynthesis in global biogeochemical cycles. Photosynth Res 39:235–258

Falkowski PG, Barber RT, Smetacek V (1998) Biogeochemical controls and feedbacks on ocean primary production. Science 281:200–206

Feely RA, Doney SC, Cooley SR (2009) Ocean acidification: present conditions and future changes in a high-CO_2 world. Oceanography 22:37–47

Feng Y, Hare CE, Leblanc K, Rose J, Zhang Y, DiTullio GR, Lee PA, Wilhelm SW, Rowe JM, Sun J, Nemcek N, Gueguen C, Passow U, Benner I, Brown C, Hutchins DA (2009) Effects of increased pCO_2 and temperature on the North Atlantic spring bloom. I. The phytoplankton community and biogeochemical response. Mar Ecol Progr Ser 388:13–25

Feng Y, Warner ME, Zhang Y, Sun J, Fu F-X, Rose JM, Hutchins DA (2008) Interactive effects of increased pCO_2, temperature, and irradiance on the marine coccolithophore *E. huxleyi* (Prymnesiophyceae). Eur J Phycol 43:87–98

Field CB (1998) Primary Production of the Biosphere: Integrating Terrestrial and Oceanic Components. Science 281:237–240

Frada M, Probert I, Allen MJ, Wilson WH, de Vargas C (2008) The "Cheshire Cat" escape strategy of the coccolithophore *Emiliania huxleyi* in response to viral infection. P Natl Acad Sci USA 105:15944–15949

Frada MJ, Bidle KD, Probert I, de Vargas C (2012) In situ survey of life cycle phases of the coccolithophore *Emiliania huxleyi* (Haptophyta). Environ Microbiol 14:1558–1569

Franklin D, Steinke M, Young J, Probert I, Malin G (2010) Dimethylsulphoniopropionate (DMSP), DMSP-lyase activity (DLA) and dimethylsulphide (DMS) in 10 species of coccolithophore. Mar Ecol Progr Ser 410:13–23

Frenz M, Baumann K-H, Boeckel B, Hoppner R, Henrich R (2005) Quantification of Foraminifer and Coccolith Carbonate in South Atlantic Surface Sediments by Means of Carbonate Grain-Size Distributions. J Sediment Res 75:464–475

Garrido M, Koeck B, Goffart A, Collignon A, Hecq J-H, Agostini S, Marchand B, Lejeune P, Pasqualini V (2014) Contrasting Patterns of Phytoplankton Assemblages in Two Coastal Ecosystems in Relation to Environmental Factors (Corsica, NW Mediterranean Sea). Diversity 6:296–322

Gattuso J-P, Brewer PG, Hoegh-Guldberg O, Kleypas JA, Pörtner H-O, Schmidt DN, 2014: Cross-chapter box on ocean acidification. In: Field CB, Barros VR, Dokken DJ, Mach KJ, Mastrandrea

MD, Bilir TE, Chatterjee M, Ebi KL, Estrada YO, Genova RC, Girma B, Kissel ES, Levy AN, MacCracken S, Mastrandrea PR, White LL (eds.) Climate Change 2014: Impacts, Adaptation, and Vulnerability. Part A: Global and Sectoral Aspects. Contribution of Working Group II to the Fifth Assessment Report of the Intergovernmental Panel on Climate Change. Cambridge University Press, Cambridge. United Kingdom and New York, USA, pp. 129-131.

Gattuso J-P, Hansson L (2011) Ocean acidification: background and history. In: Gattuso J-P, Hansson L (eds) Ocean acidification. Oxford University Press, p 1–17

Gazeau F, Sallon A, Maugendre L, Louis L, Dellisanti W, Gaubert M, Lejeune P, Gobert S, Alliouane S, Taillandier V, Louis F, Obolensky G, Grisoni J-M, Guieu C, (submitted)a. First mesocosm experiments to study the impacts of ocean acidification on plankton communities in the NW Mediterranean Sea (MedSeA project). Estuarine, Coastal and Shelf Science.

Gemayel E, Hassoun AER, Benallal MA, Goyet C, Rivaro P, Abboud-Abi Saab M, Krasakopoulou E, Touratier F, Ziveri P (2015) Climatological variations of total alkalinity and total inorganic carbon in the Mediterranean Sea surface waters. Earth Syst Dyn Discuss 6:1499–1533

Gerecht AC, Šupraha L, Edvardsen B, Langer G, Henderiks J (2015) Phosphorus availability modifies carbon production in *Coccolithus pelagicus* (Haptophyta). J Exp Mar Biol Ecol 472:24–31

Gerecht AC, Šupraha L, Edvardsen B, Probert I, Henderiks J (2014) High temperature decreases the PIC / POC ratio and increases phosphorus requirements in *Coccolithus pelagicus* (Haptophyta). Biogeosciences 11:3531–3545

Guieu C, Dulac F, Ridame C, Pondaven P (2014) Introduction to project DUNE, a dust experiment in a low Nutrient, low chlorophyll Ecosystem. Biogeosciences 11:425-442

Gotsis-Skretas O, Pagou K, Moraitou-Apostolopoulou M, Ignatiades L (1999) Seasonal horizontal and vertical variability in primary production and standing stocks of phytoplankton and zooplankton in the Cretan Sea and the Straits of the Cretan Arc (March 1994–January 1995). Prog Oceanogr 44:625–649

Gran G (1952) Determination of the equivalence point in potentiometric titrations of seawater with hydrochloric acid. Oceanol Acta 5:209–218

Green JC, Heimdal BR, Paasche E, Moate R **(**1998) Changes in calcification and the dimensions of coccoliths of *Emiliania huxleyi* (Haptophyta) grown at reduced salinities. Phycologia. 37(2):121-131

Gruber N (2011) Warming up, turning sour, losing breath: ocean biogeochemistry under global change. Philos Trans R Soc Math Phys Eng Sci 369:1980–1996

Guillard RRL, Ryther JH (1962) Studies of marine planktonic diatoms, I, *Cyclotella nanna* (Hustedt) and *Detonula convervacea* (Cleve). Can J Microbiol 8: 229–239

Hare CE, Leblanc K, DiTullio GR, Kudela RM, Zhang Y, Lee PA, Riseman S, Hutchins DA (2007) Consequences of increased temperature and CO_2 for phytoplankton community structure in the Bering Sea. Mar Ecol Progr Ser 352:9-16

Hagino K, Okada H, Matsuoka H (2000) Spatial dynamics of coccolithophore assemblage in the Euatorial Western-Central Pacific Ocean. Mar Micropaleontol 39:53–72

Hagino K, Okada H, Matsuoka H (2005) Coccolithophore assemblages and morphotypes of Emiliania huxleyi in the boundary zone between the cold Oyashio and warm Kuroshio currents off the coast of Japan. Mar Micropaleontol 55:19–47

Haidar AT, Thierstein HR (2001) Coccolithophore dynamics off Bermuda (N. Atlantic). Deep- Sea Res Part II 40:1925–1956

Hainbucher D, Rubino A, Cardin V, Tanhua T, Schroeder K, Bensi M (2014) Hydrographic situation during cruise M84/3 and P414 (spring 2011) in the Mediterranean Sea. Ocean Sci 10:669–682

Hansen HP, Koroleff F (1999) Determination of nutrients. In: Grasshoff K, Kremling K, Ehrhardt M (eds.) Methods of Seawater Analysis. Wiley-VCH. Weinheim. pp. 159–228

Hay WW, Mohler HP, Roth PH, Schmidt RR, Boudreaux JE (1967) Calcareous nannoplankton zonation of the cenozoic of the Gulf coast and Caribbean – Antillean area, and transoceanic correlation. Trans Gulf Coast Assoc Geol Soc 17:428–480

Henriksen K, Stipp SLS, Young JR, Bown PR (2003) Tailoring calcite: nanoscale AFM of coccolith biocrystals. Am Mineral 88:2040 –2044

Huertas IE, Rouco M, López-Rodas V, Costas E (2011) Warming will affect phytoplankton differently: evidence through a mechanistic approach. Proc R Soc B. doi: 10.1098/rspb.2011.0160.

Hutchins DA, Fu F-X, Webb EA, Walworth N, Tagliabue A (2013) Taxon-specific response of marine nitrogen fixers to elevated carbon dioxide concentrations. Nat Geosci 6:790–795

Hutchins DA, Fu F-X, Zhang Y, Warner ME, Feng Y, Portune K, Bernhardt PW, Mulholland MR (2007) CO_2 control of Trichodesmium N_2 fixation, photosynthesis, growth rates, and elemental ratios: Implications for past, present, and future ocean biogeochemistry. Limnol Oceanogr 52:1293

Iglesias-Rodríguez MD, Brown CW, Doney SC, Kleypas J, Kolber D, Kolber Z, Hayes PK, Falkowski PG (2002) Representing key phytoplankton functional groups in ocean carbon cycle models: Coccolithophorids. Glob Biogeochem Cycles 16:47–1–47–20

Iglesias-Rodriguez MD, Halloran PR, Rickaby REM, Hall IR, Colmenero-Hidalgo E, Gittins JR, Green DRH, Tyrrell T, Gibbs SJ, von Dassow P, Rehm E, Armbrust EV, Boessenkoo KP (2008) Phytoplankton calcification in a high-CO_2 world. Science 320:336–340.

Ignatiades L, Gotsis-Skretas O, Pagou K, Krasakopoulou E (2009) Diversification of phytoplankton community structure and related parameters along a large-scale longitudinal east-west transect of the Mediterranean Sea. J Plankton Res 31:411–428

Ignatiades L, Georgopoulos D, Karydis M (1995) Description of the phytoplanktonic community of the oligotrophic waters of the SE Aegean Sea (Mediterranean). Mar Ecol Progr Ser 16:13–26

Irwin AJ, Oliver MJ (2009) Are ocean deserts getting larger? Geophys Res Lett 36

Joos F, Spahni R (2008) Rates of change in natural and anthropogenic radiative forcing over the past 20,000 years. PNAS 105:1425–1430

Karl DM (1999) A Sea of Change: Biogeochemical Variability in the North Pacific Subtropical Gyre. Ecosystems 2:181–214

Karl D., Bidigare R., Letelier R. (2001) Long-term changes in plankton community structure and productivity in the North Pacific Subtropical Gyre: The domain shift hypothesis. Deep Sea Res Part II Top Stud Oceanogr 48:1449–1470

Keeling RF, Körtzinger A, Gruber N (2010) Ocean Deoxygenation in a Warming World. Annu Rev Mar Sci 2:199–229

Keeling RF, Walter, S. J., Piper, S. C., Bollenbacher, A. F. (2015) Mauna Loa Observatory, Hawaii | Scripps CO_2 Program. http://scrippsco2.ucsd.edu/data/mlo. 2015-07-02 11:41:10

Kester DR, Duedall IW, Conners DN, Pytkowicz RM (1967) Preparation of artificial seawater. Limnol Oceanogr 12:176–179

Keller MD (1989) Dimethyl sulfide production and marine phytoplankton: the importance of species composition and cell size. Biol Oceanogr 6:375–382

Khatiwala S, Tanhua T, Mikaloff Fletcher S, Gerber M, Doney SC, Graven HD, Gruber N, McKinley GA, Murata A, Ríos AF, Sabine CL (2013) Global ocean storage of anthropogenic carbon. Biogeosciences 10:2169–2191

Kim I-N, Lee K, Gruber N, Karl DM, Bullister JL, Yang S, Kim T-W (2014) Increasing anthropogenic nitrogen in the North Pacific Ocean. Science 346:1102–1106

Klaas C, Archer DE (2002) Association of sinking organic matter with various types of mineral ballast in the deep sea: Implications for the rain ratio: Ocean carbon-mineral flux association. Glob Biogeochem Cycles 16. http://dx.doi.org/10.1029/2001GB001765

Klausmeier CA, Litchman E, Daufresne T, Levin SA (2004) Optimal nitrogen-to-phosphorus stoichiometry of phytoplankton. Nature 429(6988):171-174

Kleijne A (1990) Distribution and malformation of extant calcareous nannoplankton in the Indonesian Seas. Mar Micropaleontol 16:293–316

Kleijne A (1991) Holococcolithophorids from the Indian Ocean, Red Sea, Mediterranean Sea and North Atlantic Ocean. Mar Micropaleontol 17:1–76.

Kleijne A (1992) Extant Rhabdosphaeraceae (coccolithophorids, class Prymnesiophyceae) from the Indian Ocean, Red Sea, Mediterranean Sea and North Atlantic Ocean. ScriptaGeol. 100: 1–63

Kleijne A, Kroon D, Zevenboom W (1989) Phytoplankton and foraminiferal frequencies in northern Indian Ocean and Red Sea surface waters. Neth J Sea Res 24:531–539.

Knappertsbusch M (1993) Geographic distribution of living and Holocene coccolithophores in the Mediterranean Sea. Mar Micropaleontol 21:219–247

Kress N, Frede Thingstad T, Pitta P, Psarra S, Tanaka T, Zohary T, Groom S, Herut B, Fauzi C. Mantoura R, Polychronaki T, Rassoulzadegan F, Spyres G (2005) Effect of P and N addition to oligotrophic Eastern Mediterranean waters influenced by near-shore waters: A microcosm experiment. Deep Sea Res Part II Top Stud Oceanogr 52:3054–3073

Kroeker KJ, Kordas RL, Crim R, Hendriks IE, Ramajo L, Singh GS, Duarte CM, Gattuso J P (2013) Impacts of ocean acidification on marine organisms: quantifying sensitivities and interaction with warming. Glob Change Biol 19:1884–1896

Krom MD, Kress N, Brenner S, Gordon LI (1991) Phosphorus limitation of primary productivity in the eastern Mediterranean Sea. Limnol Oceanogr 36(3):424–432

Langer G, Benner I (2009)b Effect of elevated nitrate concentration on calcification in *Emiliania huxleyi*. J Nannoplankton Res 30:77–80

Langer G, Bode M (2011) CO_2 mediation of adverse effects of seawater acidification in *Calcidiscus leptoporus*. Geochem Geophy Geosy 12(Q05001)

Langer G, Geisen M, Baumann K-H, Kläs J, Riebesell U, Thoms S, Young JR (2006) Species-specific responses of calcifying algae to changing seawater carbonate chemistry. Geochem Geophys Geosystems 7(9): 1525–2027

Langer G, Nehrke G, Probert I, Ly J, Ziveri P (2009) Strain-specific responses of *Emiliania huxleyi* to changing seawater carbonate chemistry. Biogeosciences 6:2637–2646

Langer G, De Nooijer LJ, Oetje K (2010) On the role of the cytoskeleton in coccolith morphogenesis: the effect of cytoskeleton inhibitors. J Phycol 46:1252–1256

Langer G, Oetjen K, Brenneis T (2012)a Calcification of *Calcidiscus leptoporus* under nitrogen and phosphorus limitation. J Exp Mar Biol Ecol 413:131–137

Langer G, Oetjen K, Brenneis T (2012)b On culture artefacts in coccolith morphology. Helgol. Mar. Res. http://dx.doi.org/10.1007/s10152-012-0328-x.

Langer G, Probert I, Nehrke G, Ziveri P (2011) The morphological response of *Emiliania huxleyi* to seawater carbonate chemistry changes: an inter-strain comparison. J Nannoplankton Res 32:29–34

Lasternas S, Tunin-Ley A, Ibañez F, Andersen V, Pizay M-D, Lemée R (2011) Short-term dynamics of microplankton abundance and diversity in NW Mediterranean Sea during late summer conditions (DYNAPROC 2 cruise; 2004). Biogeosciences 8:743–761

Lavigne H, Epitalon JM, Gattuso J-P (2014) Seacarb: seawater carbonate chemistry with R. ran.r-project.org/package=seacarb.

Leblanc K, Quéguiner B, Garcia N, Rimmelin P, Raimbault P (2003) Silicon cycle in the NW Mediterranean Sea: seasonal study of a coastal oligotrophic site. Oceanol Acta 26:339–355

Lee K, Sabine CL, Tanhua T, Kim T-W, Feely RA, Kim H-C (2011) Roles of marginal seas in absorbing and storing fossil fuel CO_2. Energy Environ Sci 4:1133

Leonardos N, Geider RJ (2005) Elevated atmospheric carbon dioxide increases organic carbon fixation by *Emiliania huxleyi* (Haptophyta), under nutrient-limited high-light conditions. J Phycol 41:1196–1203

Levitan O, Rosenberg G, Setlik I, Setlikova E, Grigel J, Klepetar J, Prasil O, Berman-Frank I (2007) Elevated CO_2 enhances nitrogen fixation and growth in the marine cyanobacterium Trichodesmium. Glob Change Biol 13:531–538

Lewis E, Wallace DWR (1998) Program developed for CO_2 system calculations ORNL/CDIAC-105. Carbon Dioxide Information Analysis Centre Oak Ridge National Laboratory. U.S. Department of Energy. Oak Ridge. Tennessee.

Loeblich JR, AR, Tappan H (1978) The coccolithophorid genus Calcidiscus Kamptner and its synonyms. J Paleontol 52:1390–1392

Lohmann H (1902) Die Coccolithophoridae, eine Monographie der Coccolithen bildenden Flagellaten, zugleich ein Beitrag zur Kenntnis des Mittelmeerauftriebs. Archiv für Protistenkunde 1:89–165

Lombard F, Guidi L, Kiørboe T (2013) Effect of Type and Concentration of Ballasting Particles on Sinking Rate of Marine Snow Produced by the Appendicularian *Oikopleura dioica* (BR MacKenzie, Ed.). PLoS ONE 8:e75676

Longhurst A, Sathyendranath S, Platt T, Caverhill C (1995 9 An estimate of global primary production in the ocean from satellite radiometer data. J Plankton Res 17:1245-1271

Louis J, Guieu C, Gazeau F (submitted) Is nutrients dynamic affected by ocean acidification? Results from two mesocosms experiments in the Mediterranean Sea. Estuarine, Coastal and Shelf Science.

Malinverno E (2003) Coccolithophorid distribution in the Ionian Sea and its relationship to eastern Mediterranean circulation during late fall to early winter 1997. J Geophys Res 108 (C9). http://dx.doi.org/10.1029/2002JC001346.

Malinverno E, Maffioli P, Corselli C, De Lange GJ (2014) Present-day fluxes of coccolithophores and diatoms in the pelagic Ionian Sea. J Mar Systems 132: 13–27

Mackinder L, Wheeler G, Schroeder D, Riebesell U, Brownlee C (2010) Molecular mechanisms underlying calcification in coccolithophores. Geomicrobiol. J 27:585–595

Maugendre L, Gattuso J-P, Poulton AJ, Dellisanti W, Gaubert M, Guieu C, Gazeau F (submitted) No effect of ocean acidification on plankton metabolism in the NW oligotrophic Mediterranean Sea: results from two mesocosm studies. Estuarine, Coastal and Shelf Science.

Margalef R (1978) Life-forms of phytoplankton as survival alternatives in an unstable environment. Oceanol Acta 1:493–509

Martinez JM, Schroeder DC, Larsen A, Bratbak G, Wilson WH (2007) Molecular dynamics of *Emiliania huxleyi* and cooccurring viruses during two separate mesocosm studies. Appl Environ Microb 73:554–562

McConnaughey TA, Whelan JF (1997) Calcification generates protons for nutrient and bicarbonate uptake. Earth-Sci Rev 42:95–117

McIntyre A, Bé AWH (1967) Modern coccolithophoridae of the Atlantic Ocean. 1. Placoliths and cyrtoliths. Deep-Sea Res 14:561–597

Mehrbach C, Culberson CH, Hawley JE, Pytkovicz RM (1973) Measurement of the apparent dissociation constants of carbonic acid in seawater at atmospheric pressure. Limnol Oceanogr 18:897–907.

Meier KJS, Beaufort L, Heussner S, Ziveri P (2014) The role of ocean acidification in *Emiliania huxleyi* coccolith thinning in the Mediterranean Sea. Biogeosciences 11:2857–2869

Merico A, Tyrrell T, Cokacar T (2006) Is there any relationship between the phytoplankton seasonal dynamics and the carbonate system?. J Marine Syst 59:120–142.

Meyer J, Riebesell U (2015) Reviews and Syntheses: Responses of coccolithophores to ocean acidification: a meta-analysis. Biogeosciences 12:1671–1682

Mohan R, Mergulhao L P, Guptha MVS, Rajakumar A, Thamban M, Anilkumar N, Sudhakar M, Ravindra R (2008) Ecology of coccolithophores in the Indian sector of the Southern Ocean,.Mar Micropaleontol 67:30–45.

Molfino B, McIntyre A (1990) Precession forcing of nutricline dynamics in the equatorial Atlantic. Science 249:766–769.

Moore CM, Mills MM, Arrigo KR, Berman-Frank I, Bopp L, Boyd PW, Galbraith ED, Geider RJ, Guieu C, Jaccard SL, Jickells TD, Roche J La, Lenton TM, Mahowald NM, Marañón E, Marinov I, Moore JK, Nakatsuka T, Oschlies A, Saito MA, Thingstad TF, Tsuda A, Ulloa O (2013) Processes and patterns of oceanic nutrient limitation. Nat Geosci 6:701–710

Moutin T, Raimbault P (2002) Primary production, carbon export and nutrients availability in western and eastern Mediterranean Sea in early summer 1996 (MINOS cruise). J Mar Syst 33:273–288

Müller MN, Antia AN, La Roche J (2008) Influence of cell cycle phase on calcification in the coccolithophore *Emiliania huxleyi*. Limnol Oceanogr 53:506–512

Murray G, Blackman VH (1898) On the nature of the Coccospheres and Rhabdospheres. Phil Trans R Soc Ser B 190:427–441

Nejstgaard JC, Gismervik I, Solberg PT (1997) Feeding and reproduction by *Calanus finmarchicus*, and microzooplankton grazing during mesocosm blooms of diatoms and the coccolithophore *Emiliania huxleyi*. Mar Ecol Progr Ser 147:197–217

Nelson DM, Goering JJ, Kilham SS, Guillard RRL (1967) Kinetics of silicic acid uptake and rates of silica dissolution in the marine diatom *Thalassiosira pseudonana*. J Phycol 12: 246–252

Nishida S (1979) Atlas of Pacific nannoplanktons, News Osaka. Micropaleonty 3:1–31.

Okada H, Honjo S (1973) The distribution of ocean coccolithophorids in the Pacific. Deep-Sea Res 20:335–374.

Okada H, Honjo S (1975) Distribution of coccolithophores in marginal seas along the western Pacific Ocean and in the Red Sea. Mar Biol 31:271–285

Okada H, McIntyre A (1977) Modern coccolithophores of the Pacific and North Atlantic Oceans. Micropaleontology 23:1–55

Okada H, McIntyre A (1979) Seasonal distribution of modern coccolithophores in the western North Atlantic Ocean. Mar Biol 54:319–328

Orr JC, Fabry VJ, Aumont O, Bopp L, Doney SC, Feely RA, Gnanadesikan A, Gruber N, Ishida A, Joos F, Key RM, Lindsay K, Maier-Reimer E, Matear R, Monfray P, Mouchet A, Najjar RG, Plattner G-K, Rodgers KB, Sabine CL, Sarmiento JL, Schlitzer R, Slater RD, Totterdell IJ, Weirig M-F, Yamanaka Y, Yool A (2005) Anthropogenic ocean acidification over the twenty-first century and its impact on calcifying organisms. Nature 437:681–686

Ortenzio F D', Antoine D, Marullo S (2008) Satellite-driven modeling of the upper ocean mixed layer and air–sea CO_2 flux in the Mediterranean Sea. Deep Sea Res Part Oceanogr Res Pap 55:405–434

Oviedo AM, Langer G, Ziveri P (2014) Effect of phosphorus limitation on coccolith morphology and element ratios in Mediterranean strains of the coccolithophore *Emiliania huxleyi*. J Exp Mar Biol Ecol 459:105–113

Oviedo A, Ziveri P, Alvarez M, Tanhua T (2015) Is coccolithophore distribution in the Mediterranean Sea related to seawater carbonate chemistry?. Ocean Sci 11:13-32
Paasche E (1964) A tracer study of the inorganic carbon uptake during coccolith formation and photosynthesis in the coccolithophorid *Coccolithus huxleyi*. Physiol Plant Suppl 3:1–82

Paasche E (1998) Roles of nitrogen and phosphorus in coccolith formation in *Emiliania huxleyi* (Prymnesiophyceae). Eur J Phycol 33:33–42

Paasche E (2002) A review of the coccolithophorid *Emiliania huxleyi* (Prymnesiophyceae), with particular reference to growth, coccolith formation, and calcification-photosynthesis interactions. Phycologia 40:503–529

Paasche E, Brubak S (1994) Enhanced calcification in the coccolithophorid *Emiliania huxleyi* (Haptophyceae) under phosphorus limitation. Phycologia 33:324–330

Passow U, Carlson CA (2012) The biological pump in a high CO_2 world. Mar Ecol Progr Ser 470:249–271

Paulino AI, Egge JK, Larsen A (2008) Effects of increased atmospheric CO_2 on small and intermediate sized osmotrophs during a nutrient induced phytoplankton bloom. Biogeosciences 5:739–748

Pearson PN, Palmer MR (2000) Atmospheric carbon dioxide concentrations over the past 60 million years. Nature 406:695–699

Pinardi N, Masetti E (2000) Variability of the large scale general circulation of the Mediterranean Sea from observations and modelling: a review. Palaeogeogr Palaeoecl 158: 153–173

Polovina JJ, Howell EA, Abecassis M (2008) Ocean's least productive waters are expanding. Geophys Res Lett 35

Probert I, Houdan A (2004) The Laboratory culture of coccolithophores. In: Thierstein H R, Young JR (eds.) Coccolithophores: From Molecular Processes to Global Impact. Springer. Germany. pp.217–250

Psarra S, Tselepides A, Ignatiades L (2000) Primary productivity in the oligotrophic Cretan Sea (NE Mediterranean): seasonal and interannual variability. Prog Oceanogr 46:187–204.

Rabitti S, Bianchi F, Boldrin A, Da Ros L, Socal G, Totti C (1994) Particulate matter and phytoplankton in the Ionian Sea. Oceanol Acta 17:297–307

Rahav E, Herut B, Levi A, Mulholland MR, Berman-Frank I (2013) Springtime contribution of dinitrogen fixation to primary production across the Mediterranean Sea. Ocean Sci 9:489–498

Ras J, Claustre H, Uitz J (2008) Spatial variability of phytoplankton pigment distributions in the Subtropical South Pacific Ocean: comparison between in situ and predicted data. Biogeosciences 5:305–369

Raven JA, Crawfurd K (2012) Environmental controls on coccolithophore calcification. Mar Ecol Progr Ser 470:137–166

Rhein M, Rintou SR, Aoki, S., Campos E, Chambers D, Feely RA, Gulev S, Johnson GC, Josey SA, Kostianoy K, Mauritzen C, Roemmich D, Talley LD, Wang F (2013) Observations: Ocean. In: Stocker TF, Qin D, Plattner G-K, Tignor M, Allen SK, Boschung J, Nauels A, Xia Y, Bex V, Midgley PM (eds) Climate change 2013: the physical science basis: Working Group I contribution to the Fifth assessment report of the Intergovernmental Panel on Climate Change. Cambridge University Press, New York

Rickaby RE, Henderiks J, Young JN (2010) Perturbing phytoplankton: a tale of isotopic fractionation in two coccolithophore species. Clim Past Discuss 6:257–294

Riebesell U (2004) Effects of CO_2 enrichment on marine phytoplankton. J Oceanogr 60:719–729

Riebesell U, Czerny J, von Bröckel K, Boxhammer T, Büdenbender J, Deckelnick M, Fischer M, Hoffmann D, Krug SA, Lentz U, Ludwig A, Muche R, Schulz KG (2013) Technical Note: A Mobile Sea-Going Mesocosm System – New Opportunities for Ocean Change Research. Biogeosciences 10(3):1835-1847

Riebesell U, Bellerby RGJ, Grossart HP, Thingstad F (2008) Mesocosm CO_2 perturbation studies: from organism to community level. Biogeosciences 5:1157-1164

Riebesell U, Zondervan I, Rost B, Tortell PD, Zeebe RE, Morel FM (2000) Reduced calcification of marine plankton in response to increased atmospheric CO_2. Nature 407:364–367

Riebesell U, Fabry VJ, Hansson L, Gattuso J-P (Eds) (2010) Guide to best practices for ocean acidification research and data reporting. Publications Office of the European Union, Luxembourg

Riegman R, Stolte W, Noordeloos AAM, Slezak D (2000) Nutrient uptake and alkaline phosphatase (ec 3:1:3:1) activity of *Emiliania huxleyi* (Prymnesiophyceae) during growth under n and p limitation in continuous cultures. J Phycol 36:87–96

Ribera d'Alcalà M, Civitarese G, Conversano F, Lavezza R (2003) Nutrient ratios and fluxes hint an overlooked processes in the Mediterranean sea. J Geophys Res 108:8106.

Robinson AR, Leslie WG, Theocharis A, Lascaratos A (2001) Mediterranean Sea circulation. In: Encyclopedia of ocean sciences, Academic Press. London. doi:10.1006/rwos.2001.0376, 2001.

Rohling EJ, Abu-Zied R, Casford JSL, Hayes A, Hoogakker BAA (2009) The marine environment: present and past. In: Woodward JC (eds.) The Physical Geography of the Mediterranean. Oxford University Press. Oxford. ISBN: 978-0-19-926803-0, 33–67

Rost B, Riebesell U (2004) Coccolithophores and the biological pump: responses to environmental changes. In: Thierstein H, Young JR (eds.) Coccolithophores: from molecular processes to global impact. Springer, Berlin, p99−125

Rost B, Riebesell U, Burkhardt S, Sültemeyer D (2003) Carbon acquisition of bloom-forming marine phytoplankton. Limnol Oceanogr 48:55–67

Rost B, Zondervan I, Wolf-Gladrow D (2008) Sensitivity of phytoplankton to future changes in ocean carbonate chemistry: current knowledge, contradictions and research directions. Mar Ecol Progr Ser 373:227–237

Rouco M, Branson O, Lebrato M, Iglesias-Rodríguez MD (2013) The effect of nitrate and phosphate availability on *Emiliania huxleyi* (NZEH) physiology under different CO_2 scenarios. Front Microbiol 4

Sabine CL (2004) The Oceanic Sink for Anthropogenic CO_2. Science 305:367–371

Sarmiento JL, Dunne J, Gnanadesikan A, Key RM, Matsumoto K, Slater R (2002) A new estimate of the $CaCO_3$ to organic carbon export ratio. Glob Biogeochem Cycles 16:54–1–54–12

Sarthou G, Timmermans KR, Blain S, Treguer P (2005) Growth physiology and fate of diatoms in the ocean: a review. J Sea Res 53:25–42

Schneider A, Tanhua T, Körtzinger A, Wallace DWR (2010) High anthropogenic carbon content in the eastern Mediterranean. J Geophys Res 115

Schneider A, Wallace DWR, Körtzinger A (2007) Alkalinity of the Mediterranean Sea. Geophys Res Lett 34

Schroeder K, Gasparini GP, Borghini M, Cerrati G, Delfanti R (2010) Biogeochemical tracers and fluxes in the Western Mediterranean Sea, spring 2005. J Mar Syst 80:8–24

Siokou-Frangou I, Christaki U, Mazzocchi MG, Montresor M, Ribera d'Alcalá M, Vaqué D, Zingone A (2010) Plankton in the open Mediterranean Sea: a review. Biogeosciences 7: 1543–1586

Stewart RIA, Dossena M, Bohan DA, Jeppesen E, Kordas RL, Ledger ME, Meerhoff M, Moss B, Mulder C, Shurin JB, Suttle B, Thompson R, Trimmer M, Woodward G (2013) Mesocosm Experiments as a Tool for Ecological Climate Change Research. In: Woodward G, Ogorman EJ (eds.) Advances in Ecological Research: Global Change in Multispecies Systems, Pt 3, pp.71-181.

Stocker TF, Qin D, Plattner G-K, Alexander LV, Allen SK, Bindoff NL, Bréon F-M, Church JA, Cubasch U, Emori S, others (2013) Technical summary. In: Climate Change 2013: The Physical Science Basis. Contribution of Working Group I to the Fifth Assessment Report of the Intergovernmental Panel on Climate Change. Cambridge University Press, p 33–115

Sverdrup HU (1953) On conditions for the vernal blooming of phytoplankton. ICES J Mar Sci 18:287–295.

Taillandier V, D'Ortenzio F, Antoine D (2012) Carbon fluxes in the mixed layer of the Mediterranean Sea in the 1980s and the 2000s. Deep Sea Res Part Oceanogr Res Pap 65:73–84

Takahashi K, Okada H (2000) Environmental control on the biogeography of modern coccolithophores in the southeastern Indian Ocean offshore of Western Australia. Mar. Micropaleontol 39:73–86

Tanhua T, Hainbucher D, Cardin V, Álvarez M, Civitarese G, McNichol AP, Key RM (2013)a. Repeat hydrography in the Mediterranean Sea, data from the Meteor cruise 84/3 in 2011. Earth Syst Sci Data 5:289–294

Tanhua T, Hainbucher D, Schroeder K, Cardin V, Álvarez M, Civitarese G (2013)b. The Mediterranean Sea system: a review and an introduction to the special issue. Ocean Sci 9: 789–803

The MerMex group: Madron XD, Guieu C, Sempéré R, Conan P, Cossa D, D'Ortenzio F, Estournel C, Gazeau F, Rabouille C, others (2011) Marine ecosystems' responses to climatic and anthropogenic forcings in the Mediterranean. Prog Oceanogr 91:97–166

Thingstad TF, Krom MD, Mantoura RFC, Flaten GAF, Groom S, Herut B, Kress N, Law CS, Pasternak A, Pitta P, Psarra S, Rassoulzadegan F, Tanaka T, Tselepides A, Wassmann P, Woodward EMS, Riser CW, Zodiatis G, Zohary T (2005) Nature of Phosphorus Limitation in the Ultraoligotrophic Eastern Mediterranean. Science 309:1068–1071

Tortell PD, DiTullio GR, Sigman DM, Morel FMM (2002) CO_2 effects on axonomic composition and nutrient utilization in an Equatorial Pacific phytoplankton assemblage. Mar Ecol Progr Ser 23:37–43

Tortell PD, Payne CD, Li Y, Trimborn S, Rost B, Smith WO, Riesselman C, Dunbar RB, Sedwick P, DiTullio GR (2008) CO_2 sensitivity of Southern Ocean phytoplankton. Geophys Res Lett 35(L04605). doi:10.1029/2007GL032583.

Touratier F, Goyet C (2011) Impact of the Eastern Mediterranean Transient on the distribution of anthropogenic CO_2 and first estimate of acidification for the Mediterranean Sea. Deep Sea Res Part Oceanogr Res Pap 58:1–15

Triantaphyllou M, Dimiza M, Krasakopoulou E, Malinverno E, Lianou V, Souvermezoglou E (2010) Seasonal variation in *Emiliania huxleyi* coccolith morphology and calcification in the Aegean Sea (Eastern Mediterranean). Geobios 43:99–110

Tyrrell T, Schneider B, Charalampopoulou A, Riebesell U (2008) Coccolithophores and calcite saturation state in the Baltic and Black Seas. Biogeosciences 5:485–494.

Tyrrell T, Young JR (2009) Coccolithophores. In: Steele JH, Turekian KK, Thorpe SA (eds) Encyclopedia of Ocean Sciences, 2nd ed. Academic Press, San Diego, US., p 3568–3576

Van Cappellen, P (2003) Biomineralization and global biogeochemical cycles. Rev Mineral Geochem 54(1):357–381

van de Waal DB, Johnm W, Ziveri P, Reichart G-J, Hoins M, Sluijs A, Rost B (2013) Ocean acidification reduces growth and calcification in a marine dinoflagellate. PLOSONE 8(6)e65987

Vardi A, Haramaty L, Van Mooy BA, Fredricks HF, Kimmance SA, Larsen A, Bidle KD. (2012) Host-virus dynamics and subcellular controls of cell fate in a natural coccolithophore population. P Natl Acad Sci USA 109:19327–19332

Volpe G, Colella S, Forneris V, Tronconi C, Santoleri R (2012) The Mediterranean Ocean Colour Observing System – system development and product validation. Ocean Sci 8:869–883

Wu J, Sunda W, Boyle EA, Karl DM (2000) Phosphate Depletion in the Western North Atlantic Ocean. Science 289:759–762

Yacobi Y, Zohary T, Kress N, Hecht A, Robarts R, Waiser M, Wood A, Li W (1995) Chlorophyll distribution throughout the southern Mediterranean in relation to the physical structure of the water mass. J Mar Syst 6:179–190

Young J, Geisen M, Cros L, Kleijne A, Sprengel C, Probert I, Østergaard J (2003) A guide to extant coccolithophore taxonomy. J Nannoplankton Res Spec Issue 1:1–125

Young JR, Westbroek P (1991) Genotypic variation in the coccolithophorid species *Emiliania huxleyi*. Mar Micropaleontol 18:5–23

Young JR, Poulton AJ, Tyrrell T (2014) Morphology of *Emiliania huxleyi* coccoliths on the northwestern European shelf – is there an influence of carbonate chemistry? Biogeosciences 11:4771–4782

Winter A, Jordan RW, Roth PH (1994) Biogeography of living coccolithophores. p. 161-178. In: Winter A, Siesser WG (eds.) Coccolithophores. Cambridge University Press, Cambridge.

Zeebe RE, Caldeira K (2008) Close mass balance of long-term carbon fluxes from ice-core CO2 and ocean chemistry records. Nat Geosci 1:312–315

Zeebe RE, Wolf-Gladrow DA (2001) CO_2 in seawater: equilibrium, kinetics, isotopes. Gulf Professional Publishing

Ziveri P, Baumann K-H, Boeckel B, Bollmann J, Young JR (2004) Biogeography of selected Holocene coccoliths in the Atlantic Ocean. In: Thierstein HR, Young JR (eds) Coccolithophores From Molecular Processes to Global Impact. Springer, Berlin Heidelberg New York, p 403–428

Ziveri P, Bernardi B de, Baumann K-H, Stoll HM, Mortyn PG (2007) Sinking of coccolith carbonate and potential contribution to organic carbon ballasting in the deep ocean. Deep Sea Res Part II Top Stud Oceanogr 54:659–675

Ziveri P, Passaro M, Incarbona A, Milazzo M, Rodolfo-Metalpa R, Hall-Spencer JM (2014) Decline in Coccolithophore Diversity and Impact on Coccolith Morphogenesis Along a Natural CO_2 Gradient. Biol Bull 226:282–290

Ziveri P, Rutten A, Lange GJ De, Thomson J, Corselli C (2000) Present-day coccolith fluxes recorded in central eastern Mediterranean sediment traps and surface sediments. Palaeogeogr Palaeoclimatol Palaeoecol 158:175–195

Ziveri P, Thoms S, Probert I, Geisen M, Langer G (2012) A universal carbonate ion effect on stable oxygen isotope ratios in unicellular planktonic calcifying organisms. Biogeosciences 9:1025–1032,

Ziveri P, Thunell RC, Rio D (1995) Seasonal changes in coccolithophore densities in the Southern California Bight during 1991–1992. Deep-Sea Res Part I 42:1881–1903